A Study of the Mechanisms of Diesel Exhaust Enhanced Allergic Lung Disease

Tina L Stevens

A dissertation submitted to the faculty of the University of North Carolina at Chapel Hill in partial fulfillment of the requirements for the degree of Doctor of Philosophy in the Curriculum of Toxicology

Chapel Hill
2008

Approved by:
Dr. David Peden
Dr. M. Ian Gilmour
Dr. Michael Madden
Dr. Ilona Jaspers
Dr. Stephen Tilley

Abstract

Tina L Stevens: A Study of the Mechanisms of Diesel Exhaust Enhanced Allergic Lung Disease
(Under the direction of Dr. M. Ian Gilmour)

Over the last several decades, epidemiologists have witnessed a rapid rise in the prevalence and severity of asthma. While the factors underlying this increase are clearly complex, environmental factors such as ambient particular matter (PM) appear to play a role. Diesel exhaust particles (DEP), a large contributor to vehicle derived PM, has been shown to act as an immunologic adjuvant when given with antigen; however, there is still a lack of understanding as to what component(s) are responsible for these effects and the underlying mechanisms through which they act. In this work, immunotoxic and genomic responses of three chemically distinct DEP samples were assessed in an ovalbumin (OVA) murine mucosal sensitization model. Immunotoxic endpoints in the lung after OVA challenge demonstrated C-DEP/OVA ≈ A-DEP/OVA > N-DEP/OVA with respect to adjuvancy. To elucidate possible mechanisms for these effects, global gene expression changes in the lung were assessed. While all three DEP/OVA treatments induced expression of cytokine and toll-like receptor pathways, only A- and C-DEP/OVA treatments altered expression of apoptosis pathways. In addition, C-DEP/OVA treatment, which induced the greatest T_H2 response post-sensitization, altered expression of DNA damage pathways. This comprehensive approach using gene expression analysis to examine changes at a pathway level provides a clearer picture of the events occurring in

the lung after DEP exposure in the presence or absence of antigen. This work also explored immune responses in mice acutely exposed to moderate doses of DE in an OVA mucosal sensitization model and identified possible mechanisms using genomics. Mice exposed to DE/OVA induced a mild adjuvant response. Expression analysis demonstrated DE/OVA altered oxidative stress and metabolism pathways. Together these results demonstrate that exposure to even moderate doses of an air pollutant, such as DE, can enhance allergic sensitization through oxidative stress and inflammatory pathways. Overall the results demonstrate all three DEP samples and DE induced adjuvancy, the extent of which was not solely dependent on the extractable organic content, and gene expression analysis was a more sensitive indicator of early signaling events than the classical immunotoxic endpoints.

To Chloe Rose Nash:

May you always follow your heart and reach for the stars

Acknowledgements

Though only my name appears on the cover of this dissertation, a great many people have contributed to its production. I owe my gratitude to all those people who have made this dissertation possible and because of whom my graduate experience has been one that I will cherish forever.

First and foremost I would like to thank the Curriculum in Toxicology for providing me with the training grants that has made this work possible. The work described here was supported by National Institute of Environmental Health Sciences Grant T32 ES007126 and the U.S. Environmental Protection Agency Grant CT 829472.

I would like to express my deepest gratitude to my advisor, Dr. M. Ian Gilmour, for his support, guidance, suggestions, and encouragement throughout my graduate studies. He has taught me innumerable lessons and insights, which have not only helped me to attain my doctorate, but also have made me a better scientist.

I also give special thanks to Dr. Susan Hester for her generous help and guidance with the genomic portion of my research. Her expertise in the field of toxicogenomics as well as her encouragement and friendship has been invaluable for the completion of my dissertation research.

Many thanks to the members of my dissertation committee, Dr. David Peden, Dr. Ilona Jaspers, Dr. Michael Madden, and Dr. Stephen Tilley for their valuable suggestions and insights.

I would like to thank Mary Daniels, Elizabeth Boykin, Judy Richards, Rick Jaskot, Charly King, and Todd Krantz for their technical assistance and Drs William Linak and Seung-Hyun Cho for their diesel particle analysis. I especially would like to thank Kymberly Gowdy, who not only helped me with my studies, but also provided me with encouragement and comic relief.

Last, but certainly not least, I would like to thank my parents, Thomas and Linda Stevens, and my sister, Laurie Stevens, for their understanding, love, support, and endless hours of babysitting during the past few years; without them this work would not have been possible. I would especially like to thank my mother for believing in me even in my darkest hours. I am eternally grateful for her unending support and encouragement. Finally, I would like to thank my daughter, Chloe Rose Nash, for her love, patience, and understanding during these busy years.

Table of Contents

List of Tables

List of Figures

List of Abbreviations

A-DEP: Automobile DEP

AHR: Airway hyperresponsiveness

AM: Alveolar macrophage

BALF: Bronchoalveolar lavage fluid

C-DEP: Compressor DEP

CB: Carbon black

CO: Carbon monoxide

COPD: Chronic obstructive pulmonary disease

CYP1A1: Cytochrome P450 1A1

CYP1B1: Cytochrome P450 1B1

DCM: Dichloromethane

DE: Diesel exhaust

DEP: Diesel exhaust particles

EOM: Extractable organic material

ES: Enrichment score

FDR: False discovery rate

GM-CSF: Granulocyte-macrophage colony-stimulating factor

GSH: Glutathione

GSEA: Gene set enrichment analysis

GSSG: Glutathione disulfide

HO-1: Heme oxygenase-1

IFN-γ: Interferon-γ

IgE: Immunoglobulin E

IgG1: Immunoglobulin G1

IL: Interleukin

iNOS: Inducible nitric oxide synthase

LDH: Lactate dehydrogenase

MAPK: Mitogen-activated protein kinase

MCP: Monocyte chemoattractant protein

MDC: Macrophage-derived chemokine

MIA: Microalbumin

MIP-2: Macrophage inflammatory protein-2

N-DEP: NIST DEP

NAG: N-acetyl-B-D-glucosaminidase

NES: Normalized enrichment score

NF-κB: Nuclear factor-κB

NIST: National institute of standard technology

NO: Nitric oxide

NO_2: Nitrogen dioxide

OVA: Ovalbumin

PAH: Polycyclic aromatic hydrocarbon

PM: Particulate matter

ROS: Reactive oxygen species

SO_2: Sulfur dioxide

T_H: T helper

TARC: Thymus and activation-regulated chemokine

TGF: Transforming growth factor

Toll-like receptor: TLR

TNFα: Tumor necrosis factor α

Treg: Regulatory T cells

Chapter 1

Introduction

1.1 Particulate Air Pollution

Epidemiological studies have demonstrated that exposure to ambient air particulate matter (PM) is positively associated with increases in mortality and morbidity due to respiratory illness [1-4]. While ambient PM can originate from natural sources such as volcanoes, forest fires, dust storms, and sea spray, a significant portion is generated from a variety of anthropogenic activity. These types of activities include agricultural operations, industrial processes, combustion of wood and fossil fuels, construction and demolition activities, and vehicle emissions. Recognizing the detrimental respiratory as well as cancer and cardiovascular health effects of PM, through the Clean Air Act initiative, the Environmental Protection Agency (EPA) set National Ambient Air Quality Standards (NAAQS) regulating PM along with five other criteria pollutants. The 2006 revised standards limits particles with a mass median aerodynamic diameter (MMAD) of < 2.5 µm (PM2.5, fine) and those which are smaller than 10 µm but larger than 2.5 (PM10, coarse). The current 24-hour exposure standards are 35 $\mu g/m^3$ for PM2.5 and 150 $\mu g/m^3$ for PM10. The annual fine particle exposure standard is 15 $\mu g/m^3$ and no annual PM10 exposure limit exists. In addition to PM10 and PM2.5 there is also PM0.1 (ultra-fine). These are generally defined as having an MMAD < 0.1 µm and are not directly regulated by the NAAQS per se because they contribute very little mass they are indirectly regulated through their presence in the PM2.5 and PM10 fractions [5].

Coarse particles, consisting of inorganic minerals from wind erosion of crustal material (Al, Si, Ca, Fe, Ti), road dust (brake linings, tire residue), and bioaerosols (pollen, mold spores) [6], mainly deposit in the upper airways where they are removed by the body's mucociliary clearance system resulting mainly in gastrointestinal exposure and

have been shown to induce pulmonary inflammation in rodents [7, 8]. Fine and ultra-fine particles, generated in combustion or formed from gases, can be more toxic to the lower airways because they are more readily inhaled [9], can reach the alveoli in a higher proportion than coarse where no cilia are present, and exhibit long atmospheric residence time [10].

In vitro and *in vivo* toxicology studies have demonstrated that ultra-fine carbon and titanium dioxide particles are more toxic than larger particles with the same chemistry with respect to pro-inflammatory and oxidative stress endpoints in A549 human epithelial cells and a slower pulmonary clearance rate and greater inflammation in rats [9, 11] These effects have been attributed to the ultra-fine particles having a larger surface area and the ability to penetrate epithelial cells more readily than their larger counterparts. This in turn leads to a greater generation of reactive oxygen species on the surface [12], as well as better ability to activate signal transduction pathways important in inflammation, injury, and repair [13]. Researchers have used diesel exhaust particles (DEP) as a model PM pollutant to understand the impact of PM on the genesis and exacerbation of asthma. Several groups have demonstrated that DEP can act as an adjuvant when combined with an allergen, resulting in enhanced IgE antibody production, increased allergic inflammation and airway hyperresponsiveness (AHR) in mice [14-16].

1.2 Diesel Exhaust Characteristics

Diesel Exhaust (DE) is produced after combustion of diesel fuel in compression-ignition on road engines such as buses, trucks, and other heavy industrial transport

vehicles, as well as numerous off-road sources such as generators. It is a common contaminant of ambient air in urban and rural environments. DE comprises of particles and gases representing thousands of different chemical substances, of which at least 40 are considered to be hazardous air pollutants by the Environmental Protection Agency (EPA). The chemical compounds in DE depend on the type and age of the engine, type of fuel and additives, type of emission control equipment, how the engine is maintained and operated, and after treatment.

Although emissions have been reduced by improved control technologies, the use of diesel engines has continued to increase as indicated by EPA trends reports of vehicle miles traveled (http://www.epa.gov/OMS/fetrends.htm). DE contains approximately 20-100 times more particles (DEP) than gasoline exhaust. About 90% of these particles are <1 µm and therefore are readily respirable and deposit in the lower respiratory tract. The particles consist of a carbon sphere surrounded by metals (i.e. iron, copper, chromium, and nickel) and thousands of organic constituents including various absorbed hydrocarbons such as aldehydes, benzene, nitrosamines, quinones, polycyclic aromatic hydrocarbons (PAHs; including phenanthrene, fluorenes, naphthalenes, pyrenes, fluoranthrenes), and nitro-PAHs. The vapor and gaseous phase includes olefins (1,3-butadiene), aromatics (benzene, ethylbenzene, toluene, and xylenes), alkanes, and aldehydes (formaldehyde and acetaldehyde) as well as oxides of nitrogen, carbon, and sulfur. After being emitted, diesel particles undergo “atmospheric ageing” (oxidation, nitration, or other chemical and physical changes) [17]. The atmospheric lifetime of the various compounds found in diesel exhaust is dependent on the particle size and can vary from hours to days. Particles smaller than 1 µm can remain in the atmosphere for up to 15

days and maybe transported over long distances.

Human exposure to DEP ranges from 1.5 to 1700 $\mu g/m^3$ depending upon proximity to source(s), ventilation rates, and dilution into surrounding air. The California Air Resources Board reported the average total DEP exposure for Californians to be 1.5 $\mu g/m^3$. While the ambient DEP concentrations nationwide are relatively low, levels of DEP in certain urban areas can be considerably higher. In 1996, PM2.5 was measured as a surrogate for DEP and found to be 37-47 $\mu g/m^3$ at an intersection in the Harlem section of New York City [18]. Concentrations as high as 130 $\mu g/m^3$ in a car following an urban transit bus making numerous stops were detected using real-time aethalometer carbon black measurements as an indicator of DEP concentrations [19]. Occupational exposure can be even greater. The Health Effects Institute estimates average exposure over an 8 hr work day to be up to 100 $\mu g/m^3$ for trucking and transportation occupations, 17-134 $\mu g/m^3$ for railroad locomotive shop workers, and 100-1700 $\mu g/m^3$ for underground miners in proximity to diesel engines [20]. Those most likely to be exposed to diesel exhaust in occupational environments include mine workers, tunnel and loading dock workers, auto mechanics, toll booth collectors, truck and forklift drivers and others who work in areas where diesel powered vehicles are used, stored and maintained.

Part of the difficulty in studying the health effects of DEP is the heterogeneous characteristic of the mixture. The chemical composition of DEP has been shown to alter its biological activity [21]. A study published in our laboratory compared the toxic effects of two DEP samples, one from an automobile DEP (A-DEP) and another from the National Institute of Standards Technology Standard Reference Material 2975 generated from a forklift engine (N-DEP). The chemical properties of these samples were

dramatically different. On a mass basis, A-DEP had more extractable organic material while the N-DEP was composed mostly of elemental carbon. Intratracheal instillation of A-DEP in mice induced macrophage influx and stimulated an increase in cytokines interleukin (IL) -5, IL-6, TNFα, and MIP-2 while N-DEP enhanced neutrophil influx and IL-6. These effects provided evidence for our hypothesis (discussed in more detail later) that DEP with different chemical profiles can have varied adjuvant potential in an allergic mouse model.

1.3 Increased Prevalence of Asthma

There has been a marked increase in the prevalence of allergic diseases such as asthma in industrialized countries over the last quarter of the 20th century [22, 23] with a trend toward more developed and westernized countries having higher asthma prevalence. In the United States, allergic diseases affect 17% of the population and are the sixth leading cause of chronic illness [24]. An estimated 22 million Americans suffer from asthma, 6.5 million of which are children. According to National Health Interview Surveys, the asthma rate among US children more than doubled from 3.6% in 1980 to 8.9% in 2005. The factors driving this increase are still not fully understood.

Epidemiology studies have suggested that socioeconomic and ethnicity are risk factors for asthma development. Asthma prevalence is higher among families with lower incomes. Racial disparities are also evident in asthma prevalence. Respectively, American Indian or Alaska Native and black children have 25% and 60%, higher prevalence rates than white children. Social and environmental risk factors are highlighted by higher asthma rates in US-born Mexican populations than non-US born

Mexicans living in the US [25].

Asthma and allergies have a strong hereditary and hence genetic component. Children with one parent who has asthma are three to six times more likely to develop the disease, and children with two parents with asthma are 10 times more at risk than those children whose parents do not have asthma. Over 100 genes have been associated with asthma , 25 of which are associated with asthma in six or more separate populations studies [26]. Many of these genes such as IL-4, STAT6, IL-13, TNFα, TGF-β, are related to the immune system or to modulating inflammation. While this does not prove a genetic cause it certainly reflects a modest effect of these genes on risk. Nevertheless, the rapid increase in the prevalence of asthma in the last decades is unlikely to be caused by genetic changes alone.

Environmental factors appear to play a role. Many researchers have contributed the rise in asthma to our "western" lifestyle suggesting our diet [27], cigarette smoke [28], and inhalation of air pollution from indoor and outdoor sources [22, 29-31]. There is sufficient epidemiologic and animal data to suggest that some synergism exists between allergen exposure and exposure to air pollutants (primarily outdoor) in the induction of asthma in children and possibly adults [32, 33].While a combination of factors mentioned probably contribute to the increased allergy prevalence among individuals living in urbanized areas, this dissertation will focus on the effects of diesel exhaust and diesel exhaust particles on the development of allergic airway disease.

1.4 Allergic Asthma

Asthma is a chronic inflammatory disease of the airways, characterized by

reversible airway obstruction and accumulation of lymphocytes and eosinophils in the lung. It can be divided into two sub-types, allergic and non-allergic asthma. Of the nearly 20 million Americans suffering from asthma, greater than 60% have allergic asthma [34]. Allergic asthma is a T_H2 lymphocyte mediated inflammatory disease which features high serum levels of allergen-specific IgE, and upon allergen challenge, results in airway eosinophilia, excess mucus production, and bronchoconstriction.

Allergy and allergic diseases like asthma normally develops in two phases. The first phase (induction) is induced when the susceptible individual initially encounters the allergen. A primary immune response is mounted that results in a state of heightened responsiveness to that particular antigen (specific sensitization). Subsequent exposures (challenge) of the now sensitized individual to the allergen evokes a more vigorous and accelerated secondary immune response. Overt outward adverse health effects are normally first recognized during this secondary immune response against the allergen and these symptoms present themselves as local tissue disruption and inflammation.

With allergic asthma, symptoms are triggered by an allergic reaction after inhalation of common allergens, such as cockroach and dust mite feces, animal dander, molds, and seasonal pollens. These environmental sensitizers have been ubiquitous as long as people have lived in the world, but in the last 50-100 years a growing and significant percentage of the population (particularly in developed countries) have developed an allergic response to these proteins [35]. This short timeframe suggests that environmental pollutant exposures are contributing to this increase as opposed to a significant change in the gene pool. Changes in lifestyle including alterations in diet, activity patterns, medication use, housing conditions, and possibly other factors have

undoubtedly had an impact on the sensitization rate. Epidemiology studies have also shown that increases in ambient particle matter (PM) are correlated with increased hospitalizations due to respiratory illness including exacerbation of pre-existing asthma [3, 36, 37]. Furthermore, there is mounting evidence linking air pollution with an increased risk of developing asthma [38-40].

1.5 Molecular and Cellular Basis for the Inflammatory Events in Asthma

1.5.1 T helper 1 (T_H1) and T helper 2 (T_H2) lymphocytes

In 1986, the existence of two CD4+ T_H cell subsets was discovered in mice, and they were designated T_H1 and T_H2 [41]. Their identification has greatly improved understanding of the regulation of immune effector functions. These T_H subsets are defined by the patterns of cytokines that they produce. T_H1 cells secrete Interleukin (IL)-2, IFNγ, IL-12 while T_H2 secrete IL-4, IL-5, IL-6, IL-10, and IL-13. The differences in the cytokines secreted by these cell types determine their biological function. T_H1 subset is responsible for many cell-mediated functions such as delayed-type hypersensitivity (DTH) and for the production of opsonization-promoting IgG antibodies. T_H2 cells stimulate eosinophil activation and differentiation, are more efficient B cell helpers, and promote the production of IgE and non-complement-activating IgG antibodies (in mice, IgG1). In addition, they cross-regulate by producing mutually antagonistic cytokines. For example, IFN-γ preferentially inhibits proliferation of the T_H2 subset, and IL-4 and IL-10 down-regulate secretion of IL-12. A shift in the predominant T cell population from T_H1 type to the T_H2 type has been associated with asthma [42] (Figure 1.1)

1.5.2 Eosinophils

Airway eosinophilic inflammation is a classical characteristic feature of allergic asthma. Eosinophils are regarded as effector cells responsible for much of the pathophysiology of asthma, playing a major role in the onset and maintenance of bronchial inflammation and tissue injury. They are known to be an indirect marker of asthmatic airway inflammation, the severity of which has been shown to be dependent on eosinophil accumulation and activation within the airways [43-45]

A series of events occurs, directed by T_H2 cells, to cause eosinophils to arrive in the airway and promote obstruction, injury, and bronchial hyperresponsiveness. These steps include proliferation and differentiation of eosinophils in the bone marrow, migration through the vascular endothelium into the lung tissue, and activation and release of toxic granules.

Cytokines such as granulocyte monocyte colony stimulating factor (GM-CSF), IL-3, and IL-5 signal bone marrow progenitor cells to proliferate, differentiate into eosinophils, and release the cells into circulation [46]. IL-5 is the most selective for eosinophil differentiation, proliferation, and maturation within the bone marrow, as IL-3 and GM-CSF can act on various other cell types [47].

Eosinophil recruitment from the circulation into the lung tissue results from the complex mechanisms that involve vascular adhesion molecules, extracellular matrix proteins, and chemokines. The initial reversible tethering and rolling of eosinophils on the endothelium results from the formation of numerous weak reversible bonds between integrins expressed on eosinophils and endothelial adhesion molecules, such as very late activation antigen-4 (VLA-4) and vascular cell adhesion molecule-1 (VCAM-1),

respectively. The tethering and rolling of eosinophils is followed by chemokine mediated stable integrin-adhesion binding which firmly tethers the cells to the endothelium[48]. Integrinβ2 (Itgβ2) binds to intercellular adhesion molecule-1 (ICAM-1) on the endothelium resulting in firm cellular arrest that is critical for transmigration. Binding of CC chemokines (eotaxin, eotaxin-2, RANTES, and MCP-3) to their receptors (CCR3 and CCR5) on eosinophils leads to the formation and retraction of lamellipodia, which gives the cells “arms” and “feet” to migrate into the tissue. Transendothelial migration also requires the function of matrix metalloprotease-9 (MMP-9) which degrades membrane fibers, allowing eosinophils to penetrate the basement membrane [49].

Once in the tissue, eosinophils can become activated and express a number of receptors for cytokines, as well as chemokines, immunoglobulins, and complement. The cytokines IL-3, IL-5, and GM-CSF prolong eosinophil survival, increase free oxygen radical production, and induce eosinophil degranulation.

The proteins stored in eosinophil granules are major basic protein (MBP) eosinophil cationic protein (ECP), eosinophil peroxidase (EPO) and eosinophil derived neurotoxin (EDN). When released these granules directly cause mucosal injury and contribute to the disturbances in lung physiology. In addition, eosinophils generate lipid mediators, including platelet-activating factor, leukotrienes B_4 and C_4, as well as cytokines and chemokines, such as IL-5 and GM-CSF, which amplify the inflammatory response by recruiting and activating leukocytes and epithelial cells [50, 51].

1.5.3 IgE and IgG1 antibodies

IgE antibodies play a major role in allergy and asthma. These antibodies are primarily synthesized in the lymphoid tissue of the respiratory and gastrointestinal tracts. The regulation of IgE production appears to be a function of T cells. T_H2 cytokines, in particular IL-4 and IL-13, stimulate B cells to switch to producing IgE antibodies [52]. Co-stimulatory interaction between CD40 ligand on the T cell surface and CD40 on the B cell surface is also essential for antibody class switching.

IL-4 further enhances IgE-mediated immune responses by up-regulation IgE receptors on the cell surface: the low-affinity IgE receptor (FcεRII or CD23) on B cells and mononuclear cells and the high-affinity IgE receptor (FcεRI) on mast cells and basophils[53]. Once an individual has become sensitized, the specific antigen binds to the IgE-Fc receptor complex and the cells release mediators such as histamine and secrete IL-4 [54].

In the mouse, mast cell activation induced by the interaction of IgE and mast cell FcεRI receptor is well characterized, however, the interaction of IgG1 and mast cell FcγRIII receptor can also induce mast cell activation and degranulation. Indeed, loss of the FcεRI alpha chain results in an enhancement of FcγRIII mast cell degranulation. It is important to note that while T_H2 cells induce IgG1 and IgE in mice, in humans T_H2 cells induce IgE and IgG4.

1.5.4 Interleukin 4 (IL-4)

IL-4 is a key cytokine in the development of allergic inflammation. Not only is it associated with induction of the ε isotype switch and secretion of IgE by B cells [52], but it also induces expression of vascular cell adhesion molecule-1 (VCAM-1), promotion of

eosinophil transmigration across endothelium, mucus secretion, and differentiation of T helper type 2 lymphocytes leading to cytokine release.

IL-4 contributes to airway obstruction in asthma through the induction of mucin gene expression and the hypersecretion of mucus in mice and human cell lines [55], and increases the expression of eotaxin and other inflammatory cytokines from human lung fibroblasts that might contribute to inflammation and lung remodeling in chronic asthma [56].

An essential biological activity of IL-4 in the development of allergic inflammation is the ability to induce differentiation of naïve T helper type 0 (T_H0) lymphocytes into T_H2 lymphocytes [57, 58]. These T_H2 cells then proceed to secrete IL-4, IL-5, IL-10 and IL-13. The induction of T_H2-like lymphocytes is a unique biological activity of IL-4 because IL-4 receptors and not IL-13 receptors are expressed on T cells [59].

An important activity of IL-4 in promoting cellular inflammation in the asthmatic lung is the induction of vascular cell adhesion molecule (VCAM)-1 on vascular endothelium[60]. Through the interaction of VCAM-1, IL-4 is able to direct the migration of T lymphocytes, monocytes, basophils, and eosinophils to the site of inflammation. IL-4 also promotes eosinophilic inflammation by inducing eosinophil chemotaxis and activation through the increased expression of eotaxin. In addition, IL-4 is important in allergic immune responses owing to its ability to prevent apoptosis of T lymphocytes and eosinophils.

1.5.5 Interleukin 5 (IL-5)

The production of IL-5 by activated T cells is a key event in the induction of eosinophilic inflammation. Although activated T-helper cell populations are the main source of IL-5, secretion from other cell types (eosinophils, mast cells, $CD4^+$ and $CD8^+$ T cells) have been reported [61]. IL-5 is the primary cytokine involved in activation and survival of eosinophils and marked proliferation and maturation of eosinophil precursors [62]. Transgenic mice in which IL-5 is constitutively expressed show a profound and lifelong eosinophilia. IL-5 has also been shown to augment airway hyperresponsiveness in asthma[63].

1.5.6 Interleukin 13 (IL-13)

IL-13 is produced by activated T cells, B cells and mast cells. In the mouse, almost exclusively T_H2 clones express IL-13, however, in humans it can be expressed in both T_H1 and T_H2 cells [64]. IL-13 is a cytokine closely related to IL-4 and binds to IL-4Rα receptors [65]. It is present in increased amounts in asthmatic airways and has very similar biological activities to IL-4 [66, 67]. IgE production and the induction of VCAM-1 are activities shared with the related cytokine IL-4. In addition both cytokines inhibit transcription of IFNγ and both α and β chains of IL-12. Thus, IL-13 may (like IL-4) suppress the development of T_H1 cells through down-regulation of IFNγ and IL-12 production by monocytes, favoring the generation of T_H2 cells. There is a significant correlation between eosinophil BALF counts and levels of IL-13 in animal models of allergic asthma [68, 69]. Mice administered IL-13 exhibited goblet cell hyperplasia and mucus glycoprotein accumulation in the airways [70].

1.5.7 Interleukin 10 (IL-10)

IL-10 is another T_H2 cytokine, but its pathophysiological role in asthma has not been clearly elucidated. Some evidence suggests that IL-10 production is reduced in patients with asthma compared with nonasthmatic control subjects [71], and murine studies provide evidence that IL-10 suppresses development of eosinophilic inflammation in the airways. Robinson et al. [72] found IL-10 mRNA was increased in BALF cells in response to allergic sensitization and challenge.

Administration of recombinant IL-10 reduced allergen-induced eosinophilic airway inflammation but increased airway hyperreactivity [73]. IL-10-induced airway reactivity may be linked to release of histamine. IL-10 has been shown to increase murine mast cell and basophil proliferation, differentiation, and degranulation [74] and stimulate MCP-1 production [75, 76]. MCP-1 suppresses monocyte production of IL-12 and is a potent stimulator of histamine release. Depletion of MCP-1 has been shown to reduce airway reactivity without attenuating eosinophilia [77]. Therefore IL-10 may induce airway hyperreactivity through MCP-1 production.

1.5.8 Interleukin 1 (IL-1)

The major cellular sources of the pro-inflammatory cytokine IL-1 are monocytes, macrophages, neutrophils, eosinophils, mast cells, platelets, lymphocytes, NK cells, endothelial cells, and airway smooth muscle cells. Nakae *et al.* [78] reported IL-1 plays important roles in the development of AHR. AHR, OVA-specific T cell proliferation, IL-4 and IL-5 production by T cells, and IgG1 and IgE production by B cells were markedly reduced in IL-1 deficient mice compared with wild-type mice in an OVA-induced AHR

model. In addition, patients with symptomatic asthma showed increased levels of IL-1 in BAL fluid compared with patients with asymptomatic asthma [79]. IL-1 increased the expression of ICAM-1, E-selectin, and VCAM-1 in human bronchial tissue [80].

1.5.9 Tumor necrosis factor α (TNFα)

TNFα is another pro-inflammatory cytokine that is present abundantly in asthmatic airways. It is produced by many cells including macrophages, T cells, mast cells, and epithelial cells, but the principal source is the macrophage. Like IL-1, TNFα also increased the expression of ICAM-1, E-selectin, and VCAM-1 in human bronchial tissue [80]. There is evidence that IgE triggering in sensitized lungs leads to increased expression in epithelial cells in both rat and human [81]. TNFα is present in the BAL fluid of asthmatic patients[82]. It is reported that TNFα is also released from alveolar macrophages of asthmatic patients after allergen challenge [83].

1.5.10 Interleukin 6 (IL-6)

The pro-inflammatory cytokine IL-6 is secreted by monocytes/ macrophages, T cells, B cells, fibroblasts, lung epithelial, and endothelial cells [84, 85]. IL-1 or TGFβ can increase IL-6 release from airway smooth muscle cells and fibroblasts [86, 87]. IgE-dependent triggering stimulates the secretion of IL-6 from both blood monocytes and alveolar macrophages *in vitro* [88] Increased production of IL-6 was observed in the BALF of patients with allergic asthma at baseline compared to control subjects and a further increase was measured after challenge[89, 90].

1.5.11 Granulocyte monocyte colony stimulating factor (GM-CSF)

GM-CSF is a pleiotropic cytokine that can stimulate and regulate growth, proliferation, maturation, and function of hematopoietic cells. Several airway cells produce GM-CSF, including macrophages, eosinophils, T-cells, fibroblast, endothelial cells, airway smooth muscle cell, and epithelial cells [91]. Elevated levels of GM-CSF have been well described in BALF, endobronchial biopsy, and sputum samples from asthmatics [92-94]. Elevated levels of GM-CSF, largely derived from epithelial cells, have been demonstrated to increase eosinophil activation and survival in asthmatics [95-97]. GM-CSF not only influences eosinophils chemoattraction and activation but also participates in the etiology of bronchial hyperresponsiveness in mild asthma. Dendritic cells have been demonstrated to be essential for presenting inhaled Ag to previously primed T_H2 cells, and thus for chronic eosinophilic airway inflammation [98, 99]. GM-CSF is a critical factor for dendritic cell maturation, increased expression of accessory molecules such as ICAM-1, B7-1 (CD80), and B7-2 (CD86), and dendritic cell recruitment into the airway in murine models of asthma [99-101]

1.5.12 Monocyte chemoattractant protein 1 (MCP1/CCL2)

MCP-1 is a member of the cc family of chemokines. It was initially identified as a monocyte-specific chemoattractant, but now has also been shown to attract activated T cells, NK cells, and basophils. MCP-1 displays immunoregulatory functions and may be involved in T_H2 differentiation. MCP-1 modulates the differentiation of monocytes into DCs. DCs generated in the presence of MCP-1 display a markedly reduced production of IL-12 and therefore may inhibit T_H1 cell development [102].

1.5.13 Thymus and activation-regulated chemokine (TARC/CCL17) and macrophage-derived chemokine (MDC/CCL22)

TARC and MDC are CC chemokines which have recently been reported to play an important role in allergic airway disease. TARC and MDC are produced by DCs amongst other pulmonary cells and bind to the CC chemokine receptor 4 (CCR4), which is found on CD4+ T_H2 cells. Upon allergen challenge, bronchial epithelial cells release the cytokine TSLP which in turn stimulates dendritic cells to produce TARC and MDC, recruiting T_H2 cells to the airways and ultimately perpetuating the disease [103, 104].

Studies have shown TARC and MDC are up-regulated in the airways and serum of human subjects with asthma after allergen challenge [105]. A mouse model of allergic airway inflammation has also shown antibody treatment against TARC can inhibit antigen-induced eosinophilia, T_H2 cytokines, and bronchial hyperresponsiveness [105].

1.5.14 Transforming growth factor-β (TGF-β)

TGF-β is a profibrotic cytokine which stimulates fibroblasts to promote the synthesis and secretion of many proteins of the extracellular matrix [106, 107]. Due to its function in promoting growth and repair, TGF-β is thought to play an important role at sites of wound healing and tissue remodeling and may play a role in the fibrotic changes occurring within asthmatic airways [108]. In addition, TGF-β is an immunomodulatory cytokine and a potent chemoattractant for several cell types including monocytes, fibroblasts, and mast cells [109-111]. Major sources of TGF-β are eosinophils, neutrophils, airway smooth muscle cells, fibroblasts, epithelial cells, and mast cells [112]. Expression of TGF-β mRNA and protein production by eosinophils in asthmatic subjects

has been correlated with the severity of asthma and the degree of subepithelial fibrosis [108].

1.6 Effect of Particles on Allergic Immune Responses

There is epidemiological evidence that certain air pollutants such as DE are associated with the development of allergic airway disease [113-117], and recent associations have been specifically linked to proximity to highways [118-120]. While these effects need to be confirmed with better personal exposure information, investigations in animals and in a few human clinical studies have reported that air pollutants may indeed contribute to the increased incidence of allergic disease and asthma [121-126].

Animal experiments have demonstrated that many types of particles including ambient PM, DEP, residual oil fly ash (ROFA), carbon black particles (CB), and polystyrene particles (PSP) can act as immunologic adjuvants when administered with an antigen via intraperitoneal, intranasal, intratracheal, and inhalation routes of exposure [127-133]. In most cases the particles alone cause inflammation, but when administered during sensitization, they also promote the development of allergic immune responses (in the form of increased IgE antibody, T_H2 cytokines, and airway hyperresponsiveness). Upon repeated challenge with antigen, these animals exhibit increased severity of allergic type disease (pulmonary eosinophils, airway hyperresponsiveness, increased mucus production, etc.) compared to control animals which received antigen exposure and vehicle control in the place of the pollutant.

The relationship between particle exposure and increased allergic symptoms has

also been examined in limited human studies with both allergic and non-allergic subjects. Individuals with allergic rhinitis and mild asthma exposed intranasally to 0.3 mg of DEP, generated from an automobile, had significantly enhanced IgE antibody production in the nasal mucosa [134]. In a later study, atopic subjects given DEP prior to nasal immunization with a neoantigen, keyhole limpet hemocyanin (KLH), produced antigen-specific IgG, IgA, and IgE as well as IL-4 in nasal lavage fluid [135], while subjects given KLH alone only produced IgG and IgA, indicating that the DEP acted as an adjuvant to promote primary allergic sensitization.

While these specific studies used a diesel particle highly enriched in organic constituents, another body of literature also shows that the carbonaceous core of the diesel as well as more inert particles like carbon black and polystyrene particles (PSP) can similarly induce adjuvant-like effects in rodents [136]. Rats instilled with 100 µg of fine (FCB) or ultrafine carbon black (UFCB) had some measure of allergic adjuvancy compared to DEP [137], while the adjuvant effects of PSP were directly related to the pro-inflammatory potential dictated by an increase in the surface area of ultrafine versus fine. In contrast, instillation of DEP, "representative of heavy duty diesel engine particulate emissions" according to the National Institute of Standards and Technology, did not induce inflammatory or allergic responses in healthy or asthmatic subjects, suggesting chemistry plays an important role in the response [138].

1.7 Dendritic Cells

Dendritic cells (DCs) are the most important antigen presenting cells in the lung and are located throughout the basement membrane of the airways, forming long

extensions or dendrites to sample the lumen on a continual basis. Antigen uptake during the presence of a "danger signal" (e.g. damage-associated molecular patterns; DAMPs) causes DC to process the antigen into the MHC complex, acquire a mature phenotype expressing co-stimulatory molecules (CD80/86), migrate to the draining lymph node, and present the antigen to naïve $CD4^+$ T cells. This "danger signal" could be induced by an allergen, microbial contaminant, or cytokines such as thymic stromal lymphopoietin (TSLP). Depending on the signal type, maturation status, and the presence of other mediators, dendritic cells can preferentially polarize T lymphocytes to a T_H1 or T_H2 response.

Recent evidence shows airway DC populations are important in determining the induction of pulmonary immunity or tolerance. Two important subtypes of DCs are myeloid DC (mDC) and plasmacytoid DC (pDC). Both of these subtypes endocytose antigen in the lung and present processed peptides to naïve T cells in the draining lymph node. Intratracheal instillation of OVA exposed bone-marrow-derived mDCs are sufficient to induce T_H2 sensitization in mice, however pDCs have been shown to down-regulate this effect [139, 140]. Depletion of pDCs during inhalation of protein allergens in mice results in the development of asthmatic symptoms such as airway eosinophilia, goblet cell hyperplasia, and T_H2 cell cytokine production [141], while adoptive transfer of mDCs before sensitization results in an allergic phenotype [141]. It has also been shown that airway pDC are more abundant compared to mDC in the draining lymph node of tolerized mice compared to the profile seen in actively sensitized animals. Airway mDCs play a central role not only in initiating specific T_H2 cell immune responses leading to asthmatic symptoms, but also in restimulating effector T cells during ongoing

airway inflammation and antigen challenge [142].

1.8 Phase I and Phase II Metabolism

The lung is a target organ for the toxicity of inhaled compounds (xenobiotics). The lung has the capability of metabolizing such compounds with the aim of reducing their potential toxicity. The metabolism of xenobiotics is often divided into two groups, called phase I and phase II. DEP or CB has been shown to significantly alter both phase I and phase II enzyme expression and activity in the lungs of rats [143].

Phase I introduces reactive and polar groups through a variety of enzymes. These reactions involve hydrolysis, reduction, and oxidation. Phase II reactions include glucuronidation, sulfonation, acetylation, methylation, and glutathione and amino acid conjugation. These reactions generally act in concert to detoxify xenobiotics and remove them from cells. In some instances, the biotransformation of a given compound can result in the generation of more reactive, and frequently more toxic, metabolites. Polycyclic aromatic hydrocarbons (PAHs) or N-nitrosamines are an example of pro-carcinogens which can be biotransformed into more reactive intermediates that more easily form DNA adducts than the parent compound.

Diesel exhaust emissions contains fine and ultra-fine PM composed of carbon core surrounded by various adsorbed organic compounds, including PAHs, quinones, and nitro-PAHs [144]. Many of these organic compounds associated with diesel exhaust particles (DEP) are suspected to be mutagenic and carcinogenic [145]. Pathways involved in phase I metabolic activation of these compounds include formation of diol epoxides catalyzed by several cytochrome P450s [146-148], radical cations catalyzed by P450

peroxidases [149, 150], and reactive and redox active o-quinones catalyzed by dihydrodiol dehydrogenases (DD) [151, 152].

In phase I, a variety of enzymes introduce reactive and polar groups into their substrates such as -OH, -NH2, -SH, or -COOH. One of the most common modifications is hydroxylation catalysed by the cytochrome P-450-dependent mixed-function oxidase system. Cytochrome P450 monooxygenases (CYP) play an important role in the defense against inhaled toxicants, and are expressed in bronchial and bronchiolar epithelium, Clara cells, type II pneumocytes, and alveolar macrophages. CYP1A1, CYP1B1, CYP2A6, CYP2B6, CYP2E1, CYP2Cs, CYP2D, CYP3A4, CYP3A5 and CYP3A5 mRNA expression has been detected in human lung cells. Exposure of rats to DEP or carbon black (CB) has been shown to induce changes in CYP1A1 and CYP2B1 protein levels in the lung. Recent studies have demonstrated that these enzymes are primarily responsible for the generation of intracellular ROS induced by DEP exposure [153] suggesting that CYP enzymes may contribute to both the inflammatory and genotoxic mechanisms of DEP carcinogensis.

A widely accepted pathway of PAH activation involves formation of electrophilic diol epoxides. For benzo[a]pyrene (B[a]P), a representative PAH, are initially converted by CYP P450 to a variety of arene oxides that can bind covalently to DNA. One metabolite, benzo[a]pyrene-4,5-oxide is rapidly inactivitated by epoxide hydrolase. However, benzo[a]pyrene-7,8-dihydrodiol-9,10-oxide is not a substrate for epoxide hydrolase and is highly mutagenic to mammalian cells.

A second pathway of PAH activation involves the formation of radical cations catalyzed by elevated levels of P450 peroxidase. The radical cations arise from one-

electron oxidation at C6 on benzo[a]pyrene [149, 154]. The radical cations form predominantly depurinating adducts. PAH-derived DNA adducts, which may play a role in DEP-mediated mutagenicity and carcinogenicity, were found in rats after a short-term (12 weeks) exposure to DEP [155]. Elevated levels of PAH-derived DNA adducts have also been observed in white blood cells of humans following DEP exposure [156].

Quinones can be reduced by two- or one-electron reduction to the hydroquinone or semiquinone form. Flavin-dependent quinone reductases and NAD(P)H quinone oxidoreductase 1 (NQO1) reduce quinones, via a two-electron reduction, to its hydroquinone form which can then be conjugated with glutathione or glucuronic acid and are rapidly excreted. The second pathway of quinone reduction is catalyzed by NAD(P)H-cytochrome P450 reductase, microsomal NADH-cytochrome b5 reductase, or mitochondrial NADH ubiquinone oxidoreductase, and results in the formation of the extremely unstable semiquinone radicals which subsequently undergo redox cycling, leading to the production of highly reactive oxygen species (ROS) in the presence of molecular oxygen. These reactive compounds induce oxidative damage and, consequently, tissue degeneration, and apoptotic cell death [60].

The phase II enzymes, which include glutathione-S-transferases (GST), epoxide hydrolases, aryl sulfotransferases, and UDP-glucuronyltransferases, conjugate the activated xenobiotic metabolites with glutathione (GSH), glucuronides, sulfate ester, or amino acid derivatives to produce polar, readily excretable compounds. The induction of phase II enzymes has been shown to protect the lung from oxidative injury [157]. The GSTs, for example play a critical role in providing protection against electrophiles and products of oxidative stress. These enzymes facilitate the conjugation of glutathione with,

and subsequent elimination of, the electrophilic compounds including quinones and epoxides.

1.9 Hierarchical Stress Response

The PM-induced oxidative stress response has been proposed to be a hierarchical event, which is characterized by the induction of antioxidant and phase II metabolism enzymes at lower tiers of oxidative stress and by pro-inflammatory followed by cytotoxic responses at higher levels of oxidative stress [158, 159] (Figure 1.2).

In this proposed response, the first tier of oxidative stress, epithelial cells and macrophages respond by increasing expression of antioxidant and phase I and phase II metabolizing enzymes such as superoxide dismutase, catalase, glutathione peroxidase, glutathione reductase, glutathione S-transferase, NADPH quinone oxidoreductase, heme oxygenase 1 (HO-1). The transcription of these enzymes is mediated in part by the transcription factor nuclear regulatory factor 2 (Nrf2) which binds to the antioxidant response element (ARE) in the promoter of these genes [160].

If the antioxidant and detoxification pathways fail to neutralize the oxidative stress response, pro-inflammatory cytokines are produced (tier 2). DEP and DEP extracts have been shown to activate the mitogen-activated protein (MAP) kinase and NFκB signaling cascades in epithelial cells and macrophages [161, 162]. Activation of these pathways leads to the production of IL-4, IL-5, IL-10, IL-13, TNFα, MCP-1, GM-CSF, ICAM-1, and VCAM-1 [163]. These cytokines, chemokines, and adhesion molecules play important roles in the pathogenesis of asthma and therefore it has been suggested to be the mechanism by which DEP exerts its adjuvant effects[125]. In addition to the

original oxidative stress insult, these signaling molecules lead to inflammation and further oxidative stress.

The third tier of oxidative stress involves mitochondrial perturbation, which can lead to apoptosis, apoptosis-necrosis, and superoxide generation [164]. Reactive species generated from phase I metabolism can disrupt the mitochondrial transmembrane potential by interfering with the electron transport chain. Uncoupling of oxidative phosphorylation interrupts ATP production which decreases mitochondrial membrane potential leading ultimately to apoptosis and necrosis. The quinone-enriched polar fraction of DEP extract decreased of membrane potential and mitochondrial membrane mass, and induced of apoptosis in RAW 264.7 cells [165]. In addition, ultra-fine particles have been observed lodged inside the damaged mitochondria suggesting direct mitochondrial damage [166].

1.10 Genomic Analysis

The human genome project, along with the sequencing of DNA from many other organisms, has led to a dramatic increase in knowledge about gene structure and function over the last two decades. Through this knowledge and the development of new technologies for monitoring genetic sequences, genetic variation, and global gene expression analysis, the field of genomics was created. Broadly speaking genomics is the study of how genes interact and influence biological pathways, networks, and cellular physiology [167, 168]. Toxicogenomics, a new sub-discipline in the field of toxicology, takes this one step farther by examining how environmental and xenobiotic exposures alter these interactions.

Toxicogenomics, combining conventional toxicological research and functional genomics, is based on the fact that most relevant toxicological effects of a compound also alter gene expression, directly or indirectly. Toxicogenomics data offers additional insights into cellular mechanisms of toxicity beyond those derived from traditional toxicological endpoints based on whole organ pathology or survival curves. Molecular profiling of toxicants through microarray technology enhances our basic understanding of some of the underlying mechanisms that cause toxicity.

Several experimental studies have employed microarray technology to study the biological effects of DEP exposures. Arrays containing a limited number of genes were used to study gene expression changes *in vivo* in rat lung. Reynolds and Richards [169] assessed the effects of intranasal instillation of DEP in rats with rat stress arrays. 10 genes out of the 207 stress-related rat genes tested, were up-regulated. These included mitogen-activated protein kinase 2, calcium-binding protein 2, 94 kDa glucose-regulated protein, G1/S-specific cyclin D1, prothymosin-alpha, MAP kinase kinase 5, M-phase inducer phosphatase 2, and nucleoside diphosphate kinase A, which are involved in the lung's damage response. Sato *et al.* [170]exposed rats to DE and surveyed cDNA expression arrays with only 588 rat cDNAs to identify genes that may be involved in DE-induced carcinogenesis. Six genes, heat-shock protein 47, superoxide dismutase, proliferating cell nuclear antigen, retinoblastoma, A-raf, and K-ras, were up-regulated in the lungs of exposed rats.

In vitro microarray studies investigating the effects of DEP extract were also conducted. Koike *et al.* [171] investigated the effects of DEP extract on rat primary alveolar macrophages by examining changes in gene expression levels after a 6 hr

exposure using a toxicology array containing 450 rat cDNAs. Six genes, heme oxygenase (HO)-1 and -2, thioredoxin peroxidase 2, glutathione S-transferase P subunit, NAD(P)H dehydrogenase, and proliferating cell nuclear antigen (PCNA) were up-regulated. The first five are involved in antioxidant response while PCNA is involved in DNA damage repair. In addition, Koike *et al* [172] also exposed epithelial cells to DEP extract and evaluated gene expression changes using a 10,000 gene spotted array. The 6 hr DEP extract exposure increased expression of HO-1 and 50 other genes associated with drug metabolism, antioxidant response, cell cycle/proliferation/apoptosis, coagulation/fibrinolysis, and expressed sequence tags. In addition, 20 genes including type II transglutaminase (TGM-2), a regulator of coagulation, were decrease. The authors concluded HO-1 and TGM-2, genes with the highest differential responses, were good biomarkers for PM exposure.

A microarray study by Verheyen *et al.* [173] exposed human alveolar macrophages for 6 or 24 hrs to DEP. Oxidative metabolism, transcription regulation, transport, signal transduction, as well as cell cycle, DNA repair, and immune response genes were altered. CYP1B1, IL-1, thrombomodulin, integrinβ 7, similar to *S. cerevisiae* Sec6p, TNF receptor superfamily member 1B, leupaxin, CGI-41 protein, and BTG family member 2 genes were up-regulated at both time points. In addition peroxiredoxin 1, collagen type 1 receptor, protein kinase cAMP-dependent catalytic beta, butyrobetaine 2-oxoglutarate dioxygenase 1, CDC-like kinase 1, stathmin 1, and high-mobility group protein 2 were down-regulated at both time points. The authors concluded a multitude of biological processes are involved in DEP toxicity.

1.11 Scope of this Dissertation

The studies performed in this dissertation were focused on elucidating the mechanisms by which diesel exhaust (DE) enhances allergic lung disease. Chapter 2 evaluates the relative potency of three chemically distinct DE particles (DEP) on allergic airway inflammation in a murine ovalbumin (OVA) sensitization model. In addition to the post-challenge adjuvant effects, this chapter also assesses early immunologic changes in lungs after exposure to DEP. This chapter has been submitted to Toxicological Sciences for publication. In chapter 3 genomic microarray technology was utilized to identify altered pathways in the lung that were associated with the effects found in chapter 2. This chapter identifies common and unique pathways associated with exposure to the three DEP samples. Chapter 4 had two goals: 1) to investigate the adjuvant effects, post antigen challenge, of a short term inhalation exposure to moderate doses (500 and 2000 $\mu g/m^3$) of DE; and 2) to identify global gene changes associated with altered immune function. To this end immunologic endpoints were examined in mice acutely exposed by whole-body inhalation to moderate doses of DE in an ovalbumin mucosal sensitization model. In addition, microarray analysis was utilized to determine global lung gene expression changes associated with the effects of DE exposure alone and with antigen. The text and data in this chapter was published in April 2008 in Toxicological Sciences.

Figures

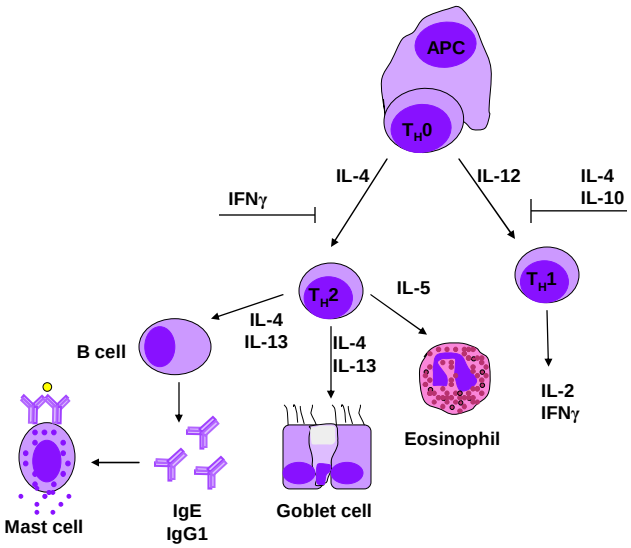

Figure 1.1 T_H2 differentiation and allergic sensitization. Antigen presenting cells (APC) present antigen to naïve T helper cells (T_H0) inducing activation and differentiation into a T_H2 or T_H1 subset, depending on the cytokines present. Differentiation into T_H1 cells occurs under the influence of IL-12. T_H1 cells produce high levels of IL-2 and IFNγ. T_H2 differentiation occurs under the influence of IL-4 and these cells produce IL-4, IL-5, and IL-13, which are cytokines known for their role in allergic airway inflammation. Both T_H cell sub-types are mutually antagonistic; IL-4 and IL-10 down-regulate IL-12 and IFNγ down-regulates IL-4.

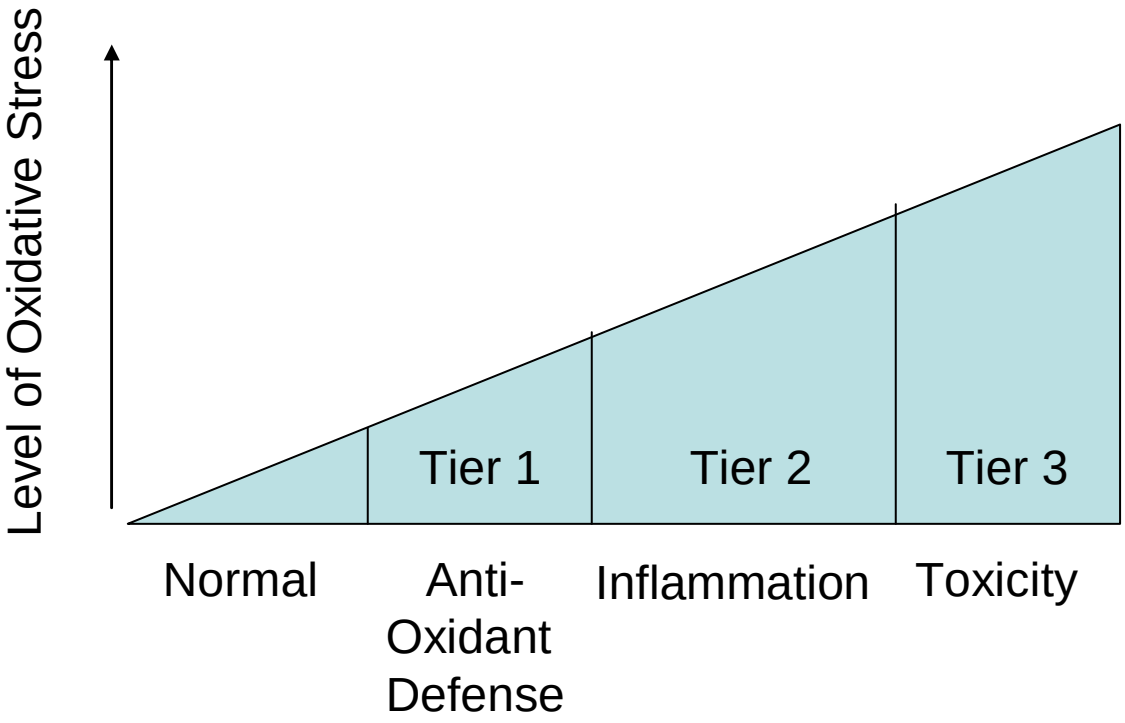

Figure 1.2 Hierarchical stress responses. At a low level of oxidative stress (Tier 1), antioxidant enzymes and phase I and II metabolizing enzymes are up-regulated to protect the cell from oxidative damage. At an intermediate level of oxidative (stress), the cells protective responses are overwhelmed and inflammation ensues. At a high level of oxidative stress (tier 3), the cell responds by inducing apoptosis or apoptosis/necrosis pathways. (Adopted from Li *et al.* [174, 175])

Chapter 2

Differential Potentiation of Allergic Lung Disease in Mice Exposed to Chemically Distinct Diesel Samples

Abstract

Numerous studies have demonstrated that diesel exhaust particles (DEP) potentiate allergic immune responses however the chemical components associated with this effect and the underlying mechanisms are not well understood. This study characterized the chemical composition of three chemically distinct DEP samples and compared post-sensitization and post-challenge inflammatory allergic phenotypes in BALB/c mice. Mice were instilled intranasally with saline or 150 µg of NIST (N-DEP), automobile (A-DEP), or compressor (C-DEP) with or without 20 µg of ovalbumin (OVA) on days 0 and 13, and were subsequently challenged with 20 µg of OVA on days 23, 26, and 29. Mice were necropsied 18 hrs post-sensitization and 18 and 48 hrs post-challenge. N-DEP, A-DEP, and C-DEP contained 1.5%, 68.6%, and 18.9% extractable organic material (EOM), respectively. The post-challenge results showed that DEP given with OVA induced a gradation of adjuvancy as follows: C-DEP ≈ A-DEP > N-DEP. The C- and A-DEP/OVA exposure groups had significant increases in eosinophils, OVA-specific IgG1, and airway hyperresponsiveness. In addition the C-DEP/OVA exposure increased the T_H2 chemoattractant chemokine, thymus and activation-regulated chemokine (TARC), and exhibited the most severe perivascular inflammation in the lung while A-DEP/OVA increased IL-5 and IL-10. In contrast, N-DEP/OVA exposure only increased OVA-specific IgG1 post-challenge. Analysis of early signaling showed that C-DEP induced a greater number of T_H2 cytokines compared to A-DEP and N-DEP. The results demonstrate that immune potentiation was not solely related to the amount of organic material and suggest that a balanced combination of carbon and EOM was the most effective adjuvant.

2.1 Introduction

Epidemiology studies have shown that the incidence of asthma has almost doubled in industrialized countries over the past 20 years [176-182]. Increases in ambient particulate matter (PM) have been correlated with a rise in hospitalization associated with respiratory illnesses such as asthma [118, 183]. Diesel exhaust particles (DEP) are an important component of ambient air PM. Several animal and limited human studies have shown that DEP can act as an immunological adjuvant to increase the severity of allergen induced asthma [114, 115, 123, 128, 134, 184-186], however, the physical and chemical composition of DEP responsible for this effect and a detailed understanding of early cellular signaling events are not well understood.

DEP are a complex mixture of organic and inorganic compounds that vary depending on factors such as type of engine, load characteristics, and method of collection. Two well studied DEP samples, an automobile derived DEP (A-DEP) and the National Institute of Standards Technology Standard Reference Material 2975 DEP (N-DEP) sample generated from a forklift engine, have been extensively studied for their pulmonary inflammatory effects [187] and mutagenicity [188], respectively. When compared, these particles were found to have contrasting physical and chemical properties and involuntary aspiration in mice showed distinct pulmonary toxicity profiles indicating that not all DEP are the same [21].

Animal studies have shown DEP exert allergic airway effects when given with an antigen [128, 137, 185, 189, 190]. These effects include increased T_H2 cytokines, eosinophils, and airway hyperresponsiveness upon antigen challenge. Studies have attributed this adjuvant effect to the organic components or the particles themselves by

examining either a DEP rich in organics and DEP organic extractable material [191, 192] or carbon black, synthetic model particles [193-195], or DEP stripped of its organics (washed DEP) [196], respectively. However, comparisons among the different studies are complicated by the variability in the sensitization and challenge regime as well as the methods of particle preparation.

The present study was conducted to evaluate the relative potency of three different DEP samples, N-DEP, A-DEP, and C-DEP (generated from a diesel engine used to power an air compressor) on allergic airway inflammation in a murine ovalbumin (OVA) mucosal sensitization model. In addition to adjuvant effects after antigen challenge, pulmonary responses post-sensitization were characterized to improve understanding of the relationship between the physical and chemical components of DEP and early signaling involved in the enhanced development of allergic immune response.

2.2 Materials and Methods

2.2.1 Animals

Female BALB/C mice (8-10 weeks old) were obtained from Charles River Laboratories (Raleigh, NC) and allowed to acclimate for a minimum of one week prior to dosing. Mice were randomly assigned to treatment groups and housed in an AAALAC-approved animal facility at the US-EPA. All animal procedures were reviewed and approved by the US-EPA's Institutional Animal Care and Use Committee. Housing environment conditions include a 12-h light/dark cycle at an ambient temperature of 22±1ºC and relative humidity of 55±5ºC. Mice were provided water and mouse chow *ad libitum*. Additional mice from each facility were routinely monitored serologically for

Sendai, mouse pneumonia, mouse hepatitis, and other murine viruses, as well as mycoplasma.

2.2.2 Particle samples

Standard Reference Material (SRM) 2975 diesel exhaust particle sample (N-DEP) was purchased from National Institute of Standard Technology (NIST) (Gaithersburg, MD). The reported mean diameter of these particles was 11.2 ±0.1 µm by area distribution, and the surface area, as determined by nitrogen adsorption, was 91μm^2/g. The certified analysis contains 11 certified concentrations and 28 reference concentrations for selected PAHs found in the DEPs. The DEP was generated by a heavy-duty forklift diesel engine and collected under "hot" conditions without a dilution tunnel (Table 2.1).

Automobile DEP (A-DEP) was generated and collected under conditions previously described [187, 197]. Briefly, the sample was generated by a light-duty (2740cc), 4-cylinder Isuzu diesel engine. DEP was collected under "cold" (50 ºC) conditions onto glass-fiber filters and on steel duct walls in a constant-volume sampling system fitted at the end of a dilution tunnel (Table 2.1).

Compressor DEP (C-DEP) was generated in-house as described by Cao et al [198] at EPA-RTP using a 30 kW (40 hp) 4-cylinder Deutz BF4M1008 diesel engine connected to a 22.3 kW Saylor Bell air compressor to provide 20% load. The generated particles were collected under "hot" conditions in a baghouse (Table 2.1).

2.2.3 Particle analysis

Organic carbon (OC) and elemental carbon (EC) were analyzed using a thermal-optical carbon analyzer with transmittance-based pyrolysis correction (Sunset Laboratory, Inc., Tigard, OR) using method 5040 found in the National Institute for Occupational Safety and Health (NIOSH) *Manual of Analytical Methods* (NIOSH 1994). DEP were extracted to determine mass distribution of initial extractable organic matter (EOM) and sub-fractions. Bulk samples of 2 g of each DEP were loaded in glass fiber thimbles and extracted with dichloromethane (DCM) using soxhlets overnight. Extracts were subsequently concentrated under nitrogen, and aliquots were dried on aluminum pans and weighed. Another aliquot of each DCM extract was further concentrated to 150 µL and readjusted to 12 mL with hexane. The hexane-insoluble fraction of the extract remained as a precipitate, and the other soluble fractions were applied to a DCM-rinsed neutral silica gel column. The EOM was then eluted serially with hexane, 50:50 hexane:DCM, DCM, and methanol. Each fraction was concentrated, and the mass was determined.

2.2.4 Experimental design

Following the protocol of Steerenberg *et al* [199], DEP samples (N-, C-, A-DEP) were suspended at a concentration of 3 mg/ml in saline alone or with 0.4 mg/ml of ovalbumin. Particles were sonicated using a Microson Ultrasonic Cell Disruptor (Micromix) for 10 min. Mice were randomly divided into 8 treatment groups, anesthetized with isofluorane, and exposed to saline, 20 µg OVA, 150 µg DEP, or DEP + OVA by intranasal instillation on Days 0 and 13. Mice were either necropsied 18 hrs later or went on to be challenged with 20 µg of ovalbumin on days 23, 26, and 29, and

necropsied 18 or 48 hrs after the last challenge (Figure 2.1).

2.2.5 Necropsy

Mice were euthanized with sodium pentobarbital and bled by cardiac puncture. The chest wall was opened and the trachea cannulated. The left lung lobe was clamped off and the right lobes lavaged with three 0.6 ml volumes of warmed Hanks balanced salt solution (HBSS) (Invitrogen, Grand Island, NY) and immediately cooled on ice. The left lung lobe was inflated with 10% buffered formalin and used for histopathological analysis.

2.2.6 Bronchoalveolar lavage fluid and characterization

The bronchoalveolar lavage fluid (BALF) was centrifuged (800rpm, 15 min, 4 ºC) and the supernatant was stored at 4 ºC for biochemical analysis or -80 ºC for cytokine detection. The pelleted cells were resuspended in 1 ml of RPMI 1640 (Gibco, Carlsbad, CA) containing 2.5 % fetal bovine serum (FBS; Gibco, Carlsbad, CA). Total cell counts in the lavage fluid of each mouse were obtained with a Coulter Counter (Beckman Dickson, Hialeah, FL). Each sample (200 µl) was centrifuged in duplicate onto slides using a Cytospin (Shandon, Pittsburgh, PA) and subsequently stained with Diff Quik solution (American Scientific, McGraw Park, PA) for cell differentiation determination, with at least 200 cells counted from each slide.

2.2.7 Biochemical analysis

BALF supernatant was analyzed using commercially available kits adapted for

automated analysis using a Cobas Fara II centrifugal spectrophotometer (Hoffman-La Roche, Branchburg, NJ). All assays were modified for use on the Konelab 30 clinical chemistry analyzer (Espoo, Finland). Microalbumin (MIA) levels were determined using a MALB SPQ kit (INCSTAR, MN) with a standard curve prepared with bovine serum albumin (BSA). N-acetyl-B-D-glucosaminidase (NAG) was measured using a commercially prepared kit containing sodium 3-cresolsulfonphthaleinyl-N-acetyl-B-D-glucosinamide, which can be hydrolyzed by NAG, releasing 3-cresolsulfonphthalein sodium salt (3-cresol purple), and standards from Roche Diagnostics (Mannheim, Germany). BALF supernatants were assayed for total protein using Pierce Coomassie Plus Protein Assay Reagent (Pierce Biotechnology, Inc, Rockford, IL). Concentrations were determined from a standard curve using BSA standards obtained from Sigma Chemical Co. (St. Louis, MO). Supernatants were also assayed for LDH activity using a commercially prepared kit and controls from Sigma Chemical Co. Both assays were modified for use on a KONELAB 30 clinical chemistry spectrophotometer analyzer (Thermo Clinical Lab Systems, Espoo, Finland).

2.2.8 Cytokine analysis

Cytokine proteins in cell supernatants were assessed using the Luminex 100 (Luminex Corp., Austin, TX) and LINCOplex kits (Linco Research, Inc., St. Charles, MO) for simultaneous detection and measurement of cytokines IL-4, IL-5, IL-6, IL-10, IL-12, IL-13, IL-15, IL-17, TNF-α, GM-CSF, IFN-γ, and a monocyte chemotactic protein (MCP-1). The limits of detection of the Luminex assays were 0.3, 0.6, 0.7, 10.3, 3.7, 4.7, 9.3, 1.7, 0.9, 4.6, 0.7, and 6.3 pg/ml, respectively. Enzyme-linked immunosorbent assays

(ELISA) for thymus and activation-regulated chemokine (TARC) were conducted using a commercially available kit (R&D systems, Minneapolis, MN) following manufacturer's protocol. The limit of detection was 15 pg/ml.

2.2.9 Antigen-specific serum IgE and IgG1

Antigen-specific IgE and IgG1 serum immunoglobulin production was measured by sandwich ELISA. Serum was prepared and kept frozen at -80 ºC until assay. Briefly 96 well flat bottom plates are coated with 100 µl/well of ovalbumin (OVA) (Sigma-Aldrich, St. Louis, MO) at a concentration of 100 µg/ml in PBS and incubated overnight at 4 ºC. The following day, after a blocking step and washing, 100 µl of each serum sample (IgE-neat and IgG1-diluted 1:10000) and 7 2-fold serial dilutions of mouse anti-OVA IgE (beginning at 1000 ng/ml; Serotec, Raleigh, NC) and IgG1 (beginning at 100 ng/ml; Zymed, San Francisco, CA) was added in duplicate wells to the plates. After an overnight incubation at 4 ºC and washing, the plates were treated successively with 100 µl/well of biotinylated IgE or IgG1 and horseradish peroxidase-streptavidin (diluted 1:1000; Zymed, San Francisco, CA), with washes and incubation for 1hr at room temperature between each of these steps. Tetramethylbenzidine substrate (TMB; DAKO Corp., Carpinteria, CA) was added (20 min, RT), the reaction was stopped using 2 M H2SO4, and absorbance was measured at 450 nm and compared between treatment groups. Optical density was read on a Spectramax 340PC Plate Reader (Molecular Devices Corp., Menlo Park, CA). Softmax Pro version 2.6.1 Software (Molecular Devices Corp.) was used for data collection and conversion from optical density to antibody concentration was calculated with reference to standard curves of the known

amounts of each antibody.

2.2.10 Histopathology

The left lung lobe of the lung was inflated and fixed with 10% buffered formalin, immersed in 10% buffered formalin for 24 hrs then transferred into 70% ethanol. Samples were sent to Experimental Pathology Laboratories (Research Triangle Park, NC) for processing and histopathological evaluation by a board certified veterinary pathologist. Lung sections were stained with hematoxylin and eosin (H&E) to determine inflammatory changes. Specifically, lung sections were scored for perivascular and peribronchial inflammation: 0-normal, 1-minimal, 2-mild, 3-moderate or 4-severe. The total scores for each group (n=3) were averaged. Statistical analysis of the data was not performed, but the data were assessed for any immediately obvious trends.

2.2.11 Airway hyperresponsiveness (AHR)

Nonspecific airway responsiveness to increasing concentrations of aerosolized methacholine (Mch) in unrestrained mice in a 12-chamber whole-body plethysmograph system (Buxco Electronics, Troy, NY) was measured on Day 31, 48 h after intranasal challenge. Pressure signals were analyzed with BioSystem XA software (SFT3812, version 2.0.2.4, Buxco Electronics) to derive whole-body flow parameters that were used to calculate enhanced pause (Penh). Penh was used as an index of airflow obstruction, which has been correlated with changes in airway resistance [200]. After measuring baseline parameters for 7 min, an aerosol of saline or Mch in increasing concentrations

(6.25, 12.5, and 25 mg/ml) was nebulized through an inlet of the chamber. The recorded Penh values were averaged during the baseline periods and the Mch challenges to obtain mean values for each event and were represented as change from the mean during the baseline period to the mean during each Mch challenge.

2.2.12 Statistical analysis

The data were analyzed using a two-way analysis of variance (ANOVA) model. The two independent variables were OVA (at levels present and absent) and treatment (at levels A-DEP, C-DEP, N-DEP and Saline). Pair-wise comparisons were performed as subtests of the overall ANOVA, subsequent to a significant main or interactive effect. If the usual ANOVA assumptions were not satisfied, either the data were transformed so as to satisfy the assumptions or, in cases where the assumptions could not be satisfied, a distribution free test was substituted for the ANOVA. The level of significance was set at 0.05. No adjustment was made to the significant level as a result of multiple comparisons.

2.3 Results

2.3.1 Chemical characteristics of diesel exhaust particles (DEP)

From the OC/EC ratios, the A-DEP comprised six times the amount of organic carbon compared to elemental carbon, while the C-and N-DEP contained more elemental carbon. The significant enrichment of organics in A-DEP was also shown by the amount of DCM-extracted organics (approximately 70% of particles mass), which was much larger than the 19% and 1.5% for C-DEP and N-DEP, respectively (Table 2.1). However,

the mass distribution of sub-fractions of EOM of A-DEP and C-DEP were found to be similar, showing that the EOM of A-and C-DEP were mostly hexane soluble (less polar; 58-74% in organic extracts), while the EOM of N-DEP was soluble in hexane or methanol (more polar) at the same degree (Table 2.1). A previous study [201] suggested that A-DEP comprised a large amount of unburned fuel, which was indicated by GC/MS as a large amount of aliphatic hydrocarbons. GC/MS analysis on C-DEP also showed a similar organic composition with A-DEP, with a large amount of alkanes by single chemical quantitative identification analyses (data not shown), suggesting that organics in C-DEP could also result from incomplete combustion of diesel fuel, albeit at a lower degree.

2.3.2 Post-challenge results

BALF cell differential counts

Mice were given either saline or DEP alone (non-sensitized) or with OVA (sensitized) on days 0 and 13, challenged with OVA on days 23, 26, and 29, and necropsied 18 and 48 hrs later (Figure 2.1). The C-DEP + OVA group at 18 hrs had a significantly greater number of macrophages than all groups (Table 2.2). At the 48 hr time point the total cell numbers in the BALF of all sensitized mice exposed to DEP was increased compared to saline or DEP alone treatments, of which macrophages and eosinophils were the predominant cell type (Table 2.3). Statistical analysis revealed an interactive effect of DEP exposure combined with antigen with respect to the number of

eosinophils in the BALF at 48 hrs for the A- and C-DEP + OVA exposures. Eosinophils in all DEP + OVA treated mice were significantly greater than saline and DEP alone at the 48 hr time point, however A- and C-DEP + OVA treated mice had a significantly greater amount of eosinophils compared to the OVA control and N-DEP + OVA groups. OVA control and non-sensitized A-DEP groups exhibited a significant increase in eosinophils at the 48 hr time point compared to saline and N- and C-DEP alone. Neutrophil and lymphocyte infiltration was highest in the C-DEP + OVA treatment for both time points (Table 2.2 & 2.3). A significant interactive effect from the combined DEP and OVA exposures, with respect to the number of lymphocytes in the BALF, was apparent for both N- and C-DEP + OVA exposures at both time points and the A-DEP + OVA exposure at the 48 hrs. Only the C-DEP + OVA exposure demonstrated a synergistic effect with respect to neutrophil infiltration at both time points. These data show that after DEP + OVA sensitization and allergen challenge, (a) mice had increased airway inflammatory cell influx compared with saline, OVA, and DEP alone; (b) the magnitude of inflammatory cell influx was greater at the 48 hr time point; (c) while C- and A-DEP + OVA mice displayed the strongest inflammatory response at 48 hrs, this response was initially stronger in C-DEP + OVA; and (d) at the 48 hr time point OVA and A-DEP alone also resulted in a significant increase in inflammatory cells.

BALF biochemical analyses

To determine if the increased lung inflammation present in DEP + OVA exposed mice after allergen exposure was accompanied by changes in alveolar epithelial permeability, BALF total protein and microalbumin (MIA) were measured. Protein

(Figure 2.2) and MIA levels (data not shown) in non-sensitized DEP treated mice were not significantly different from each other or saline control. In sensitized mice, only C-DEP + OVA displayed an increase in both biomarkers at the early time point. However, by 48 hrs protein both protein and MIA levels in A- and C-DEP + OVA groups were significantly greater than saline, OVA, all non-sensitized DEP, and N-DEP + OVA exposed groups, suggesting that increased epithelial permeability accompanied the inflammatory process (Figure 2.2).

To explore whether the allergen-induced inflammation in mice was accompanied by increased lysosomal enzyme release, we measured BALF NAG, an established marker of alveolar macrophage activation[202]. A- and C-DEP + OVA sensitized mice exhibited a significant increase in BALF NAG at the 48 hr time point compared with saline, OVA, and DEP alone (data not shown). LDH levels in the BALF were measured as an index of cellular toxicity. C-DEP + OVA exposed mice had a significant increase in LDH levels at both points compared to saline, OVA, and non-sensitized N- and A-DEP (Figure 2.3). The A-DEP + OVA exposure induced a significant increase in LDH compared to saline and non-sensitized N- and C-DEP at the 48 hr time point (Figure 2.3b). These results suggest that the increased inflammation in mice was associated with increased alveolar epithelial permeability, release of lysosomal enzymes from activated macrophages, and cellular toxicity.

Serum antibody levels

To evaluate the influence of DEP exposure on sensitization, OVA specific IgE and IgG1 serum levels were measured 18 and 48 hrs post-challenge. Saline and non-

sensitized DEP exposed mice had undetectable levels of OVA specific IgE and IgG1. There were no significant changes in IgE levels across all groups (data not shown). OVA specific IgG1 antibody titers in the serum of all DEP + OVA sensitized mice were significantly increased compared to saline control for both time points (Figure 2.4). Only N- and C-DEP + OVA at 18 hrs and N-DEP + OVA at 48 hrs had a significant increase in IgG1 antibodies compared to OVA control.

BALF cytokine analyses

To determine the effects of DEP on T_H2 polarization, local production of T_H1 (IL-12 and IFN-γ) and T_H2 cytokines and chemokines (IL-4, 5, 6, 10, 13, 15, and 17, TNF-α, GM-CSF, MCP-1, TARC) in BALF was quantified 18 hrs post-challenge. Although an increase was seen in the OVA treatment group, all DEP + OVA exposures did not enhance IL-4, 6, 12, 13, 15, 17, TNF-α, GM-CSF, IFN-γ, or MCP-1 above OVA control concentrations (data not shown). A-DEP + OVA treatment resulted in a significant increase in IL-5 and IL-10 compared to saline, OVA, and N-DEP + OVA (Figure 2.5a + b). IL-10 was also significantly greater than C-DEP + OVA (Figure 2.5b). Thymus and activation-regulated chemokine (TARC) levels were significantly increased compared to saline, OVA, and N- and A-DEP + OVA in C-DEP + OVA exposed mice (Figure 2.5c).

Airway hyperresponsiveness

Airway hyperresponsiveness (AHR) to methacholine was measured by whole body plethysmography. Forty-eight hrs after the last OVA challenge, all mice had similar baseline readings but OVA and all DEP + OVA exposures resulted in an overall

increased Penh for all methacholine challenges (Figure 2.6) compared to saline and DEP alone exposures (data not shown). Intranasal instillation of A- and C-DEP + OVA and OVA control significantly increased Penh in response to 6 mg/ml of methacholine compared to saline controls (Figure 2.6). In addition, A- and C-DEP + OVA had a significantly greater PenH than saline in response to 12 and 25 mg/ml of methacholine.

Histopathology

Histology specimens from all animals were scored for the degree of perivascular and peribronchial inflammation, with a score of 1 indicating mild to a score of 4 indicating severe change. Where appropriate, airways were identified as being mainstem bronchus versus secondary airways. Lung sections from non-sensitized mice given DEP demonstrated minimal to mild perivascular inflammation. In contrast, all DEP + OVA exposures appeared to mildly potentiate the inflammatory response above that observed with OVA sensitization alone. Specifically C-DEP + OVA groups had the highest scores for all measurements with perivascular inflammation (3.67) being the highest at 48 hrs (Table 2.4).

2.3.3 Post-sensitization

BALF cell counts

To elucidate early cellular mechanisms that lead to the development and intensity of allergic inflammation seen after antigen challenge, cellular profiling of the BALF was

investigated. Mice were given either saline or DEP with or without OVA on days 0 and 13 and necropsied 18 hrs later. As shown in Table 2.5, non-sensitized A-DEP exposed mice had a significant increase in the number of macrophages in the BALF (Table 2.5). Eosinophils were significantly increased in C-DEP + OVA exposed mice compared to OVA control, A-DEP, C-DEP, and A-DEP + OVA. Non-sensitized N-DEP and C-DEP + OVA mice had a significantly greater number of neutrophils in the BALF. In addition, C-DEP + OVA exposure induced a significant increase in lymphocytes in the BALF compared to all groups. Statistical analysis indicated a synergistic effect from the combined exposure of C-DEP and OVA with respect to eosinophil and lymphocyte lung infiltration.

BALF biochemical analyses

To determine if the DEP exposure with or without antigen directly induced cellular lung injury and toxicity, the BALF was analyzed for total protein, MIA, NAG, and LDH. MIA levels were unchanged across all groups (data not shown). Only the non-sensitized N-DEP exposure induced a significant increase in NAG compared to saline and OVA control (data not shown). In the context of antigen, significant increases in LDH compared to OVA control were measured in A- and N-DEP + OVA exposures. C- and N-DEP + OVA exposures significantly increased BALF NAG levels. Total protein levels were also elevated in A-DEP + OVA exposure compared to OVA control (data not shown)

BALF cytokine analysis

To determine the effects of DEP given with antigen on early cell signaling events, T_H2 cytokines (IL-4, 5, 10, 13, 15, and 17) and chemokines (TARC, and MCP-1), and proinflammatory cytokines (IL-6 and TNF-α) concentrations in BALF post-sensitization were quantified. All DEP + OVA exposures increased the production of IL-5 compared to saline and OVA controls, however this increase was only significant in N- and C-DEP + OVA exposed mice (Figure 2.7a). Instillation of C-DEP + OVA significantly increased the concentration of the T_H2 cytokine IL-4 above saline and OVA controls (Figure 2.7b). The T_H2 chemoattractant chemokine TARC was significantly increased in all DEP + OVA exposures (Figure 2.7c). Monocyte chemoattractant protein (MCP-1) protein levels were only significantly greater in C-DEP + OVA compared to all groups (Figure 2.7d). The proinflammatory cytokine IL-6 was greatly increased in response to C-DEP + OVA exposure compared to all treatment groups (data not shown). OVA and C-DEP + OVA exposure significantly decreased the concentration of the T_H1 cytokine IL-12 (Figure 2.8). In contrast, N- and A-DEP + OVA exposures increased the production IL-12 compared to OVA, however this increase was not significant.

2.4 Discussion

Studies in humans and animals have shown diesel exhaust particles (DEP) can act as an immunological adjuvant to enhance the development of allergic lung disease, and this effect is influenced by the chemical composition of the DEP. The chemical components of DEP associated with allergic adjuvancy and the underlying mechanisms are not well understood. Furthermore, the heterogeneous nature of DEP samples adds to

the difficulty in determining what effects are common among all DEP samples versus specific characteristics of a particular sample. Previous studies have shown the organic components such as polycyclic aromatic hydrocarbons (PAHs) as well as the particles themselves can induce allergic adjuvancy [191-195]. The present study investigated the relative adjuvant potency of three different DEP samples, N-DEP, A-DEP, and C-DEP which differed in the percentage of DCM extractable organic material (1.5%, 68.6%, and 18.9%, respectively) in a mucosal sensitization model adopted from Steerenberg *et al.* [199]. This study demonstrated a synergistic effect from the combined exposure of DEP and antigen with respect to injury and inflammation. Overall the results showed that on a comparative mass basis, the three samples induced a gradation of post-challenge adjuvancy and this was not solely dependent on the organic content. The inflammatory component characterized by increased numbers of eosinophils, neutrophils, and lymphocytes was significantly increased in OVA, A-DEP alone, and all DEP + OVA treatment groups, with the C- and A-DEP + OVA groups exhibiting the most robust responses. Recruitment of these inflammatory cells was accompanied by increases in alveolar epithelial permeability, macrophage activity, and general cellular toxicity as measured by protein and MIA, NAG, and LDH levels, respectively. AHR and histology results were in overall agreement with these findings.

Antigen-specific IgE antibodies have been shown to increase in response to DEP when given with antigen [128, 189, 190]. In the present study, all DEP + OVA induced a significant increase in OVA-specific IgG1 serum antibodies after antigen challenge, but not OVA-specific IgE. However, other indicators of allergic airway disease such as eosinophilic airway inflammation and airway hyperresponsiveness were present in mice

exposed to A- and C-DEP + OVA. In addition it has previously been reported that antigen specific IgG1, but not IgE, induced eosinophil degranulation *ex vivo* in the sera from ragweed pollen sensitive asthmatics [203]. Furthermore, late asthmatic reactions are correlated with high IgG1 but not IgE antibodies [204]. Therefore, antigen-specific IgG1 appears to be an important indicator of adjuvancy in this model.

Human and rodent studies have shown DEP induced allergic asthma is characterized by recruitment of T helper 2 (T_H2) lymphocytes and subsequent production of T_H2 cytokines like IL-4, IL-5, IL-10, and IL-13, which perpetuate the inflammatory response. The importance of T_H2 cells in allergic asthma is underlined by a study in which adoptive transfer of these cells into naïve mice led to an allergic asthma phenotype [205]. Conversely, removal of these cells prevented induction of asthma in sensitized mice. Thymus activation regulated chemokine (TARC), mainly produced by dendritic cells, selectively induces the migration of CCR4-expressing T_H2 cells [206, 207] and is thought to play a crucial role in allergic asthma. Elevated TARC levels have been observed in the BALF of patients with allergic asthma after allergen challenge [208], and rodent studies have shown that neutralization of this chemokine attenuates OVA induced lung eosinophilia, T_H2 cytokine expression, and associated increases in bronchial responsiveness after antigen challenge [209]. In the present study, TARC levels post-challenge in the BALF were significantly increased in C-DEP + OVA exposed mice compared to all groups and this was accompanied by a significant increase in lymphocytes.

We and others have shown A-DEP alone and with antigen induces the T_H2 cytokine IL-5 in the BALF of mice and humans [124, 201, 210]. In agreement with these studies, IL-5 levels in the BALF of mice exposed to A-DEP + OVA were significantly increased above saline and OVA controls post-challenge. IL-5 is an important factor in the proliferation and activation of eosinophils and may explain the eosinophilia seen in those mice. IL-10 is described as a T_H2 cell factor that inhibits cytokine synthesis by T_H1 cells [211, 212]. Although others have found IL-10 to down-regulate IL-5 production [213-215], in this study IL-10 was increased along with IL-5 in the BALF of mice exposed to A-DEP + OVA providing more evidence for their cooperative effect.

While most reports on PM-induced adjuvancy have focused on immune effects post-challenge, we were also interested in assessing early signaling events caused by DEP alone or in the context of antigen sensitization. The direct injury and proinflammatory effects of intranasal instillation of DEP with or without OVA on the airways was assessed by analyzing biochemistry, cell differential counts, and cytokine profiling of the BALF 18 hours after the last DEP exposure. All DEP exposures alone caused no changes in the biochemical indicators of injury which suggests no direct local airway damage. The molecule NAG was also measured as an indicator of macrophage activation. Although A-DEP exposure increased the number of macrophages and N-DEP increased neutrophil influx, NAG levels were significantly elevated in the BALF of N-DEP exposed mice. C-DEP alone had no direct effect on lung injury, NAG, or cellular infiltration.

In the context of antigen sensitization, N-DEP + OVA induced a slight increase in

LDH and NAG levels. This cellular injury and macrophage activation was accompanied by an increase in lymphocytes and the T_H2 chemokines MCP-1 and TARC in the BALF. This mild T_H2 phenotype post-sensitization was followed by a low level of adjuvancy post-challenge. Exposure to A-DEP with antigen induced a significant increase in LDH and protein levels but exhibited no significant cellular influx or cytokine production compared to OVA control, although this treatment group led to a robust adjuvant response post-challenge. On the other hand, C-DEP + OVA was a strong adjuvant post-challenge and induced a significant increase in NAG, eosinophils, neutrophils, and lymphocytes, as well as IL-4, 5, 6, MCP-1 and TARC post-sensitization. This indicates an early induction of a T_H2 phenotype in C-DEP + OVA exposure.

In the present study, C-DEP + OVA exposure induced the strongest T_H2 response post-sensitization although this sample was more balanced with respect to organic and elemental carbon levels compared to the N-DEP and A-DEP, which contained very low or very high OC/EC ratios, respectively. This immune skewing induced by C-DEP + OVA exposure was followed by a robust adjuvant effect post-challenge. On the other hand, the organic rich A-DEP did not display a T_H2 response when given with antigen but did in fact induce a strong adjuvant effect post-challenge. This suggests that the kinetics of the response or the mechanism may be different for inducing the post-challenge adjuvant response in the A-DEP + OVA exposure.

There is much evidence that the organic chemical compounds, such as PAHs, quinones, and nitro-PAHs, absorbed on the surface of DEP play a role in ROS production which in turn causes oxidative stress. If the level of oxidative stress exceeds the cells

natural antioxidant defense mechanisms then inflammatory cytokines and chemokines, which may contribute to the adjuvant effect of DEP, are produced. The amount of DCM extractable organic material present in the A-DEP sample was about 3.5 times greater than C-DEP; however, both samples when given with allergen induced similar degrees of adjuvancy post challenge. An alternate explanation for these effects induced by exposure to the different DEP samples is the presence of particular species of compounds in the organic fraction, rather than the overall amount, could be responsible for the toxic effects. Xia *et al* [165] demonstrated the quinone-enriched polar fraction of DEP was more potent than the PAH-enriched aromatic fraction in ROS production suggesting a greater ability to cause oxidative stress. Further chemical analysis of the compounds present in the fractionated DCM EOM of the DEP samples is needed.

This research highlights the capacity of different diesel particles to modulate the induction of an immune response. On an equal mass basis all three particle samples could enhance allergic sensitization as measured by antigen-specific IgG1 antibodies in the BALF after antigen challenges; however, the effects were more pronounced with the C-DEP and A-DEP samples which are composed of a higher percentage of extractable organic material. The adjuvant effects can be summarized as follows: C-DEP ≈ A-DEP >> N-DEP. To date investigations of underlying mechanisms have mainly focused on ROS production. Since these studies have investigated a single DEP sample a comparative study analyzing different samples using a global inspection approach of transcriptional regulation is needed. This study identifies the importance of chemical composition when studying heterogeneous mixtures. The expanding knowledge of the

immune effects of DEP could ultimately have wider implications for unraveling the mechanisms of air pollution enhanced allergic lung disease.

Tables

Table 2.1 Characteristics of A-DEP, C-DEP, and N-DEP

Compound	A-DEP	C-DEP	N-DEP
Source	4-cylinder 4JB1 type Isuzu automobile, Light duty (2740cc); on-road	30 kW (40hp) 4-cylinder Deutz BF4M1008 diesel engine used to power a 22.3 kW Saylor Bell air compressor; stationary	Industrial forklift; off-road
Collection method	Dilution tunnel terminus onto glass fiber filter (GD-100R, 203×254mm) at 50°C, Particles were scraped off from the filter	Diluted, cooled to 35°C, and directed to a small baghouse (Dusyex model T6-3.5-9 150 ACFM pyramidal baghouse)	Diesel exhaust filter system, under hot conditions
Collection Date	Early 1990's	October 2004	Late 1980's
Organic carbon (OC)/Elemental carbon (EC)mass ratio	5.56	0.33	0.08
DCM EOM (% of DEP)	68.6	18.9	1.5
Sub-fractions of EOM (% of EOM)			
Hexane	57.3	73.6	37.9
Hexane/DCM	3.2	7.1	4.4
DCM	0.7	1.1	1.5
Methanol	6.6	10.4	30.2
Precipitates (hexane-insoluble)	32.3	7.9	26.0

Table 2.2 Differential cell counts in the BALF 18 hrs after OVA challenge

Group	**Macrophages** ($x10^4$/ml BALF)	**Eosinophils** ($x10^4$/ml BALF)	**Neutrophils** ($x10^4$/ml BALF)	**Lymphocytes** ($x10^4$/ml BALF)
Saline	24.27 ± 2.01	0.13 ± 0.05	4.61 ± 1.16	0.49 ± 0.14
OVA	32.19 ± 5.03	8.33 ± 4.67	6.62 ± 2.01	1.90 ± 1.00
NDEP	35.51 ± 6.54	2.49 ± 2.46	7.61 ± 3.63	1.96 ± 1.52
ADEP	28.68 ± 3.99	2.45 ± 0.93	5.54 ± 1.72	1.35 ± 0.33
CDEP	32.82 ± 6.47	0.22 ± 0.19	9.71 ± 2.05	2.16 ± 0.57
OVA + NDEP	39.11 ± 5.28	25.67 ± 13.18^{*,a,c}	19.68 ± 6.64	10.68 ± 4.41$^{*,\#,a,b}$
OVA + ADEP	38.09 ± 8.61	29.24 ± 15.12^{*,a,c}	17.31 ± 5.15	7.35 ± 2.59*
OVA + CDEP	68.54 ± 10.15$^{*,\#,a,b,c,d,e}$	38.01 ± 17.82^{*,a,b,c}	36.16 ± 9.79$^{*,\#,a,b,c}$	19.42 ± 5.39$^{*,\#,a,b,c}$

$^{*}P<0.05$: significantly greater than saline control. $^{\#}P<0.05$: significantly greater than OVA control. $^{a}P<0.05$: significantly greater than N-DEP. $^{b}P<0.05$: significantly greater than A-DEP. $^{c}P<0.05$: significantly greater than C-DEP. $^{d}P<0.05$: significantly greater than N-DEP/OVA. $^{e}P<0.05$: significantly greater than A-DEP/OVA.

Table 2.3 Differential cell counts in the BALF 48 hrs after antigen challenge

Group	**Macrophages** ($x10^4$/ml BALF)	**Eosinophils** ($x10^4$/ml BALF)	**Neutrophils** ($x10^4$/ml BALF)	**Lymphocytes** ($x10^4$/ml BALF)
Saline	21.97 ± 3.53	0.40 ± 0.28	0.19 ± 0.09	0.25 ± 0.09
OVA	29.38 ± 4.38	12.37 ± 4.67^{*,a,c}	0.62 ± 0.18	3.62 ± 1.01^{*,a,c}
NDEP	25.52 ± 2.99	0.00 ± 0.00	0.64 ± 0.08	0.50 ± 0.15
ADEP	30.18 ± 6.37	11.32 ± 5.31^{*,a,c}	4.32 ± 2.62^{*,c}	3.41 ± 2.35*
CDEP	31.49 ± 1.70	0.23 ± 0.15	0.40 ± 0.08	0.57 ± 0.22
OVA + NDEP	43.79 ± 6.62*	28.42 ± 5.72^{*,a,b,c}	2.67 ± 1.13^{*,c}	13.86 ± 3.94$^{*,\#,a,b,c}$
OVA + ADEP	81.66 ± 11.09$^{*,\#,a,b,c,d}$	77.74 ± 12.29$^{*,\#,a,b,c,d}$	4.11 ± 1.22$^{*,\#,a,c}$	19.82 ± 2.66$^{*,\#,a,b,c}$
OVA + CDEP	83.72 ± 12.86$^{*,\#,a,b,c,d}$	81.96 ± 14.52$^{*,\#,a,b,c,d}$	11.47 ± 3.98$^{*,\#,a,c}$	43.41 ± 13.83$^{*,\#,a,b,c,d}$

$^{*}P<0.05$: significantly greater than saline control. $^{\#}P<0.05$: significantly greater than OVA control. $^{a}P<0.05$: significantly greater than N-DEP. $^{b}P<0.05$: significantly greater than A-DEP. $^{c}P<0.05$: significantly greater than C-DEP. $^{d}P<0.05$: significantly greater than N-DEP/OVA.

Table 2.4 Histopathology scores 18 and 48 hrs after challenge

	18 hrs		48 hrs	
Group	**Perivascular Inflammation**	**Peribronchial Inflammation**	**Perivascular Inflammation**	**Peribronchial Inflammation**
Saline	0.33	0.33	0.33	0.00
OVA	1.00	0.33	1.67	0.00
NDEP	1.00	0.33	0.00	0.00
ADEP	1.33	1.00	2.00	0.33
CDEP	0.00	0.00	0.33	0.00
OVA + NDEP	2.00	0.33	3.33	1.33
OVA + ADEP	2.33	1.33	2.00	1.33
OVA + CDEP	2.33	1.67	3.67	1.67

Table 2.5 Differential cell counts in the BALF 18 hrs after sensitization

Group	**Macrophages** ($x10^4$/ml BALF)	**Eosinophils** ($x10^4$/ml BALF)	**Neutrophils** ($x10^4$/ml BALF)	**Lymphocytes** ($x10^4$/ml BALF)
Saline	5.32 ± 2.26	0.15 ± 0.13	5.53 ± 2.50	0.28 ± 0 .13
OVA	9.12 ± 2.70	0.03 ± 0.03	9.27 ± 3.13	0.21 ± 0.06
NDEP	6.81 ± 1.34	0.16 ± 0.07	31.89 ± 3.70$^{*,\#}$	0.07 ± 0.06
ADEP	14.16 ± 2.39^{*,c}	0.00 ± 0.00	23.44 ± 6.40	0.06 ± 0.05
CDEP	5.62 ± 1.61	0.00 ± 0.00	16.89 ± 1.72	0.03 ± 0. 03
OVA + NDEP	6.97 ± 1.60	0.09 ± 0.05	13.85 ± 2.86	0.3 9 ± 0.03^{a,b,c}
OVA + ADEP	6.25 ± 1.31	0.03 ± 0.03	13.85 ± 4.00	0.1 7 ± 0.07
OVA + CDEP	7.72 ± 1.14	1.60 ± 0.80$^{\#,b,c,e}$	25.51 ± 7.02*	0.72 ± 0.07$^{*,\#,a,b,c,d,e}$

$^{*}P<0.05$: significantly greater than saline control. $^{\#}P<0.05$: significantly greater than OVA control. $^{a}P<0.05$: significantly greater than N-DEP. $^{b}P<0.05$: significantly greater than A-DEP. $^{c}P<0.05$: significantly greater than C-DEP. $^{d}P<0.05$: significantly greater than N-DEP/OVA.. . $^{e}P<0.05$: significantly greater than A-DEP/OVA.

Figures

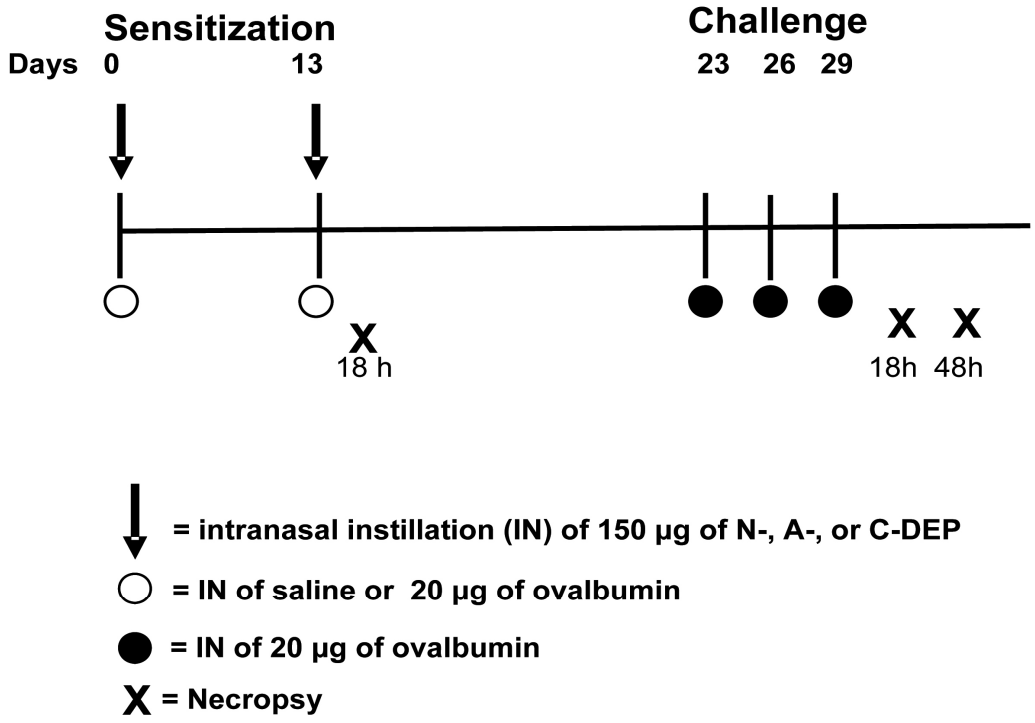

Figure 2.1 Schematic of exposure regime. BALB/c mice were intranasally instilled with saline or 150 µg of N-, A-, or C-DEP, with or without 20 µg of OVA on days 0 and 12. Mice were challenged with an intranasal instillation of 20 µg of OVA on days 23, 26, and 29 and necropsied 18 or 48 hrs later.

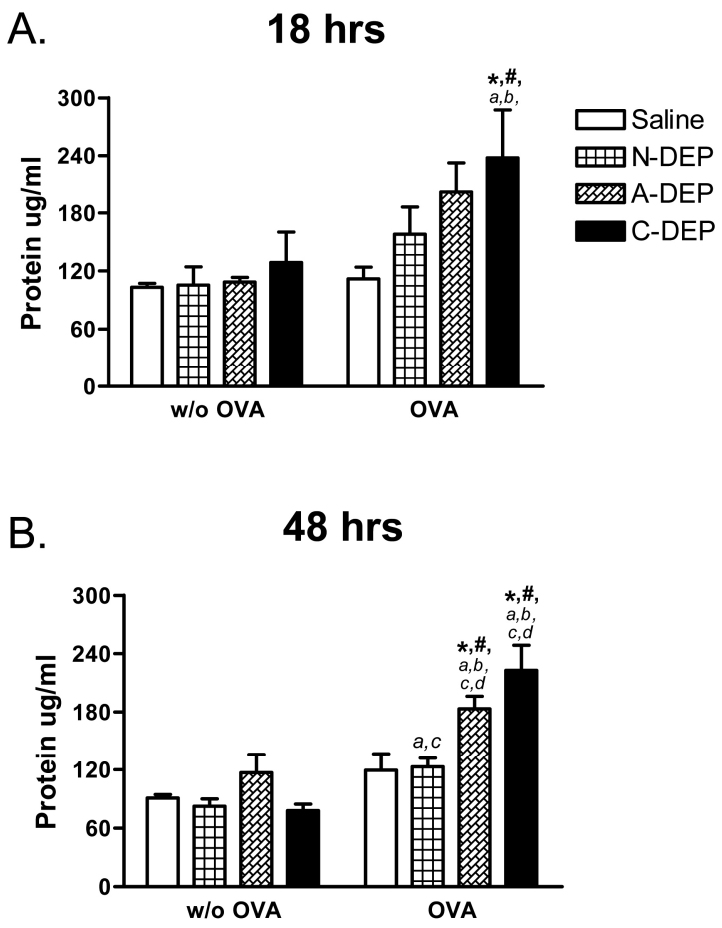

Figure 2.2 Protein concentrations in the BALF after challenge. Protein levels @ 18 hrs (A) and 48 hrs (B). $^{*}P<0.05$: significantly greater than saline control. $^{\#}P<0.05$: significantly greater than OVA control. $^{a}P<0.05$: significantly greater than N-DEP. $^{b}P<0.05$: significantly greater than A-DEP. $^{c}P<0.05$: significantly greater than C-DEP. $^{d}P<0.05$: significantly greater than N-DEP/OVA.

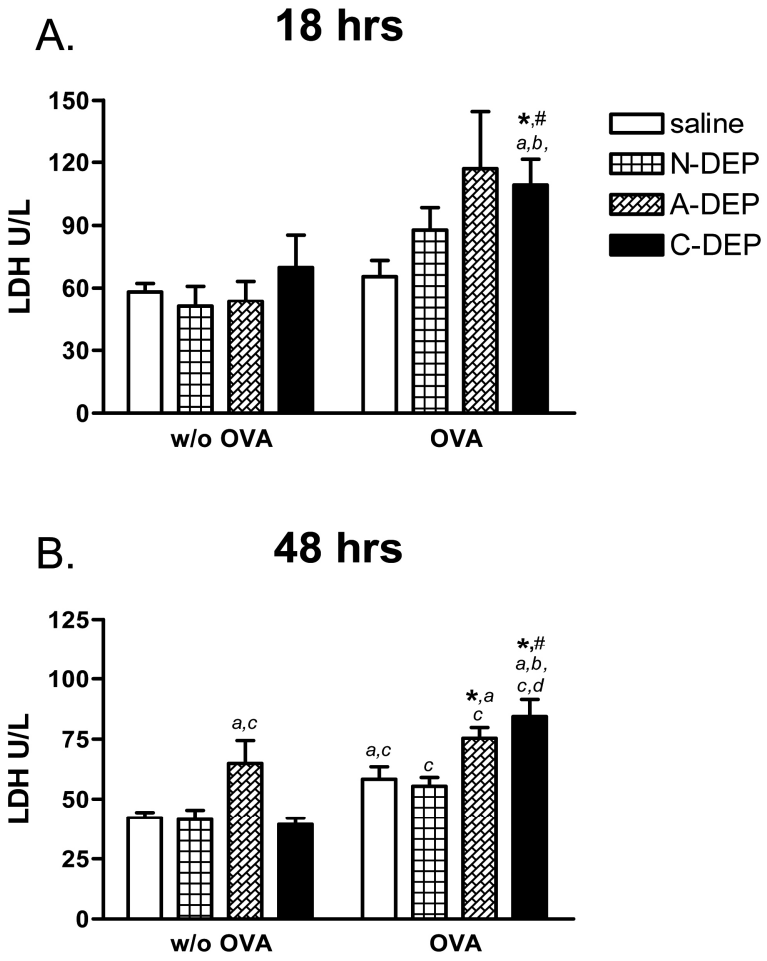

Figure 2.3 LDH levels in the BALF after challenge. LDH levels @ 18 hrs (A) and 48 hrs (B). $^{*}P<0.05$: significantly greater than saline control. $^{\#}P<0.05$: significantly greater than OVA control. $^{a}P<0.05$: significantly greater than N-DEP. $^{b}P<0.05$: significantly greater than A-DEP. $^{c}P<0.05$: significantly greater than C-DEP. $^{d}P<0.05$: significantly greater than N-DEP/OVA.

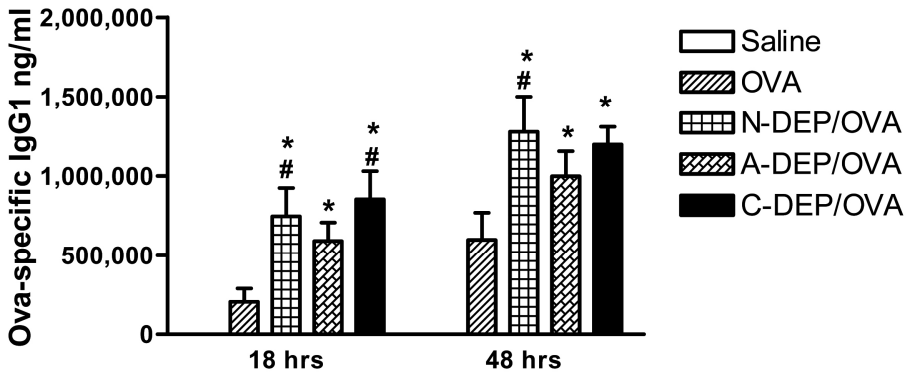

Figure 2.4 Kinetic development of OVA-specific IgG1 serum antibodies in mice exposed to diesel exhaust during allergic sensitization. Mice were intranasally instilled with 20 μg of OVA alone or in combination with 150 μg of N-, A-, or C-DEP on days 0 and 12. Mice were challenged with 20 μg of OVA on days 23, 26, and 29 and necropsied after 18 or 48 hrs. OVA-specific IgG1 antibody levels were measured in the serum by ELISA. $^{*}P<0.05$: significantly greater than saline control. $^{\#}P<0.05$: significantly greater than OVA control.

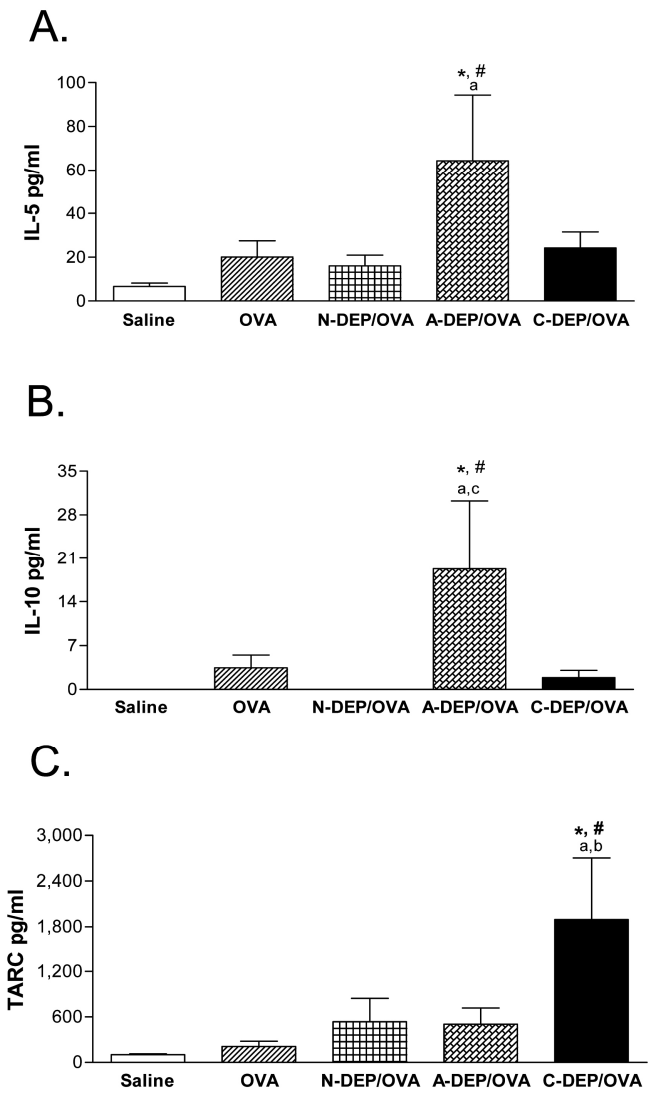

Figure 2.5 IL-5, IL-10, and TARC production levels in the BALF 18 hrs after challenge. Mice were intranasally instilled with saline, 20 μg of OVA alone or in combination with 150 ug of N-, A-, or C-DEP on days 0 and 12. Mice were challenged with 20 μg of OVA on days 23, 26, and 29 and necropsied after 18 hrs. IL-5 (A), IL-10 (B), and TARC (C) levels were measured in the BALF by ELISA. $^{*}P<0.05$: significantly greater than saline control. $^{\#}P<0.05$: significantly greater than OVA control. $^{a}P<0.05$: significantly greater than N-DEP + OVA. $^{b}P<0.05$: significantly greater than A-DEP + OVA. $^{c}P<0.05$: significantly greater than C-DEP + OVA.

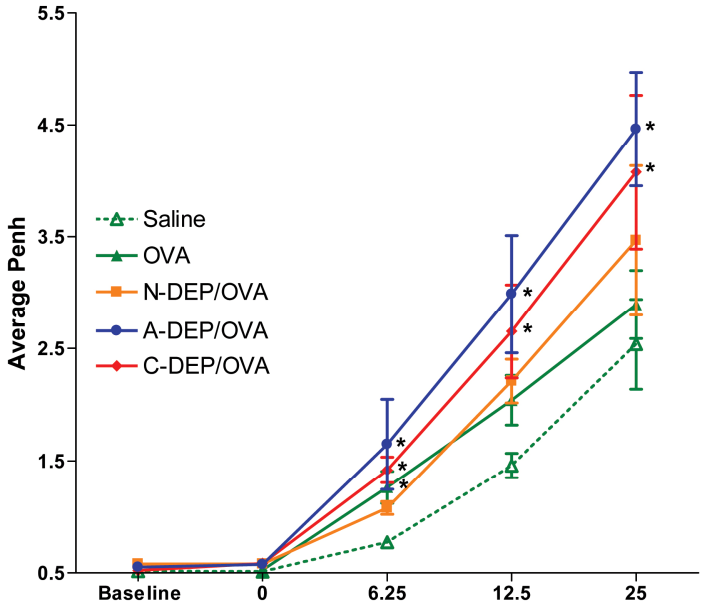

Figure 2.6 Airway hyperresponsiveness in mice 48 hrs after OVA challenge. Mice were intranasally instilled with saline, 20 μg of OVA alone or in combination with 150 ug of N-, A-, or C-DEP on days 0 and 12. Mice were challenged with 20 μg of OVA on days 23, 26, and 29 and Airway hyperresponsiveness (AHR) was measured 48 hrs after the last challenge. AHR was determined by an increase in enhanced pause (Penh) in response to increasing concentrations to methacholine. $^{*}P<0.05$: significantly greater than saline control.

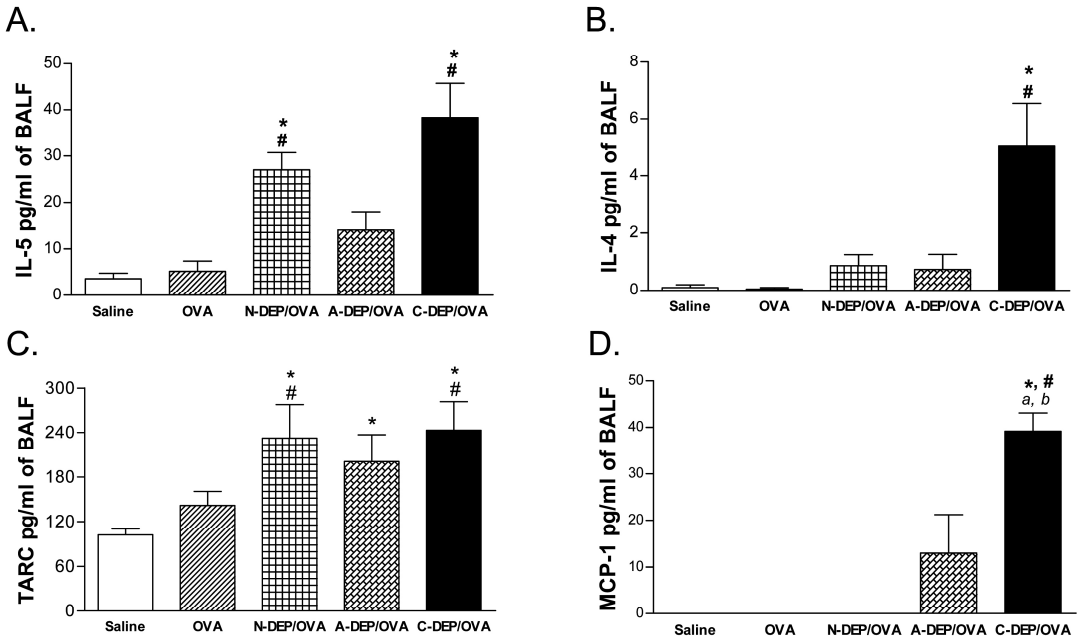

Figure 2.7 T_H2 cytokine and chemokine levels in the BALF 18 hrs after sensitization. Mice were intranasally instilled with saline, 20 μg of OVA alone or in combination with 150 ug of N-, A-, or C-DEP on days 0 and 12 and necropsied 18 hrs later. IL-5 (A), IL-4 (B), TARC (C), and MCP-1 (D) levels were measured in the BALF by ELISA. $^{*}P<0.05$: significantly greater than saline control. $^{\#}P<0.05$: significantly greater than OVA control. $^{a}P<0.05$: significantly greater than N-DEP + OVA. $^{b}P<0.05$: significantly greater than A-DEP + OVA.

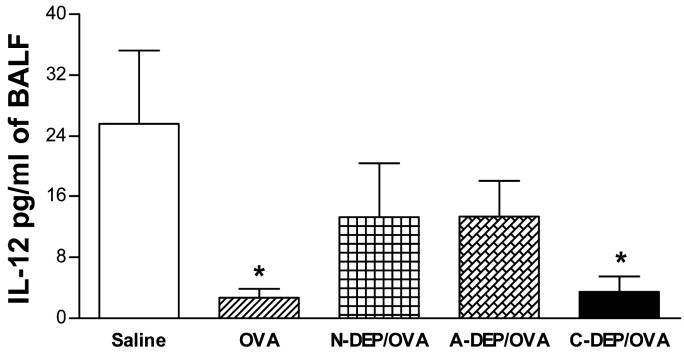

Figure 2.8 IL-12 production levels in the BALF 18 hrs after sensitization. Mice were intranasally instilled with saline, 20 μg of OVA alone or in combination with 150 ug of N-, A-, or C-DEP on days 0 and 12 and necropsied 18 hrs later. IL-12 levels were measured in the BALF by ELISA. $^{*}P<0.05$: significantly less than saline control.

Chapter 3

Differential Transcriptional Changes in Mice Exposed to Chemically Distinct Diesel Samples

Abstract

Epidemiological studies have linked ambient particulate matter with exacerbation of asthmatic symptoms and pulmonary inflammation. Diesel exhaust particles (DEP) are a predominant source of vehicle derived ambient PM and experimental studies have benn shown to be an allergic adjuvant when given with an antigen. We previously assessed the effects of three chemically distinct DEP samples: N-DEP, A-DEP, and C-DEP in a murine ovalbumin (OVA) mucosal sensitization model. The present study exposed mice to these DEP samples with and without OVA on days 0 and 13 and analyzed gene expression changes in the lungs 18 hrs after the last exposure. Transcription expression profiling demonstrated DEP altered cytokine and toll-like receptor pathways regardless of the sample or combination with antigen. Further analysis of DEP exposure with OVA demonstrated the C-DEP/OVA treatment to induce the greatest number of altered genes. While all three DEP/OVA treatments induced cytokine and toll-like receptor pathways to a greater extent than DEP alone, only A- and C-DEP/OVA treatments induced differential expression of apoptosis pathways. The induction of apoptosis pathways by these treatments was associated with a strong adjuvant response post-challenge in the previous study. In addition, the C-DEP/OVA treatment, which had the greatest T_H2 response post-sensitization in the previous study, altered expression of DNA damage pathways. This comprehensive approach using gene expression analysis to examine changes at a pathway level provides a clearer picture of the events occurring in the lung after DEP exposure in the presence or absence of antigen.

3.1 Introduction

Epidemiology studies have reported an association between rises in ambient particle matter (PM) levels and increases in hospital rates due to respiratory illnesses including asthma [216]. Diesel exhaust particles (DEP) are an important contributor to ambient PM and many studies have focused on DEP as a model anthropogenic pollutant. These particles consist of a carbon core surrounded by various amounts of adsorbed organic compounds, including polycyclic aromatic hydrocarbons (PAHs), quinones, and nitro-PAHs [144]. Human and rodent studies have shown DEP to induce allergic lung disease when given with an antigen [15, 121, 217, 218]. Although the biologic mechanisms associated with the adverse health effects of DEP are not well understood, it is likely to involve oxidative stress and inflammation.

The composition of DEP varies greatly depending on the type of engine, load, and method of collection, which in turn can alter its biological function. Singh *et al.* [201] investigated the chemical characteristics and pulmonary toxicity of two different particles, an automobile derived DEP (A-DEP) and National Institute of Standard Technology standard reference material 2975 (N-DEP) generated from a heavy forklift. The two particle samples exhibited disparate pulmonary toxicity which reflected their dissimilar chemical composition.

We previously assessed the effects of N-DEP, A-DEP, and C-DEP (generated from a diesel engine used to power a compressor) in a murine ovalbumin (OVA) mucosal sensitization model [219]. These samples differed in their percentage of dichloromethane (DCM) extractable organic material (EOM); N-DEP, C-DEP, and A-DEP contained 1.5%, 18.9%, and 67%, respectively. Immune and inflammatory endpoints showed that

the potency of C-DEP/OVA ≈ A-DEP/OVA >> N-DEP/OVA with respect to post-challenge adjuvancy as measured by eosinophilic inflammation and T_H2 cytokines in the BALF, serum OVA-specific IgG1 antibodies, and airway hyperresponsiveness. C-DEP/OVA, consistent with the strong degree of adjuvancy post-challenge, increased the influx of eosinophils, neutrophils, and lymphocytes, increased the production of T_H2 cytokines, and decreased the production of the T_H1 cytokine IL-12 in the BALF, 18 hrs after sensitization. On the other hand, post-sensitization differential cell counts and production of T_H1 and T_H2 cytokines were not significantly different for the organic rich A-DEP/OVA compared to OVA control although this group induced a strong adjuvant effect post-challenge. The relatively elemental carbon rich N-DEP/OVA exposures induced a mild T_H2 phenotype post-sensitization followed by a mild adjuvant effect post-challenge. This suggests either the kinetics or the mechanism by which A-DEP/OVA induces allergic lung disease differs from the other DEP samples. The results also demonstrated the degree of adjuvancy was not solely dependent on organic content.

While *in vitro* and *in vivo* microarray studies have been conducted to identify potential mechanisms for the adverse health effects of DEP, there are no reports of global transcriptional changes induced by DEP given with an allergen. In addition, there have not been studies comparing the transcriptional profiles of chemically distinct DEP samples. The present study used microarray analysis of whole-lung RNA to elucidate the pathways and networks involved in the effects of N-DEP, A-DEP, and C-DEP given with or without allergen in BALB/C mice.

3.2 Materials and Methods

3.2.1 Animals

Female BALB/C mice (8-10 weeks old) were obtained from Charles River Laboratories (Raleigh, NC) and allowed to acclimate for a minimum of one week prior to dosing. Mice were randomly assigned to treatment groups and housed in an AAALAC-approved animal facility at the US-EPA. All animal procedures were reviewed and approved by the US-EPA's Institutional Animal Care and Use Committee. Housing environment conditions include a 12-h light/dark cycle at an ambient temperature of 22±1ºC and relative humidity of 55±5ºC. Mice were provided water and mouse chow *ad libitum*. Additional mice from each facility were routinely monitored serologically for Sendai, mouse pneumonia, mouse hepatitis, and other murine viruses, as well as mycoplasma.

3.2.2 Particle samples

Standard Reference Material (SRM) 2975 diesel exhaust particle sample (N-DEP) was purchased from National Institute of Standard Technology (NIST) (Gaithersburg, MD). The reported mean diameter of these particles was 11.2 ±0.1 µm by area distribution, and the surface area, as determined by nitrogen adsorption, was 91μm^2/g. The certified analysis contains 11 certified concentrations and 28 reference concentrations for selected PAHs found in the DEPs. The DEP was generated by a heavy-duty forklift diesel engine and collected under "hot" conditions without a dilution tunnel.

Automobile DEP (A-DEP) was generated and collected under conditions previously described [187, 197]. Briefly, the sample was generated by a light-duty (2740cc), 4-cylinder Isuzu diesel engine. DEP was collected under "cold" (50 ºC) conditions onto glass-fiber filters and on steel duct walls in a constant-volume sampling system fitted at the end of a dilution tunnel.

Compressor DEP (C-DEP) was generated in-house as described by Cao et al [198] at the EPA using a 30 kW (40 hp) 4-cylinder Deutz BF4M1008 diesel engine connected to a 22.3 kW Saylor Bell air compressor to provide 20% load. The generated particles were collected under "hot" conditions in a baghouse.

3.2.3 Experimental design

DEP samples (N-, C-, A-DEP) were suspended at a concentration of 3 mg/ml in saline alone or with 0.4 mg/ml of ovalbumin. Particles were sonicated using a Microson Ultrasonic Cell Disruptor (Micromix) for 10 min. Mice were randomly divided into 8 treatment groups, anesthetized with isofluorane, and exposed to saline, 20 µg OVA, 150 µg DEP, or DEP + OVA intranasal instillation on Days 0 and 13 and necropsied 18 hrs later.

3.2.4 Necropsy and RNA isolation

Mice were euthanized with sodium pentobarbital and bled by cardiac puncture. The chest wall was opened and the left lung lobe was removed, quick frozen in liquid nitrogen, and stored at -80° C. RNA from frozen lung tissue was isolated using RNeasy (Qiagen, Valencia, CA) following manufacture's protocol. Quantity and quality of the

RNA was measured using a Nanospot and Agilent Bioanalyzer (Agilent Technologies, Palo Alto, CA), respectively.

3.2.5 Microarray

RNA samples were prepared, processed, and hybridized to the Affymetrix Mouse 430A gene chip at Expression Analysis (Durham, NC), as described in the GeneChip Expression Analysis Manual (Affymetrix; Santa Clara, CA). The hybridized probe array was stained with streptavidin phycoerythrin conjugate and scanned by the GeneChip® Scanner 3000 (Affymetrix; Santa Clara, CA). The amount of light emitted at 570 nm is proportional to the bound target at each location on the probe array.

The Mouse 430A Genome chip contains over 22,000 probe sets representing over 14,000 well-characterized mouse genes. A detailed description can be found at http://www.affymetrix.com/products/arrays/specific/mouse430.affx. A total of 24 gene chips representing lung samples from 24 individual mice (8 treatments, N=3) were used in this study.

3.2.6 Overall data analysis strategy

The analysis approach of this data set, consisting of 2 controls and 6 treatment groups, was to use a binary comparison approach of each treatment group compared to its respective control: N-DEP and saline, A-DEP and saline, C-DEP and saline, N-DEP/OVA and OVA, A-DEP/OVA and OVA, and C-DEP/OVA and OVA. The analysis of these data sets consisted of: 1) evaluating the data quality; 2) performing principal

components analysis (PCA) for a global inspection of within group sample correspondence and to examine model and dose effects; 3) performing Gene Set Enrichment Analysis (GSEA) to determine differentially expressed gene sets between treatment groups and controls; 4) extracting core genes responsible for a particular gene set identified as significant from the GSEA analysis; 5) determining common genes across treatment groups; 6) mapping core genes to functional pathways using KEGG pathways and MetaCore GENEGO® to identify altered pathways and networks unique or in common among the treatments.

3.2.7 Principal component analysis (PCA)

PCA transforms microarray data from all gene chips to a new coordinate system using an orthogonal linear transformation, which reduces the data to a 3 dimensional coordinate system while retaining those characteristics of the data set that contribute most to the variance. This analysis was employed to survey the data for within-group outliers and model and dose effects using Rosetta Resolver (Rosetta Inpharmatics, Agilent Technologies, Palo Alto, CA) following linear weighting normalization ($p<0.001$). Each individual gene chip or gene expression profile was represented by a single data point and the variance between each gene chip was comparable to the distance between the data points whereby two similar gene expression profiles were projected as two adjacent points and vice versa. This analysis was employed as a visual tool to initially inspect the data for within group and across group similarities and dissimilarities.

3.2.8 Gene set enrichment analysis (GSEA)

GSEA is a powerful computational method that utilizes an *a priori* defined set of genes to determine statistically significant, concordant differences between two phenotypes. For this analysis, raw data from 24 gene chips were quantile normalized using Robust Multichip Average (RMA) in Gene Pattern (www.genepattern.org) to generate estimated expression summaries. The RMA values were imported into GSEA to determine gene sets associated with each diesel treatment group compared to its respective control. The molecular signature database (MSigDB) C2 provided on the website http://www.broad.mit.edu/gsea/msigdb/msigdbindex.html, which contains 1687 gene sets, was queried for association with a particular treatment in each pairwise comparison (N-DEP/OVA and OVA, A-DEP/OVA and OVA, C-DEP/OVA and OVA, N-DEP and saline, A-DEP and saline, and C-DEP and saline). Only gene sets with a minimal gene set size of 15 genes per pathway and a maximum of 90 were queried. We acknowledge our use of GSEA software and Molecular Signature Database (MSigDB) (http://www.broad.mit.edu/gsea/) [220].

3.2.9 Pathway level analysis

The gene sets with an FDR q-value of < 0.01 were used to create a core gene list. The core gene list comprised of genes responsible for a gene set being considered significant. These genes were exported and then applied to two pathway analysis programs, KEGG Pathway Analysis (http://gather.genome.duke.edu/) and MetaCore GENEGO® (http://www.genego.com/metacore), which maps genes to pathways and determines significance. All pathways with a p-value of <0.001 and at least 5 or more differentially expressed genes were reported.

3.3 Results

3.3.1 Principle component analysis (PCA)

PCA was applied to provide a multidimensional gene expression profile of each gene chip in a 3 dimensional space to reveal clusters in the experimental data. All data from the 24 gene chips were analyzed with each dot representing a gene chip (Figure 3.1a). After analysis the gene chips were then highlighted in either blue (OVA treatment) or red (saline control). Good separation of the two groups was observed illustrating a model effect between antigen and saline. The saline group appeared to be more tightly clustered than OVA indicating low within group variability. To determine if exposure to chemically different DEP samples induces diverse genetic profiles, the gene chips were highlighted according to diesel sample (purple- A-DEP and A-DEP/OVA, blue- C-DEP and C-DEP/OVA, green- N-DEP and N-DEP/OVA, and yellow- saline and OVA) (Figure 3.1b). The plot reveals a separation of the saline and OVA treatment groups from DEP treated groups. In addition, clustering of the A-DEP exposed mice regardless of antigen is seen while the N-DEP and C-DEP exposures were clustered separately from N- and C-DEP/OVA groups.

3.3.2 Gene set enrichment analysis (GSEA)

GSEA was developed to overcome the limitations of relatively small individual differential gene expression changes and small sample size. In contrast to conventional microarray analysis programs, the algorithm employed by GSEA derives its power by focusing on gene sets with biological relevance rather than individual genes. [220, 221].

To test for sets of related genes that were altered in the lungs of mice exposed to the various treatments, we employed GSEA. The arrays were separated into 6 binary groups; N-DEP/saline and saline, A-DEP/saline and saline, C-DEP/saline and saline, N-DEP/OVA and OVA, A-DEP/OVA and OVA, and C-DEP/OVA and OVA. The C2 collection of curated gene sets from the MSigDB were queried and a detailed description of each gene set can be found on the website http://www.broad.mit.edu/gsea/msigdb/msigdb_index.html. Gene sets with a false discovery rate (FDR) q-value of < 0.001 were considered significant. The number of significant gene sets associated with N-DEP, A-DEP, and C-DEP, as determined by the pairwise comparisons (DEP exposure and saline control), was 101, 90, and 98, respectively. In the context of antigen, 60, 68, and 113 gene sets were associated with N-, A-, and C-DEP/OVA, respectively. The complete list of the significant gene sets is found in Appendices 1-6.

3.3.3 Venn analyses

Venn analyses were performed to identify the common genes to all DEP exposures. The core genes (those genes responsible for a gene set being considered significant with a FDR q-values of <0.001) were extracted from the significant gene sets associated with each diesel exposure identified by GSEA. A venn diagram was constructed to identify genes common among the 3 DEP/saline exposure pairwise comparisons (Figure 3.2a). ADEP/saline exposure resulted in the greatest number of differentially expressed genes (545). 200 genes were common among all 3 DEP treatments. Similarly a venn diagram was constructed for the genes associated with each

DEP/OVA exposure (Figure 3.2b). CDEP/OVA exposure resulted in greatest number of differentially expressed genes (800). 236 genes were found common to all DEP + OVA exposures. The two sets of common genes were applied to another venn diagram to identify the 117 common genes among all DEP exposures (Figure 3.2c).

3.3.4 KEGG pathway analyses

To understand the biological significance of the common genes associated with the 3 DEP/saline exposures, the 200 genes were imported into the gene annotation tool, Gather (http://gather.genome.duke.edu/), and the genes were mapped to KEGG pathways, using the criteria that pathways must have 5 or more differentially expressed genes and be overrepresented based on a hypergeometric test with p-value <0.001. Cytokine-cytokine receptor interaction and toll-like receptor signaling pathway were common to all DEP/saline exposures (Table 3.1). The 236 genes common among the 3 DEP/OVA exposures also significantly populated the cytokine-cytokine receptor interaction and toll-like receptor signaling pathway as well as the KEGG apoptosis pathway (Table 3.2). Table 3.3, representing the 117 common genes for all DEP/saline and DEP/OVA exposures, contains all but 3 of the genes found in the 2 pathways common to the DEP/saline (Table 3.1). These genes included common proinflammatory cytokines and chemokines such as IL1, IL6, Ccl2, 3, 4, 6, 7, 8, 9, 11, 17, and 22.

To understand the effects of the individual DEP/OVA exposures, the extracted core genes were mapped to KEGG pathways and the results represented in Tables 3.4-3.6. CDEP/OVA altered the most number of pathways. All 3 exposures populated the cytokine-cytokine receptor pathway similarly with 56, 56, and 51 genes for NDEP/OVA,

ADEP/OVA, and CDEP/OVA, respectively. Additionally, the toll-like receptor pathway contained similar amounts of genes with 23, 26, and 28 genes for NDEP/OVA, ADEP/OVA, and CDEP/OVA, respectively. This pathway contained toll-like receptors as well as many proinflammatory cytokines and transcription factors. N-DEP/OVA and C-DEP/OVA altered the expression of genes in the neuroactive ligand-receptor interaction pathway. ADEP/OVA and C-DEP/OVA altered the apoptosis pathway. Pyrimidine metabolism and aminoacyl-tRNA biosynthesis pathways were unique to C-DEP/OVA exposures.

3.3.5 GeneGo analysis

The C-DEP/OVA exposure gave the highest transcriptional changes based on the numbers of significant gene sets, extracted core genes, and the KEGG pathways, however, these analyses were not specific enough to allow an inference as to why or how C-DEP was able to elicit a stronger T_H2 response post-sensitization. We therefore mapped the 3 sets of genes to GeneGo curated databases and the results can be found in Figures 3.3 and 3.4. Figure 3.3 depicts the significance of the top 20 differentially affected GeneGo process networks for all 3 DEP/OVA exposures (N-DEP/OVA-blue; A-DEP/OVA-red; C-DEP/OVA-orange). Using this approach the similarities and differences of the groups are clear. All groups significantly altered networks related to antigen presentation, inflammation, and cell adhesion. In addition the C-DEP/OVA exposure also altered cell cycle, DNA damage, and protein degradation networks.

Differentially affected GeneGo analysis on a pathway level revealed the common pathways were associated with MHC class I antigen presentation, inflammation, and

other pathways related to the innate immune response. The A-DEP/OVA and C-DEP/OVA common pathways were involved with TNF mediated apoptosis pathways whereas C-DEP/OVA alone also induced altered expression of FAS, IAP, and mitochondrial mediated apoptosis and cell cycle regulation pathways (Figure 3.4).

3.4 Discussion

It has been established that DEP can act as an immunologic adjuvant when given with antigen [15, 121, 217, 218]; however, there is still a lack of understanding as to what component or components are responsible for these effects and the underlying mechanisms through which they act. The organic extractable material (EOM) as well as the particle itself has been shown to be responsible for the inflammatory and adjuvant effects [131, 133, 222]. In addition, it has been demonstrated that the physicochemical composition of DEP influences its biological function [1].

We recently reported the adjuvant effects of three DEP samples with different amounts of dichloromethane (DCM) EOM (N-, A-, and C-DEP samples contained 1.5, 67, and 18.9%, respectively) in a murine mucosal sensitization model [219]. The results demonstrated A-DEP/OVA and C-DEP/OVA exposures induced strong allergic responses after antigen challenge, while N-DEP, when given with OVA, was a mild adjuvant. To understand the mechanism behind these responses, we examined changes in the BALF 18 hrs after the last sensitization. The results were C-DEP/OVA > N-DEP/OVA > A-DEP/OVA with respect to cellular influx and T_H2 cytokine production [219].

The present study was designed to identify the global transcriptional changes in

the lung after exposure to the three chemically distinct DEP samples (N-, A-, and C-DEP) with or without OVA. While it is important to identify individual genes that are associated with a toxic response, most toxicity occurs through interactions of multiple genes. Therefore, our approach was to identify pathways common and unique to the DEP/OVA exposures and to associate their transcriptional responses to their allergic phenotype.

It is known that DEP exposure induces lung inflammation. DE and DEP have been shown to induce pulmonary inflammation manifested by neutrophil infiltration and elevated levels of total protein, albumin, LDH, and ROS in the lung as well as up-regulation of inflammatory pathways [201, 217, 219, 223, 224]. Based on these observations, it was no surprise that the cytokine-cytokine receptor pathway was a significantly altered pathway common to all DEP/saline exposures. The genes in this pathway included inflammatory, T_H1, and T_H2 cytokines and chemokines, but the majority of them were associated with neutrophil signaling in the DEP/saline exposures. In agreement with these findings, all three DEP/saline samples induced an increase in neutrophils in the BALF at this time point, although the increase was not significant [219].

Toll-like receptor signaling was also altered in all DEP/saline exposures. Toll-like receptors (TLRs) play important roles in the initiation of both innate and adaptive immune responses [225, 226]. Their activation is usually associated with viral or bacterial exposure; however, TLRs can also signal in response to endogenous molecules and environmental pollutants. NO_2 adjuvant effects are dependent on TLR2 [227], and airway hyperresponsiveness, induced by chronic ozone exposure, is dependent on TLR4

[228]. In addition, Zhou *et al.* [229] reported heat shock induced increases in TLR2 and TLR4 mRNA and protein expression in monocytes. Furthermore, DEP has been shown to induce TLR4 expression in the lung [230] and TLR4 deficient mice develop airway inflammation to a lesser degree in response to DEP compared to control [231]. Our results demonstrated that the toll-like receptor interaction pathway was altered by all three DEP/saline exposures, providing further evidence that the TLR pathway is involved in DEP induced inflammatory responses.

The cytokine-cytokine receptor interaction and toll-like receptor signal pathways were also common pathways associated with all three DEP/OVA exposures but with a greater enrichment of genes in both pathways. In addition, GeneGo pathway analysis revealed significantly altered immune response, inflammatory, and apoptosis pathways. We have previously shown all three DEP/OVA exposures induced allergic adjuvancy after antigen challenge suggesting the pathways presented here may be important early signaling pathways in DEP induced allergic disease.

Li *et al.* [174] proposed a hierarchical oxidative stress model to explain DEP induced effects whereby low levels of oxidative stress induce antioxidant defense mechanisms to restore redox balance in the cell (tier 1). Intermediate levels of oxidative stress (tier 2) activate MAPK and NF-κB cascades, which induce inflammation, while high levels of oxidative stress (tier 3) activate apoptosis and apoptosis/necrosis pathways [174]. The study presented here confirmed similar effects *in vivo.* Antioxidant transcription factor and enzymes such as Nrf2, heme oxygenase 1 (HO-1), and superoxide dismutase 2 (SOD2) were up-regulated in response to all three DEP/OVA exposures indicative of the tier 1 response. The tier 2 responses were also up-regulated:

MAPKs, NF-κB, as well as inflammatory, T_H1, and T_H2 cytokines and chemokines. In addition, A- and C-DEP/OVA exposures altered apoptosis (tier 3) pathways; however, C-DEP/OVA significantly altered the greatest number of these pathways. Furthermore, the apoptosis pathway representation appears to coincide with the combined phenotypic allergic responses of the three DEP/OVA. Although ROS production was not measured, the results suggest that C-DEP/OVA, according to the hierarchical stress model, induced high levels of oxidative stress.

It has been established that DEP organic compounds can generate reactive oxygen species (ROS) [232] and excessive ROS production can lead to a variety of cellular responses including DNA damage [233]. In fact, oxidative DNA damage (8-hydroxydeoxyguanosine) has been detected in mouse lung DNA after DEP exposure [234]. Although the A-DEP sample contained the greatest amount of DCM EOM, in the present study, C-DEP/OVA exposure was unique in significantly altering cell cycle and DNA damage pathways. Global transcriptional analysis of lung tissue revealed up-regulation of cell cycle control genes including 6 cyclin genes, 7 cell division cycle genes, 7 members of the family of MAP kinases, 2 cyclin-dependent kinases, RAS p21 protein activator 3 (Rasa3), and 5 other RAS related proteins.

In conclusion mice exposed to all three DEP samples with or without OVA had altered cytokine and toll-like receptor pathways suggesting these responses are a DEP chemical class signature rather than an effect of a particular component of DEP (i.e. the percentage of DCM EOM). All DEP/OVA exposures increased transcription of genes involved in the hierarchical stress response model described by Li *et al*. [166, 174, 175]. CDEP/OVA exposure significantly altered the most number of apoptosis pathways as

well as cell cycle and DNA damage pathways suggesting the C-DEP is the most bioactive sample. This comprehensive approach using gene expression analysis to examine pathway changes at a transcriptional level provides a clearer picture of the events occurring in the lung after DEP exposure in the presence or absence of antigen. Genomic analysis revealed a wide range of altered pathways suggesting this method may be more sensitive and can be used for identifying mechanisms involved in adverse effects of inhaled pollutants.

Tables

Table 3.1 KEGG pathways mapped from the 200 common genes associated with DEP/saline exposure

KEGG Pathway	# Genes	p Value
Cytokine-cytokine receptor interaction	28	< 0.0001
Ccl17 Ccl2 Ccl22 Ccl3 Ccl4 Ccl6 Ccl7 Ccl8 Ccl9 Ccr1 Ccr2 Csf2 Csf2rb1 Cxcl1 Cxcl10 Cxcl13 Cxcl2 Cxcl5 Ifngr2 Il1b Il1r2 Il8rb Inhba Ltb Osmr Tnf Tnfrsf1b Tnfrsf9		
Toll-like receptor signaling pathway	11	< 0.0001
Ccl3 Ccl4 Cd14 Cxcl10 Il1b Nfkb2 Nfkbia Pik3cd Rac2 Tlr2 Tnf		

Table 3.2 KEGG pathways mapped from the 236 genes common to all DEP/OVA exposure

KEGG Pathway	# Genes	p Value
Cytokine-cytokine receptor interaction	40	< 0.0001
Ccl11 Ccl17 Ccl2 Ccl22 Ccl3 Ccl4 Ccl6 Ccl7 Ccl8 Ccl9 Ccr1 Ccr2 Ccr5 Csf1 Csf2 Csf2ra Csf2rb1 Csf2rb2 Csf3r Cxcl1 Cxcl10 Cxcl11 Cxcl13 Cxcl2 Cxcl5 Cxcl9 Ifngr2 Il1a Il1b Il1r1 Il1r2 Il2rg Il6 Il8rb Osmr Tgfb1 Tnf Tnfrsf1b Tnfrsf5 Tnfrsf9		
Toll-like receptor signaling pathway	17	< 0.0001
Ccl3 Ccl4 Cd14 Cxcl10 Cxcl11 Cxcl9 Ikbke Il1b Il6 Lbp Nfkb1 Nfkb2 Pik3cd Rac2 Stat1 Tlr2 Tnf		
Apoptosis	11	0.0002
Birc3 Cflar Csf2rb1 Csf2rb2 Il1a Il1b Il1r1 Nfkb1 Nfkb2 Pik3cd Tnf		

Table 3.3 KEGG pathways mapped from the 117 genes common to both DEP/OVA and DEP/saline exposure

KEGG Pathway	# Genes	p Value
Cytokine-cytokine receptor interaction	26	< 0.0001
Ccl17 Ccl2 Ccl22 Ccl3 Ccl4 Ccl6 Ccl7 Ccl8 Ccl9 Ccr1 Ccr2 Csf2 Csf2rb1 Cxcl1 Cxcl10 Cxcl13 Cxcl2 Cxcl5 Ifngr2 Il1b Il1r2 Il8rb Osmr Tnf Tnfrsf1b Tnfrsf9		
Toll-like receptor signaling pathway	10	< 0.0001
Ccl3 Ccl4 Cd14 Cxcl10 Il1b Nfkb2 Pik3cd Rac2 Tlr2 Tnf		

Table 3.4 KEGG pathway mapped from the 526 genes associated with N-DEP/OVA exposure

KEGG Pathway	# Genes	p Value
Cytokine-cytokine receptor interaction Ccl11 Ccl17 Ccl2 Ccl22 Ccl3 Ccl4 Ccl6 Ccl7 Ccl8 Ccl9 Ccr1 Ccr2 Ccr5 Ccr6 Ccr7 Csf1 Csf1r Csf2 Csf2ra Csf2rb1 Csf2rb2 Csf3r Cxcl1 Cxcl10 Cxcl11 Cxcl13 Cxcl2 Cxcl5 Cxcl9 Ifnar1 Ifnar2 Ifngr2 Il10ra Il15 Il18rap Il1a Il1b Il1r1 Il1r2 Il2 Il2ra Il2rg Il3ra Il6 Il7r Il8rb Ltb Osmr Tgfb1 Tnf Tnfrsf10b Tnfrsf13c Tnfrsf1b Tnfrsf5 Tnfrsf9 Tnfsf9	56	< 0.0001
Toll-like receptor signaling pathway Ccl3 Ccl4 Cd14 Cd86 Cxcl10 Cxcl11 Cxcl9 Fos Ifnar1 Ifnar2 Ikbke Il1b Il6 Lbp Nfkb1 Nfkb2 Nfkbia Pik3cd Rac2 Stat1 Tlr2 Tlr7 Tnf	23	< 0.0001
Neuroactive ligand-receptor interaction Adora2b C3ar1 Ctsg Fpr1 P2ry6 Ptger4	6	0.0002

Table 3.5 KEGG pathways mapped from the 483 genes associated with A-DEP/OVA exposure

KEGG Pathway	# Genes	p Value
Cytokine-cytokine receptor interaction Ccl11 Ccl17 Ccl2 Ccl22 Ccl3 Ccl4 Ccl6 Ccl7 Ccl8 Ccl9 Ccr1 Ccr2 Ccr4 Ccr5 Csf1 Csf2 Csf2ra Csf2rb1 Csf2rb2 Csf3r Cxcl1 Cxcl10 Cxcl11 Cxcl13 Cxcl2 Cxcl5 Cxcl9 Ifnar2 Ifnb1 Ifng Ifngr2 Il12a Il12b Il12rb1 Il1a Il1b Il1r1 Il1r2 Il2 Il2rg Il4 Il5 Il6 Il8rb Inhba Osmr Tgfb1 Tgfbr1 Tnf Tnfrsf1a Tnfrsf1b Tnfrsf5 Tnfrsf9 Tnfsf10 Tnfsf13 Tnfsf13b	56	< 0.0001
Toll-like receptor signaling pathway Ccl3 Ccl4 Cd14 Cxcl10 Cxcl11 Cxcl9 Ifnar2 Ifnb1 Ikbke Il12a Il12b Il1b Il6 Lbp Map3k7ip1 Mapk13 Myd88 Nfkb1 Nfkb2 Nfkbia Pik3cd Rac2 Stat1 Tlr1 Tlr2 Tnf	26	< 0.0001
Apoptosis Bax Birc3 Capn1 Casp3 Cflar Csf2rb1 Csf2rb2 Il1a Il1b Il1r1 Myd88 Nfkb1 Nfkb2 Nfkbia Pik3cd Ripk1 Tnf Tnfrsf1a Tnfsf10	19	< 0.0001

Table 3.6 KEGG pathways mapped from the 800 genes associated with C-DEP/OVA exposure

KEGG Pathway	Genes	p Value
Apoptosis Apaf1 Bax Bid Birc2 Birc3 Casp3 Casp7 Casp8 Cflar Chuk Csf2rb1 Csf2rb2 Dffa Ikbkb Il1a Il1b Il1r1 Il3ra Irak1 Myd88 Nfkb1 Nfkb2 Pik3cd Ripk1 Tnf Tnfrsf1a Tradd Traf2	28	< 0.0001
Cytokine-cytokine receptor interaction Ccl11 Ccl17 Ccl2 Ccl22 Ccl3 Ccl4 Ccl6 Ccl7 Ccl8 Ccl9 Ccr1 Ccr2 Ccr5 Csf1 Csf2 Csf2ra Csf2rb1 Csf2rb2 Csf3r Cxcl1 Cxcl10 Cxcl11 Cxcl13 Cxcl2 Cxcl5 Cxcl9 Ifngr2 Il10ra Il1a Il1b Il1r1 Il1r2 Il2rb Il2rg Il3ra Il6 Il7r Il8rb Inhba Ltb Osmr Tgfb1 Tgfbr1 Tnf Tnfrsf1a Tnfrsf1b Tnfrsf25 Tnfrsf5 Tnfrsf9 Tnfsf13b Tnfsf9	51	< 0.0001
Aminoacyl-tRNA biosynthesis Aars Cars Fars1 Farslb Gars Iars Kars Nars Rars Tars Vars2 Wars Yars	13	< 0.0001
Toll-like receptor signaling pathway Casp8 Ccl3 Ccl4 Cd14 Chuk Cxcl10 Cxcl11 Cxcl9 Ikbkb Ikbke Il1b Il6 Irak1 Lbp Ly96 Map2k4 Map3k7 Mapk13 Myd88 Nfkb1 Nfkb2 Pik3cd Rac2 Stat1 Tlr2 Tlr4 Tlr7 Tnf	28	< 0.0001
Pyrimidine metabolism Ctps Dck Dtymk Dut Ecgf1 Nme1 Nme2 Pola2 Pold1 Pold2 Pole2 Polr2g Polr2h Polr3k Prim1 Rrm2 Txnrd1 Umpk Umps Upp1	21	< 0.0001
Neuroactive ligand-receptor interaction Adora2b Bzrp C3ar1 Grik5 Gzma P2ry6 Ptger4	7	< 0.0001

Figures

A.

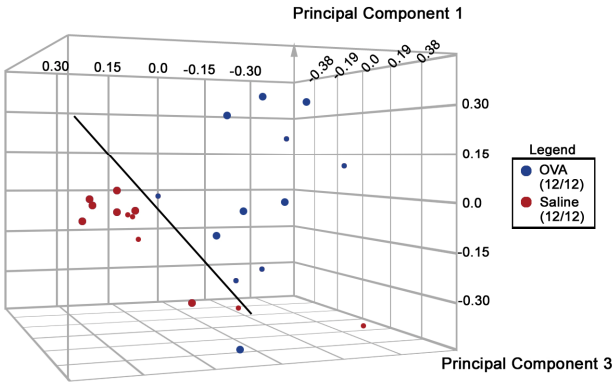

B.

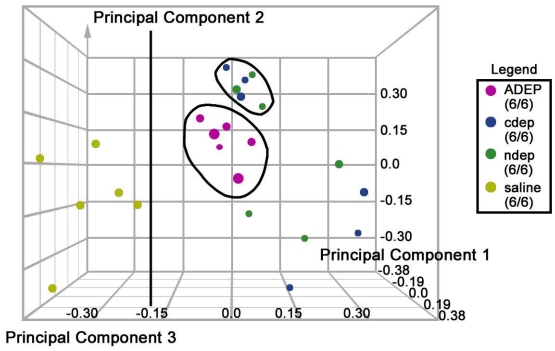

Figure 3.1 Principle component analysis plot from microarray data. PCA plots were created in Rosetta Resolver. Each plot contains gene chips from all mice and each dot represents a gene chip. Gene chips were highlighted according to the immunization protocol (blue-OVA treatment or red-saline treatment) (**A**) or the diesel exposure (yellow- saline and saline/OVA, pink- A-DEP and A-DEP/OVA, blue- C-DEP/saline and C-DEP/OVA, and green- N-DEP/saline and N-DEP/OVA) (**B**).

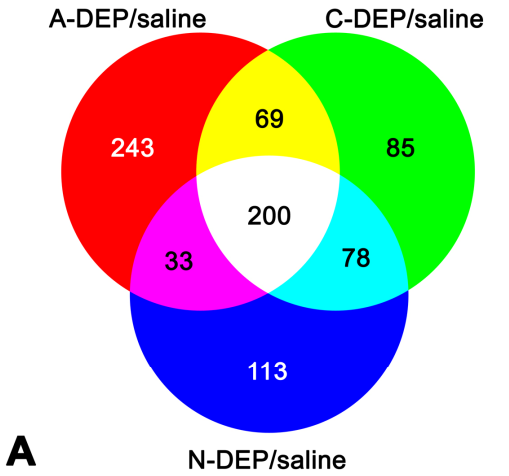

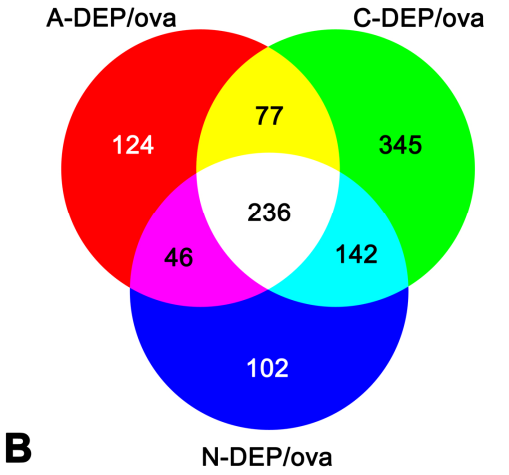

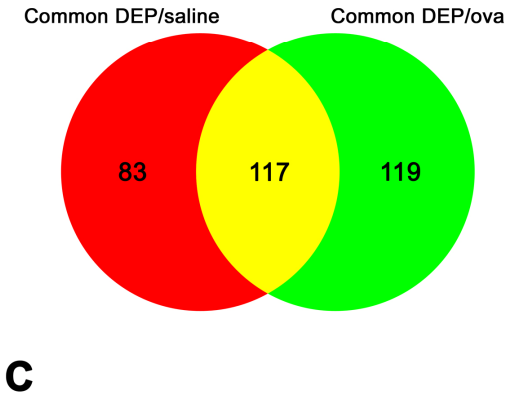

Figure 3.2 Venn analyses. Venn analyses of the core genes from significantly altered gene sets associated with each exposure

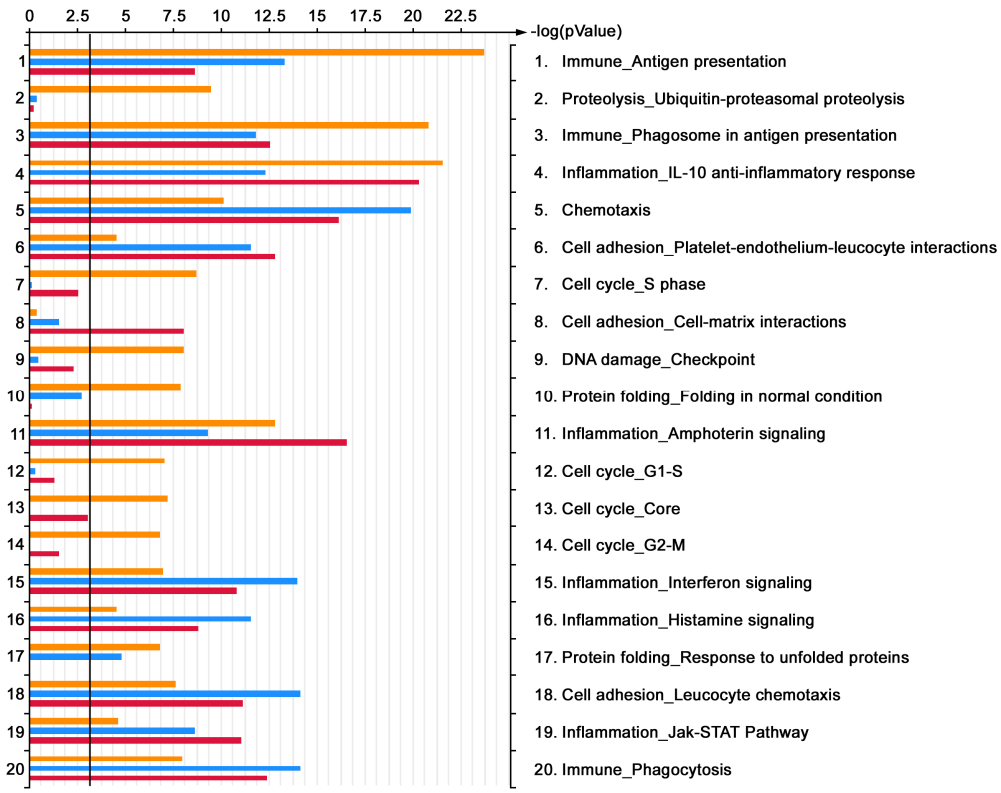

Figure 3.3 Results of GeneGo mapping of differentially affected networks.

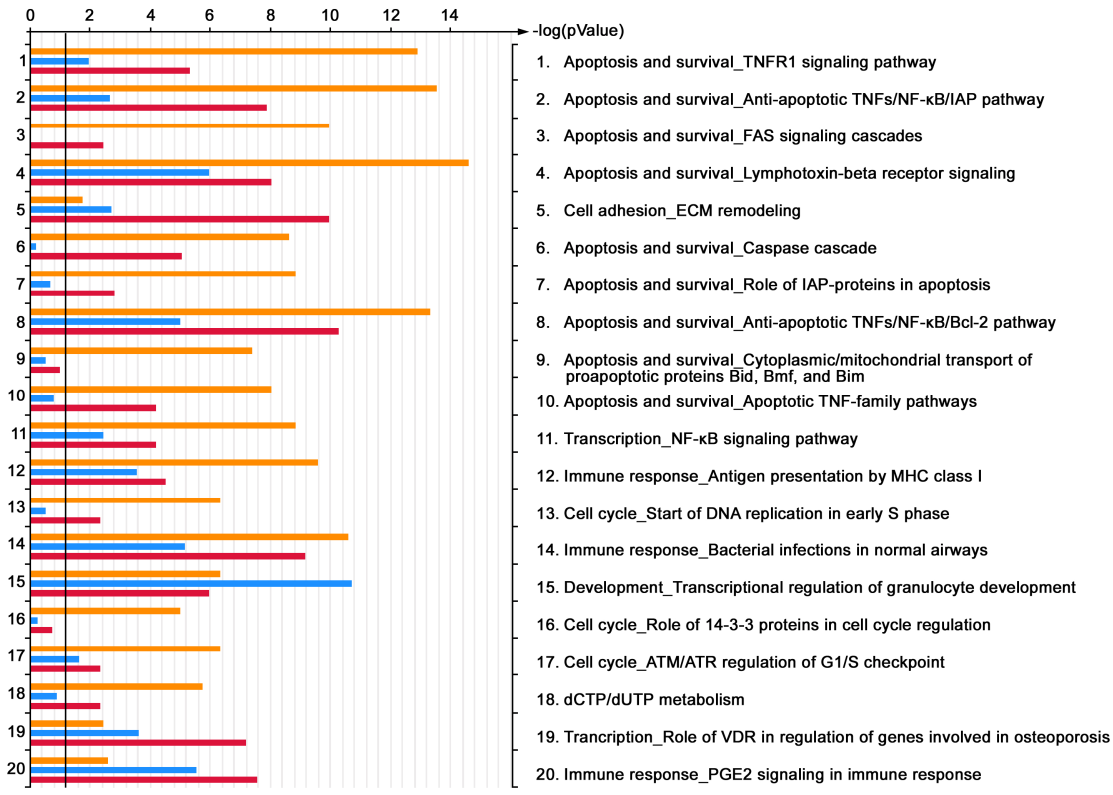

Figure 3.4 Results of GeneGo mapping of differentially affected pathways.

Chapter 4

Increased Transcription of Immune and Metabolic Pathways in Naïve and Allergic Mice Exposed to Diesel Exhaust

Abstract

Diesel exhaust (DE) has been shown to enhance allergic sensitization in animals following high dose instillation or chronic inhalation exposure scenarios. The purpose of this study was to determine if short term exposures to diluted DE enhance allergic immune responses to antigen, and identify possible mechanisms using microarray technology. BALB/c mice were exposed to filtered air or diluted DE to yield particle concentrations of 500 or 2000 $\mu g/m^3$ 4 hr/day on days 0-4. Mice were immunized intranasally with ovalbumin (OVA) antigen or saline on days 0-2, challenged on day 18 with OVA or saline, and all mice were challenged with OVA on day 28. Mice were necropsied either 4 hrs after the last DE exposure on day 4, or 18, 48, and 96 hrs after the last challenge. Immunological endpoints included OVA-specific serum IgE, biochemical and cellular profiles of bronchoalveolar lavage (BAL), and cytokine production in the BAL. OVA-immunized mice exposed to both concentrations of DE had increased eosinophils, neutrophils, lymphocytes, and IL-6 post-challenge compared to OVA control, while DE/saline exposure yielded increases in neutrophils at the high dose only. Transcriptional microarray analysis 4 hrs after the last DE exposure demonstrated distinct gene expression profiles for the high dose DE/OVA and DE/saline groups. DE/OVA induced oxidative stress and metabolism pathways while DE in the absence of immunization modulated cell cycle control, growth and differentiation, G-proteins, and cell adhesion pathways. This study shows for the first time early changes in gene expression induced by the combination of diesel exhaust inhalation and mucosal immunization, which resulted in stronger development of allergic eosinophilia.

4.1 Introduction

The prevalence of allergic asthma has risen over the last 4 decades and has been linked to increased urbanization and exposure to airborne pollutants [235-237]. Recent studies have shown that the actual incidence of asthma could be related to residential highway proximity [238, 239] or average ozone exposure concentrations [240, 241]. A large contributor to urban air pollution and ambient particulate matter (PM) is diesel exhaust (DE). Human occupational exposures to DE range from 1-100 µg/m3 (eight-hour averages) in the trucking and transportation industry, average 225 µg/m3 (time-weighted average with adjustment for background levels) for Boston and New York firefighters, and 100-1700 µg/m3 for underground miners [242, 243]. Experiments in mice have shown that inhalation of fresh DE or intrapulmonary instillation of diesel exhaust particles (DEPs) results in adjuvant activity that increases the sensitization to allergens [14, 15, 244]. Most of these studies used high dose instillation or chronic inhalation exposure scenarios to demonstrate this detrimental health effect while some limited instillation studies showed similar effects in humans [122, 135].

The mechanisms by which DE acts as an adjuvant are complex. The adjuvant potential of DE has been attributed to the generation of reactive oxygen species (ROS) by pro-oxidative organic chemical compounds on the surface of the particles [158, 164, 165, 245]. There is good evidence, however, that the carbon core of DEPs also imparts adjuvant activity through ROS production, as can accompanying gases such as NO_2 [123, 189, 246-248]. ROS generation by any of these components of DE may lead to a 3 tier hierarchical oxidative stress response described by Li and co-workers (2003). Initial responses to oxidative stress first lead to the induction of antioxidant and detoxification

mechanisms which restore cellular homeostasis (tier 1). If the capacity of these systems is overwhelmed, the ensuing inflammation (tier 2) leads to apoptosis (tier 3) [174]. The importance of oxidative stress in promoting allergic immune responses is supported by reversal of these effects with thiol anti-oxidants [158, 249].

After DE exposure in the context of antigen, components of the immune response responsible for allergic sensitization, such as IL-4, IL-5 and IL-13, are upregulated. This immune skewing results in a bias towards T-helper 2 immune activity, and increased development of IgE antibodies [42]. Following antigen challenge there are subsequent increases in clinical indicators of asthma such as eosinophilic lung inflammation, airway hyperresponsiveness, and airway mucous production [42]. While the chemical components of DE that cause these adjuvant effects under high dose conditions are diverse, demonstrating significant affects with more realistic inhalation exposure scenarios has been challenging because resultant changes in response are much smaller in magnitude.

Inhalation exposure studies are important from a dosimetry perspective for risk assessment calculations. Because low levels of DE exposure cause minimal changes in disease over short exposure periods, we sought to investigate more sensitive measures of altered immune function and early signaling pathways. The field of toxicogenomics has allowed simultaneous comparison of thousands of genes following experimental perturbations. Accompanying data sets and analytical software packages have been critical in identifying pathways as opposed to comparing single genes [250]. While some *in vitro* genomic studies of DEPs have been reported, no data are currently available for *in vivo* inhalation exposures. Furthermore, the interaction with antigen sensitization has

not been studied with a broad toxicogenomic pathway analysis approach.

In this study mice were exposed by whole-body inhalation to filtered air or DE diluted to yield 500 or 2000 µg/m^3 of DEP. Exposures were conducted for 4 hr/day over 5 consecutive days (days 0-4). On days 0, 1, and 2, mice were intranasally instilled with 100 µg of OVA or saline. Day 18 mice were either challenged with OVA or saline and all mice were challenged with OVA on day 28. Effects were assessed after the 2° challenge to confirm that mild adjuvancy was accomplished. Lung tissues taken 4 hrs after the last DE exposure on day 4 were assessed for alterations in global gene expression as an indicator of changes associated with later development of clinical disease.

4.2 Materials and Methods

4.2.1 Animals

Pathogen-free BALB/c female mice, 10-12 wk old, weighing 17-20 g, were purchased from Charles River (Raleigh, NC). All of the animals were housed in AAALAC-approved animal facilities with high-efficiency particulate air filters and received access to food and water *ad libitum*. The studies were conducted after approval by the laboratory's Institutional Animal Care and Use Committee.

4.2.2 Diesel Exhaust Exposure and Monitoring

Diesel exhaust was generated in-house using a 30 kW (40 hp) 4-cylinder Deutz BF4M1008 diesel engine connected to a 22.3 kW Saylor Bell air compressor to provide a load. Diesel fuel was purchased from a local (Research Triangle Park, NC) service station and stored in drums. Replicate analysis (ultimate, elemental, heating value, and

specific gravity) of multiple batches of fuel purchased over time indicated consistent fuel properties and composition (data not shown). Engine lubrication oil (Shell Rotella, 15W-40) was changed before each set of exposure tests. The engine and compressor were operated at steady-state to produce 0.8 m^3/min of compressed air at 400 kPa. This translates to approximately 20% of the engine's full-load rating. From the engine exhaust, a small portion of the flow (14 L/min) was educted by an aspirator (3:1 dilution) to a second cone diluter (10:1 dilution), and then through approximately 15 m of flexible food grade polyvinyl chloride (PVC) tubing (7.62 cm inside diameter) to two stainless steel 0.3 m^3 Hinners inhalation exposure chambers housed in an isolated animal exposure room. The dilution air used was drawn from the animal exposure room through a high efficiency particulate air (HEPA) filter. Target DEP concentrations in the two chambers were 2000 µg/m^3 (high) and 500 µg/m^3 (low). Control animals were housed in a third chamber supplied with the same HEPA filtered room air. DEP concentrations in the low (500 µg/m^3) chamber were achieved by additional dilution using HEPA filtered room air just prior to entering the chamber. All three chambers were operated at the same flow rate (142 L/min) which resulted in 28 air exchanges per hour.

Integrated 4 h filter samples (14.1 L/min) were collected once daily from each chamber and analyzed gravimetrically to determine particle concentrations. In addition, 8 and 20 min quartz filter samples (14.1 L/min) were collected from the high and low chambers, respectively, and analyzed using a thermal/optical carbon analyzer (Sunset Laboratory Inc., model 107, Tigard, OR) to determine organic carbon/elemental carbon (OC/EC) partitioning of the collected DEP. Continuous emission monitors (CEMs) were used to measure chamber concentrations of PM by tapered element oscillating

microbalance (TEOM, Rupprecht and Patashnick Co., series 1400, Albany, NY); oxygen (O_2, Beckman Corp., model 755, La Habra, CA); and carbon monoxide (CO., model 48, Franklin), nitric oxide and nitrogen dioxide (NO and NO_2, model 42c., Franklin), and sulfur dioxide (SO_2, model 43c, Franklin) by Thermo Electron Corp., Franklin (Waltham, MA). Samples were extracted through fixed stainless steel probes in the exposure chambers. Gas samples were passed through a particulate filter prior to the individual gas analyzers. Dilution air was adjusted periodically to maintain target PM concentrations as measured by the TEOM. Particle size distributions were characterized using a scanning mobility particle sizer (SMPS, TSI Inc., model 3080/3022a, St. Paul, MN) and an aerodynamic particle sizer (APS, TSI Inc., model 3321, St. Paul, MN). Chamber temperatures, relative humidity, and noise were also monitored, and maintained within acceptable ranges.

4.2.3 Experimental Design

Figure 4.1 depicts the exposure regimen utilized for diesel exhaust exposure and intranasal ovalbumin (OVA) immunization and challenge. Mice were exposed to HEPA filtered air or DE at a particle concentration of 500 or 2000 $\mu g/m^3$ 4 hr/day for 5 consecutive days. The intranasal antigen exposure regimen used was a modification of that used by Farraj *et al.* [251]. Mice were anesthetized in a small plexiglass box using vaporized isofluorane (Webster Veterinary Supply Inc., Sterling, MA). Anesthetized mice were treated with an intranasal instillation (IN) of 100 µg of ovalbumin (OVA; Sigma-Aldrich Inc, St. Louis, MO) in 20 µl of sterile saline (Hospira Inc., Lake Forest, IL) or saline only (as negative control) divided evenly between each nare. The

immunization phase consisted of a single instillation of OVA or saline once per day, 40 min after DE exposure, for 3 consecutive days (days 0-2). Immunized mice were challenged on days 18 and 28 with the same volume and concentration of antigen as the instillations during the immunization phase and naïve mice were instilled with saline on day 18 and OVA on day 28. Mice were either necropsied 4 hrs after the final chamber exposure on day 4, or 18, 48, or 96 hrs after the 2° OVA challenge.

4.2.4 Bronchoalveolar lavage fluid

Mice from each treatment group were euthanized with sodium pentobarbital and the trachea was exposed, cannulated, and secured with suture thread. The left mainstem bronchus was isolated and clamped with a microhemostat. The right lungs lobes were lavaged 3 times with a single volume of warmed Hanks balanced salt solution (HBSS) (Invitrogen, Grand Island, NY) (35ml/kg). The resulting lavage was centrifuged (717 x g, 15 min, 4° C) and 150 µl was stored at 4° C (for biochemical analysis) or -80° C (for cytokine measurement). The pelleted cells were resuspended in 1 ml of RPMI 1640 (Gibco, Carlsbad, CA) containing 2.5 % fetal bovine serum (FBS; Gibco, Carlsbad, CA). Total cell counts in the lavage fluid of each mouse were obtained with a Coulter Counter (Beckman Dickson). Each sample (200 µl) was centrifuged in duplicate onto slides using a Cytospin (Shandon, Pittsburgh, PA) and subsequently stained with Diff Quik solution (American Scientific, McGraw Park, PA) for cell differentiation determination, with at least 200 cells counted from each slide. The left lobe was removed for RNA isolation at the 4 hr time point post immunization.

4.2.5 Cytokine measurements

Macrophage inflammatory protein-2 (MIP-2), IL-4, IL-5, IL-6, IL-10, IL-12, and TNFα concentrations in bronchoalveolar lavage fluid (BALF) were measured by enzyme-linked immunosorbent assay (ELISA) with commercially available paired antibodies per manufacturer's instructions (Pharmingen, Franklin Lakes, NJ).

4.2.6 Cellular biochemistry

Lactate dehydrogenase (LDH) and total protein were modified for use on a Konelab 30 clinical chemistry analyzer (Thermo Clinical Lab systems Espoo, Finland). Activity for LDH was determined using a commercially available kit from Thermo DMA Corp (Cincinnati, OH). Total protein concentrations were determined with the Coomassie plus protein Reagent (Pierce Chemical, Rockford, IL) with a standard curve prepared with bovine serum albumin from Sigma-Aldrich (St. Louis, MO).

4.2.7 Antigen-specific serum IgE

Antigen-specific serum IgE production was measured by enzyme-linked immunosorbent assay (ELISA). Briefly, 96 well flat-bottom ELISA plates were coated with 100 µl of OVA at a concentration of 2 µg/ml and incubated overnight at 4°C. The following day, after a nonspecific protein blocking step using bovine serum albumin (BSA) and washing, 100µl of each serum sample and an OVA-specific IgE antibody (Serotec, Ltd., Oxford, UK) for the standand control was added in duplicate wells to the plates. Following an overnight incubation at 4°C and washing, the plates were treated successively with 100 µl/well of biotinylated rat anti-mouse IgE (Serotec, Ltd., Oxford,

UK), horseradish peroxidase-streptavidin (diluted 1:1500), with washes and incubation for 1 hr at room temperature between each of these steps. Finally, 100 µl/well TM Blue (Dako Corporation, Carpinteria, CA) was added as a substrate for horseradish peroxidase and reactions were allowed to develop at room temperature for at least 10 minutes. Plates were read at 650 nm by a Spectromax ELISA plate reader (Molecular Devices, Menlo Park, CA).

4.2.8 RNA isolation

RNA from frozen lung tissue was isolated using RNeasy (Qiagen, Valencia, CA) following manufacture's protocol. Quantity and quality of the RNA was measured using a Nanospot and Agilent Bioanalyzer (Agilent Technologies, Palo Alto, CA), respectively.

4.2.9 Microarray

RNA samples were prepared, processed, and hybridized to the Affymetrix Mouse 430A gene chip at Expression Analysis (Durham, NC), as described in the GeneChip Expression Analysis Manual (Affymetrix; Santa Clara, CA). The Mouse 430A Genome chip contains over 22,000 probe sets representing over 14,000 well-characterized mouse genes. A detailed description can be found at http://www.affymetrix.com/products/arrays/specific/mouse430.affx. A total of 24 gene chips representing 4 hr samples from 24 individual mice (6 treatments, N=4) were used in this study. The microarray data have been deposited at Genome Expression Omnibus

database (http://www.ncbi.nlm.nih.gov/geo/) and are accessible through GEO series accession number GSE9383.

4.2.10 Statistical analysis of inflammatory, biochemical, and immune endpoints

The data were analyzed using a two-way analysis of variance (ANOVA) model. The two independent variables were exposure (DEP at levels 0, 500, and 2000 $\mu g/m^3$) and treatment (at levels saline and OVA). Pair-wise comparisons were performed as subtests of the overall ANOVA, subsequent to a significant main or interactive effect. If the usual ANOVA assumptions were not satisfied, either the data were log transformed so as to satisfy the assumptions or a distribution free test was substituted for the ANOVA. The level of significance was set at 0.05. No adjustment was made to the significance level as a result of multiple comparisons.

4.2.11 Overall data analysis strategy

The analysis of this data set consisted of 6 groups (filtered air, 500 $\mu g/m^3$ [low], or 2000 $\mu g/m^3$ [high] DE with or without OVA). Steps were made to: 1) evaluate the data quality; 2) perform principal components analysis (PCA) for a global inspection of within group sample correspondence and to examine model and dose effects; 3) perform Gene Set Enrichment Analysis (GSEA) to determine differentially expressed gene sets between groups; 4) extract core genes responsible for a particular gene set identified as significant from the GSEA analysis; and 5) map core genes to functional pathways using MetaCore GENEGO® to identify altered pathways unique or in common among the treatments.

4.2.12 Principal component analysis (PCA)

PCA transforms microarray data from all gene chips to a new coordinate system using an orthogonal linear transformation, which reduces the data to a 3 dimensional coordinate system while retaining those characteristics of the data set that contribute most to the variance. This analysis was employed to survey the data for within-group outliers and model and dose effects using Rosetta Resolver (Rosetta Inpharmatics, Agilent Technologies, Palo Alto, CA) following linear weighting normalization ($p<0.001$). Each individual gene chip or gene expression profile was represented by a single data point and the variance between each gene chip was comparable to the distance between the data points whereby two similar gene expression profiles were projected as two adjacent points and vice versa. This analysis was employed as a visual tool to initially inspect the data for within group and across group similarities and dissimilarities.

4.2.13 Gene set enrichment analysis (GSEA)

GSEA is a powerful computational method that utilizes an *a priori* defined set of genes to determine statically significant, concordant differences between two phenotypes. For this analysis, raw data from 24 gene chips were normalized using Robust Multichip Average (RMA) in Gene Pattern (www.genepattern.org) to generate estimated expression summaries. The molecular signature database (MSigDB) C2 provided on the website http://www.broad.mit.edu/gsea/msigdb/msigdbindex.html, which contains 1687 gene sets, was queried for association with a particular treatment in each pairwise comparison (low DE/OVA vs. air/OVA, high DE/OVA vs. air/OVA, high DE/saline vs. air/saline,

air/OVA vs. air/saline, low DE/OVA vs. low DE/saline, and high DE/OVA vs. high DE/saline). Only gene sets with a minimal gene set size of 15 genes per pathway and a maximum of 500 were queried. To determine the significance of a gene set for each pairwise comparison, GSEA ranked all genes according to the difference in expression using a signal-to-noise metric. A running sum statistic termed the enrichment score (ES) was determined for each gene set and the maximum ES (MES) over all gene sets in the actual data was recorded. The ES reflects the degree to which a gene set is overrepresented at the top or bottom of the ranked genes. To determine the significance of the MES, a comparison was made between the actual MES and that seen in 1000 permutations that shuffled the gene set labels creating a null distribution. In addition the data were normalized based on the size of the gene set (normalized expression set [NES]). A false discovery rate (FDR) was calculated corresponding to each NES. Gene sets with a FDR of <25% were considered significant. Heatmaps were generated from the top 50 genes that were most strongly associated with the DE or DE/OVA treatment. GSEA software and Molecular Signature Database (MSigDB) are available at http://www.broad.mit.edu/gsea/[220].

4.2.14 Pathway level analysis

The gene sets with an FDR of <25% were used to create a core gene list. The core gene list comprised genes responsible for a gene set being considered significant. These genes were then applied to a pathway analysis program called MetaCore GENEGO® (http://www.genego.com/metacore), which maps genes to pathways and determines significance. All pathways with a p-value of <0.01 were reported.

4.3 Results

4.3.1 Diesel exposures

Table 4.1 shows a summary of the 5 day average exposure data for the low (500 $\mu g/m^3$) and high (2000 $\mu g/m^3$) DE concentrations. These target chamber concentrations, determined and adjusted based on continuous TEOM measurements were achieved with relatively low variability either within a particular 4 hr exposure or between different days. Chamber particle concentrations determined gravimetrically from integrated filter samples (one 4 hr sample per exposure day), agreed with the TEOM measurements within 10%. CO, NO, NO_2, and SO_2 concentrations in the high chamber averaged 4.3, 9.2, 1.1, and 0.2 ppm, respectively. Concentrations in the low chamber were below detection limits, as indicated. Particle number concentrations were relatively high, and corresponded to particle size distributions (PSDs) with a well established accumulation mode and little evidence of notable nuclei or coarse modes. Geometric median number and volume (assuming spherical particles) diameters of 86 and 195 nm, respectively, were measured in both chambers. OC/EC wt ratios of 0.7 from both chambers indicate that approximately 41% of the DEP was comprised of organic carbon.

4.3.2 Post-challenge endpoints

Ovalbumin specific IgE antibodies

Mice exposed to the low and high DE during local immunization produced increasing OVA-specific IgE antibodies over time. Mice exposed to the high dose of DE

(2000 µg/m^3) had a mild but non-significant increase (relative to OVA control) in these antibodies at the 48 hr time point (Figure 4.2). In the absence of immunization with OVA, OVA-specific IgE antibodies were not detected (data not shown).

Bronchoalveolar lavage cell differential counts

To evaluate the effect of DE exposure with or without OVA immunization on airway inflammation post-challenge, the cellular profile of BALF fluid 18, 48, and 96 hrs after OVA challenge was assessed. Cell profiles at the 18 and 96 hr time points did not differ across treatment groups. At the 48 hr time point however, eosinophils, neutrophils, and lymphocytes were statistically increased in ova immunized mice exposed to both concentrations of DE (Figure 4.3). With DE exposure alone, only neutrophils were statistically increased in the high DE concentration.

Cytokine production in the bronchoalveolar lavage fluid

To characterize the role of local cytokine production on the effects of DE in an ovalbumin immunization model, the production of macrophage inflammatory protein-2 (MIP-2), IL-4, IL-5, IL-6, IL-10, IL-12, and TNFα were quantified. IL-6 production was significantly increased in mice exposed to the high dose DE (2000 µg/m^3) at the 96 hr time point (Figure 4.4A). Although not significant, IL-10 was seen to increase in mice exposed to the high dose DE for the 48 and 96 hr time points (Figure 4.4B). All other cytokines measured were unchanged compared to controls.

4.3.3 Post-immunization endpoints

Pulmonary inflammation and lung injury

Mice were exposed to filtered air or diesel exhaust (DE) at a concentration of 500 or 2000 µg/m^3 on days 0-4, given an intranasal instillation of either saline or 100 µg of ovalbumin (OVA) 40 min after the chamber exposure on days 0-2, and necropsied 4 hrs after the last chamber exposure as depicted in Figure 1. Cell differential counts in the BALF were quantified to assess pulmonary inflammation. No differences among the groups were observed for macrophage, lymphocyte, neutrophil, and eosinophil counts (data not shown). Protein and LDH levels were quantified to determine if DE and/or antigen exposure induced cellular lung injury. These biomarkers were not found to be increased in BALF of any group (data not shown).

Principle component analysis (PCA)

PCA was applied to provide a multidimensional gene expression profile of each gene chip in a 3 dimensional space to reveal clusters in the experimental data. All data from the 24 gene chips were analyzed with each dot representing a gene chip (Figure 4.5). The first 3 PCs combined reflected approximately 40% of the variance among all samples. After analysis the gene chips were then highlighted in either blue (OVA treatment) or red (saline control). Good separation of the two groups was observed reflecting different expression profiles illustrating a model effect between antigen and saline (Figure 4.5A). To determine if there was a diesel dose effect, the gene chips were highlighted according to diesel concentrations (blue- air/saline and air/OVA, red-500 µg DE/m^3/saline and 500 µg DE/m^3/OVA, green- 2000 µg DE/m^3/saline and 2000 µg DE/m^3/OVA) (Figure 4.5B). The plot was rotated to reveal clustering among the 2000

$\mu g/m^3$ DE exposure groups.

Gene set enrichment analysis (GSEA)

To test for sets of related genes that might be altered in the lungs of mice exposed to the various treatments we employed GSEA. In contrast to conventional microarray analysis programs, the algorithm employed by GSEA derives its power by focusing on gene sets with biological relevance rather than individual genes. [220, 221]. Pairwise comparisons revealed significant gene set differences between high DE/saline vs. air/saline and high DE/OVA vs. air/OVA. For each comparison, a heatmap was constructed of the top 50 genes associated with the treatment of interest. The degree of correlation in each chip is represented by a range of colors reflecting the strength of correlation (red: high, pink: moderate, light blue: low, and dark blue: lowest). Visual inspection of the high DE/saline heatmap (Figure 4.6) showed striking contrast of the top 50 genes between the diesel and air treatments. A similar map was also constructed for the high DE/OVA vs. air/OVA comparison, where the top 50 genes associated with DE in the context of OVA are shown (Figure 4.7). While the contrast was less strong in this comparison, a binary response was still evident. For both heat maps there was good consistency across each of the 4 animals per group represented by individual gene chips (individual animals). 10 genes from the top 50 genes, 1190003K14RIK, CD14, CXCL1, CXCL5, IFITM1, LCN2, PIGR, PROM1, REG3G, and RETNLA, were in common between both heat maps.

The C2 collection of curated gene sets from the MSigDB were queried and a detailed description of each gene set can be found on the website

http://www.broad.mit.edu/gsea/msigdb/msigdb_index.html. A table was contructed for the high DE/saline vs. air/saline comparison of the top 20 gene sets associated with the DE phenotype, as ranked by normalized enrichment scores (Appendix 7). The core genes in these gene sets are involved in cellular proliferation and inflammatory effects. The top 20 gene sets associated with the DE/OVA phenotype generated from the high DE/OVA vs. air/OVA comparison (Appendix 8) contained genes involved in oxidative stress responses. The gene set WANG_MLL_CBP_VS_GMP_UP was associated with both high DE/saline and high DE/OVA phenotypes.

Pathway analysis

A total of 49 enriched gene sets with a FDR < 25% were identified in the high DE/saline compared to air/saline. The combined 619 core genes from these significant gene sets were extracted and imported into a pathway analysis program MetaCore GENEGO®. The list of pathways significantly altered by DE compared to air in the absence of antigen was clearly related to immune function and cell signaling pathways (Table 4.2). Specifically pathways included those for cell adhesion, cell cycle control, apoptosis, growth and differentiation, and cytokine signaling among others.

The pairwise comparison of high DE/OVA vs. air/OVA yielded 23 enriched gene sets with a FDR < 25%. The 412 core genes were imported into the MetaCore pathway program. The pathways associated with the high DE/OVA phenotype were distinct from those associated with the DE/saline phenotype. The majority of these pathways could be functionally classified under metabolic processes with oxidative stress systems including oxidative phosphorylation, mitochondrial and peroxisomal oxidation, ubiquinone,

glutathione, vitamin E, and PPAR regulation of lipid metabolism being very prominent (Table 4.3).

4.4 Discussion

Diesel exhaust has been shown to act as an adjuvant for allergic inflammation in animals and humans but the precise signaling pathways are not clear. Many studies have used instillation boluses of DEP or DEP extracts to explore the mechanisms of diesel enhanced allergic immune responses. While these methods are simpler and cheaper than inhalation, and can be used for hazard identification, they are not representative of real world exposures. Previous inhalation studies have used chronic exposures, between 5-34 weeks, and antigen administration has often been systemic or in combination with adjuvants such as alum. These studies have shown increases in neutrophils and eosinophils in the BALF [14, 252] but it is not clear if short term, moderate dose exposures would have the same effect on mucosal immunization. Moreover, these inhalation studies have not investigated the signaling mechanisms responsible for increased immunity and clinical disease. The present study had two goals: 1) to investigate the adjuvant effects, post antigen challenge, of a short term inhalation exposure to moderate doses (500 and 2000 $\mu g/m^3$) of DE; and 2) to identify global gene changes associated with altered immune function. Our data demonstrate for the first time that even short term inhalation exposure to moderate concentrations of DE, when given with an antigen, can induce allergic lung disease after antigen challenge. Furthermore, these adjuvant effects were associated with changes in gene expression 4 hrs after DE exposure in mice given antigen that were distinct from changes in animals exposed to DE

alone.

The post-challenge results demonstrate DE exposure with antigen resulted in mild adjuvancy as evidenced by significant increases in eosinophils, neutrophils, lymphocytes, and IL-6 in the BALF. Saline and OVA control mice did not induce an asthma phenotype after the 2° OVA challenge and DE alone only increased neutrophils, indicating the combination exposure of DE and antigen was essential to promote the development of allergic lung disease. In life measures showed that none of the animals lost weight or experienced any indicators of the lung injury.

For the second goal, microarray analysis was employed to examine global gene changes 4 hrs after the last DE exposure to understand the mechanisms involved in promoting adjuvancy. While cellular and biochemical measures showed no changes in clinical indicators of inflammation, principal component analysis (PCA) of the gene expression data revealed a model (OVA) and a high dose DE (2000 $\mu g/m^3$) effect. Gene set enrichment analysis (GSEA) was applied to further investigate gene changes associated with adjuvancy. The pairwise comparison of air/OVA vs. air/saline yielded no significant gene sets. A plausible explanation for this is the last OVA dose was given on day 2 while the lungs were harvested for gene expression analysis on day 4 (figure 1) when the mild immune stimuli could have subsided. The GSEA comparison of low DE (500 $\mu g/m^3$)/OVA vs. air /OVA resulted in no significant gene sets associated with the low DE/OVA treatment. Comparison of the high (2000 $\mu g/m^3$) DE/OVA vs. air/OVA however showed significant changes in 23 gene sets. For this reason subsequent analyses were focused on the high DE/OVA vs. OVA comparison and the high DE/saline vs. saline comparison.

DE inhalation has been shown to induce lung inflammation in humans [253] and in rodents [14, 254]. *In vitro* studies have demonstrated DEP exposure induced release of inflammatory cytokines, IL-1β, IL-8, and granulocyte-macrophage colony-stimulating factor (GM-CSF) [216, 217, 255, 256]. Here the diesel exposures caused an up-regulation of neutrophil homing chemokines genes (CCL4, CXCL1, -5, and -6) and inflammatory cytokines (IL-1β, CXCL2 [mouse equivalent to IL-8], and GMCSF). In addition, 32 other signaling molecules were also associated with diesel exposures including numerous interleukins and TNF subtypes, and an array of CC and CXC chemokines.

Chronic DE exposures induce epithelial cell proliferation in the airways and alveoli, and increase the number of resident macrophages [257-259]. An *in vitro* study reported that serum starved A549 cells proliferated in response to a low dose (up to 10 µg/ml) DEP exposure [260]. Analysis of diesel exposed lungs revealed increases in growth and differentiation pathways such as IGF-RI and PDGF signaling, and granulocyte development. Jak-STAT cascades involved in cell growth and survival, as well as genes in G1/S transition cell cycle control were also altered. While cell cycle control genes such as cyclin E2, cell division cycle associated 7, cyclin-dependent kinase 8, E2F transcription factor 5, mitogen-activated protein kinase kinase kinase 5 (MAP3K5), and mitogen-activated protein kinase 6 (MAPK6), retinoblastoma 1 (Rb1) were increased, we also observed up-regulation of several genes up-stream of this pathway such as Jun-B oncogene (JunB), trans-acting transcription factor 1 (Sp1), and early growth response 1 (Egr1) that could be driving this proliferative response.

A substantial amount of evidence has shown that PM including DEP acts as an

adjuvant when given with antigen. The proposed mechanism is a hierarchical model whereby low levels of oxidative stress induce antioxidant defense mechanisms to restore redox balance in the cell. Intermediate levels of oxidative stress activate MAPK and NF-κB cascades, which induce inflammation, while high levels of oxidative stress disrupt the mitochondrial permeability transition pore and electron transport chain resulting in cell death [174]. *In vitro* studies have shown that DEP extracts and ultrafine particles (UFPs) induce ROS production and oxidative stress by interfering with the mitochondrial electron transport chain [165, 166]. The study presented here confirmed similar effects *in vivo.* Global transcriptional analysis of lung tissue from mice in the high DE/OVA treatment group expressed increased transcription of 45 genes involved in the NADH and $FADH_2$ respiratory chain located in the inner membrane of the mitochondria. These include 6 ATP synthases, 6 ATPases, 8 cytochrome c oxidases, 20 NADH dehydrogenases, and 2 ubiquinol-cytochrome c reductases, the majority of which were up-regulated. The genomic profile for the DEP/OVA group also altered a significant number of genes reflecting phase I metabolism, including cytochrome P450s, dehydrogenases, carboxylesterases, and reductases, and a consistent induction of phase II transferases. These data confirm *in vitro* findings that have shown polycyclic aromatic hydrocarbons (PAH) induce oxidative stress indirectly, through biotransformation by cytochrome P450, expoxide hydrolase, and dihydrodiol dehydrogenase to generate redox active quinones [261].

In conclusion mice exposed to high DE alone had altered inflammatory, cell cycle control, growth and proliferation, and cell adhesion pathways. Consistent with the Li et al premise, DE exposure in the context of antigen immunization induced oxidative stress

pathways, possibly through disruption of the inner mitochondrial membrane. These effects were associated with mild adjuvancy as evidenced by increases in eosinophils, neutrophils, and lymphocytes as well as IL-6 post-challenge. Genomic alterations in lung tissues after both high DE/saline and high DE/OVA exposures are more likely to reflect molecular changes within the resident lung cell population rather than the infiltration of new cells because the cell differential counts were unchanged compared to saline and OVA controls at that time point. This comprehensive approach using gene expression analysis to examine changes at a cellular and molecular level combined with more traditional immunotoxicity endpoints provide a clearer picture of the events occurring in the lung after DE exposure in the presence or absence of antigen. The results show that relatively short exposures to DE, at concentrations seen in severe occupational environments, cause mild increases in immunologic sensitization to allergen. Genomic analysis revealed a wide range of altered pathways suggesting this method may be more sensitive and can be used for identifying mechanisms involved in adverse effects of inhaled pollutants.

Tables

Table 4.1 Summary of concentrations and characteristics of the diesel exhaust particles and gases within the animal exposure chambers[a]

Constituent	**Units**	**Low exposure**	*High exposure*
Particle mass concentration (TEOM)	$\mu g/m^3$	561±9	2136±63
Particle mass concentration (filter)[b]	$\mu g/m^3$	546±29	1983±55
Particle number concentration[c]	$\#/cm^3$	5.6×10^5 $\pm4.1\times10^3$	2.0×10^6 $\pm9.9\times10^3$
Oxygen (O_2)	%	20.7±0.11	20.3±0.07
Carbon monoxide (CO)	ppm	<1.0	4.3±0.07
Nitric oxide (NO)	ppm	<2.5	9.2±0.30
Nitrogen dioxide (NO_2)	ppm	<0.25	1.1±0.05
Sulfur dioxide (SO_2)	ppm	<0.06	0.2±0.10
Number median D_p[d]	nm	80±2	86±2
Volume median D_p[d]	nm	184±2	195±2
OC/EC[e]	wt ratio	0.7±0.05	0.7±0.05

[a]Tapered element oscillating microbalance (TEOM), O_2, CO, NO, NO_2, and SO_2 data represent mean values from continuous measurements taken over the five day exposure ± SE.

[b]Filter data represent mean values from one measurement per day taken over the five day exposure ± SE.

[c]Particle number concentration data represent mean values from two measurements (low exposure) and three measurements (high exposure) taken over one representative exposure day ± SE.

[d]D_p indicates particle geometric number and volume median diameters for a single representative particle size distribution ± geometric standard deviation. Note that volume information is calculated from number based mobility diameters and assume spherical particles.

[e]OC/EC (organic carbon to elemental carbon ratio) data represent mean values from one measurement per day taken over the five day exposure ± SE.

Table 4.2 Significantly altered pathways by high DE/saline compared to air/saline

Pathway	p-Value	Genes
Cell Adhesion		
Chemokines and adhesion	6.98E-05	18/153
Cytoskeleton remodeling	7.32E-03	15/177
FAK signaling	2.43E-03	9/70
PLAU signaling	3.14E-03	7/47
Cell Cycle Control		
Regulation of G1/S transition (p.1)	4.08E-03	8/62
Cell Death/Apoptosis		
FAS signaling cascades	9.45E-03	6/44
Cell Survival		
EPO-induced Jak-STAT pathway	7.37E-04	7/37
Cyto/chemokines		
CXCR4 signaling pathway	1.68E-03	8/54
IL4 - antiapoptotic action	1.20E-03	7/40
IL6 signaling pathway	2.18E-03	6/33
G-proteins		
A3 receptor signaling	1.60E-03	10/79
A2B receptor: action via G-protein alpha s	9.23E-03	7/57
cAMP signaling	9.29E-04	13/114
CREB pathway	9.48E-03	10/101
M-RAS regulation pathway	7.07E-03	4/19
RAB5A regulation pathway	6.97E-03	3/10
Regulation of CDC42 activity	2.74E-03	5/24
Growth and Differentiation		
IGF-RI signaling	7.54E-06	13/72
Membrane-bound ESR1: interaction with G-proteins signaling	2.96E-03	9/72
PDGF signaling via STATs and NF-kB	5.91E-03	6/40
Leptin signaling via JAK/STAT and MAPK cascades	6.45E-03	5/29
Membrane-bound ESR1: interaction with growth factors signaling	7.53E-03	6/42
TPO in cell process	4.83E-05	10/52
Transcription regulation of granulocyte development	4.84E-04	8/45
PIP3 signaling in cardiac myocytes	1.19E-03	10/76
Growth factors		
Prolactin receptor signaling	4.08E-03	8/62
Hormones		
Androgen Receptor nuclear signaling	1.19E-03	10/76
Insulin signaling:generic cascades	7.61E-03	7/55
Non-genomic (rapid) action of Androgen Receptor	2.43E-03	9/70
Kinases		
AKT signaling	2.39E-03	8/57
Metabolism - Lipid		
Insulin regulation fatty acid metabolism	2.29E-04	9/51
Insulin regulation of glycogen metabolism	9.23E-03	7/57
Metabolism - Regulators		
Transcription regulation of aminoacid metabolism	2.96E-04	8/42
Insulin receptor signaling pathway	1.86E-03	7/43
Neuroscience		
Regulation of CDK5 in CNS	1.30E-03	6/30
GDNF signaling	3.31E-03	5/25
Phosphatases		
PTEN pathway	4.13E-04	9/55

Transcription Factors		
PPAR Pathway	7.58E-04	8/48
Translation Regulation		
Insulin regulation of the protein synthesis	7.61E-03	7/55
Regulation activity of EIF2	8.39E-03	7/56

Table 4.3 Significantly altered pathways by high DE/OVA compared to air/OVA

Pathway	p-Value	Genes
Cell Cycle Control		
Role of Brca1 and Brca2 in DNA repair	1.60E-06	9/40
Metabolism - Aminoacid		
Leucune, isoleucine and valine metabolism p.1	4.00E-04	4/13
Leucune, isoleucine and valine metabolism p.2	4.92E-06	7/25
Phenylalanine metabolism	1.12E-05	7/28
TCA	8.99E-07	7/20
Metabolism - Carbohydrates		
Glycolysis and gluconeogenesis (short map)	3.55E-03	5/36
Glycolysis and gluconeogenesis	5.53E-03	3/13
Propionate metabolism p.1	5.48E-04	4/14
Propionate metabolism p.2	1.88E-06	7/22
Pyruvate metabolism	5.39E-03	4/25
Metabolism - Energy		
Oxidative phosphorylation	7.31E-36	40/99
Metabolism - Lipid		
Mitochondrial long chain fatty acid beta-oxidation	2.57E-10	9/17
Mitochondrial unsaturated fatty acid beta-oxidation	2.46E-09	8/15
Mitochondrial ketone bodies biosynthesis and metabolism	4.41E-06	5/10
Peroxisomal branched chain fatty acid oxidation	1.55E-05	6/20
Peroxisomal straight-chain fatty acid beta-oxidation	5.48E-04	4/14
PPAR regulation of lipid metabolism	3.02E-09	10/28
Regulation of fatty acid synthesis	1.77E-03	3/9
Metabolism - Nucleotide		
ATP metabolism	1.66E-03	7/60
ATP/ITP metabolism	1.79E-08	14/73
CTP/UTP metabolism	1.75E-15	20/67
dATP/dITP metabolism	6.99E-04	7/52
dCTP/dUTP metabolism	3.05E-06	9/43
dGTP metabolism	9.40E-04	6/40
GTP-XTP metabolism	1.41E-07	12/61
TTP metabolism	1.04E-05	8/38
Metabolism - Vitamin and Cofactor		
Glutathione metabolism	7.64E-13	14/37
Heme metabolism	8.48E-03	5/44
Ubiquinone metabolism	3.30E-18	23/73
Vitamin E (α-tocopherol) metabolism	9.16E-05	5/17
Regulation of Transcription		
Ligand-Dependent Transcription of Retinoid-Target genes	4.24E-03	10/129

Figures

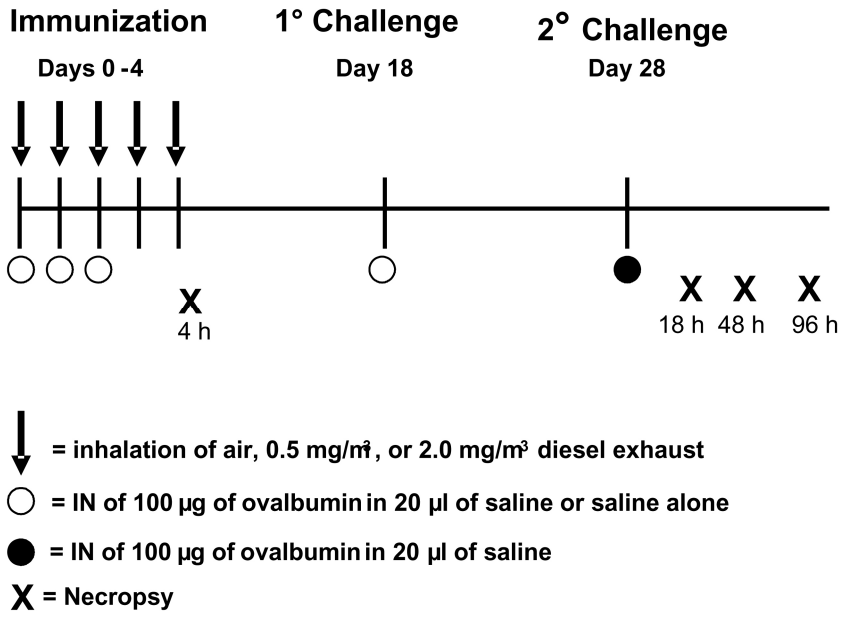

Figure 4.1 Schematic of exposure regime. BALB/c mice were exposed to filtered air, 500, or 2000 µg/m^3 of DE on days 0-4. After the first three days of exposure, mice were treated with an intranasal instillation of 100 µg in 20 µl of saline or saline alone. Mice were challenged with the same dose and concentration of either OVA or saline alone on day 18 and all mice were challenged with OVA on day 28. Necropsies were either 4 hrs (n=4) after the last air or DE exposure or 18, 48, or 96 hrs (n=6-8) after the last challenge.

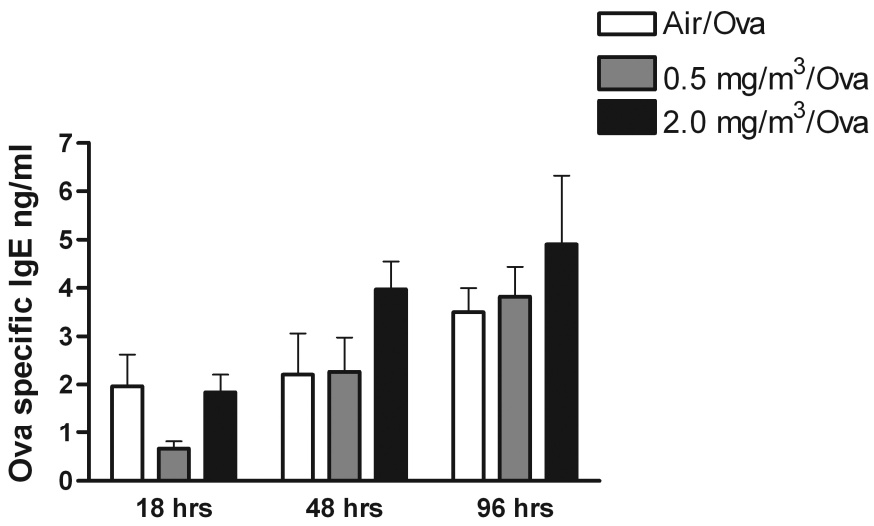

Figure 4.2 Kinetic development of OVA-specific serum antibodies in mice exposed to diesel exhaust during allergic immunization. Mice were exposed to filtered air or DE at a particle concentration of 500 or 2000 $\mu g/m^3$ on days 0-4 for 4 hr/day, intranasally instilled with OVA on days 0, 1, 2, 18, challenged with OVA on day 28, and necropsied 18, 48, and 96 hrs later. OVA-specific IgE antibody levels were measured in the serum by ELISA. n=6-8

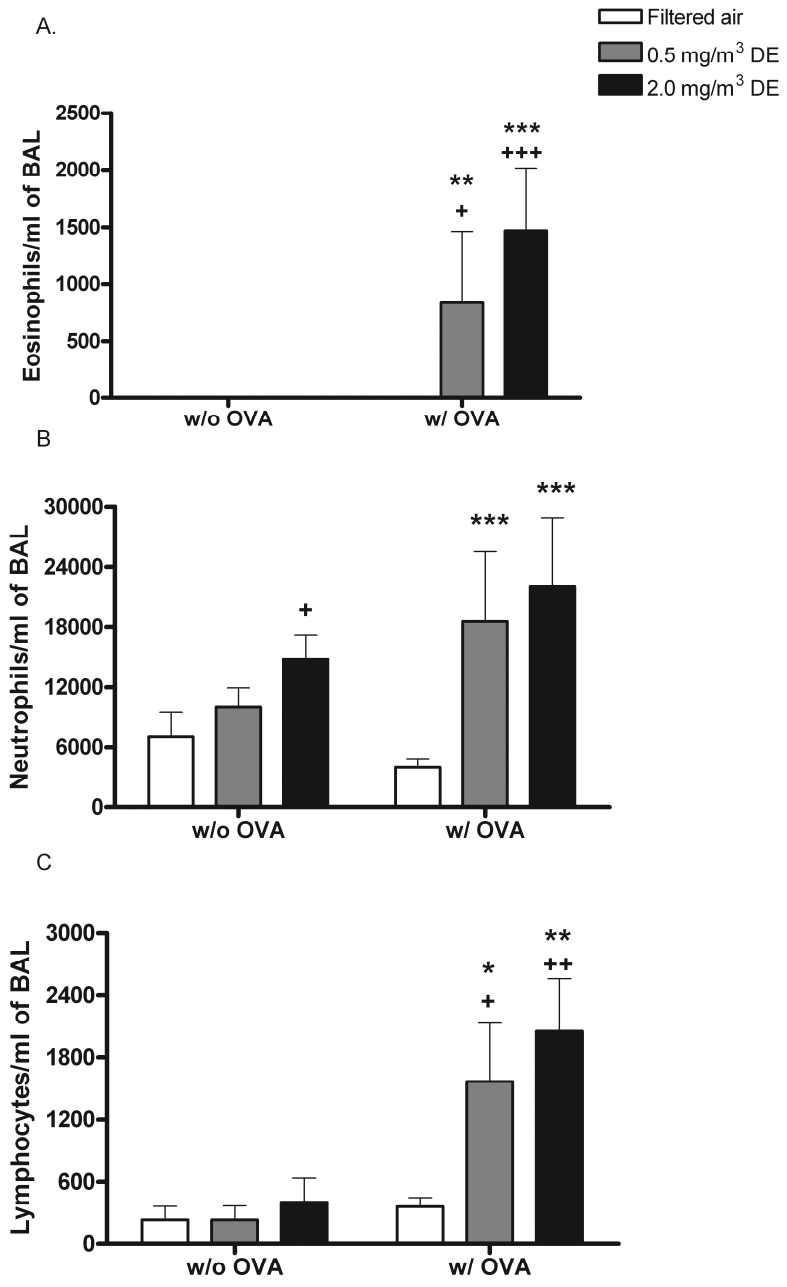

Figure 4.3 Allergen-induced pulmonary inflammatory cells in mice exposed to filtered air or diesel exhaust with or without OVA. Mice were exposed to filtered air or DE at a particle concentration of 500 or 2000 µg/m^3 on days 0-4 for 4 hr/day, intranasally instilled with OVA or saline on days 0, 1, 2, 18, challenged with OVA on day 28, and necropsied 18, 48, and 96 hrs later. Data is shown for 48 hr time point only. Eosinophils (**A**), Neutrophils (**B**), and lymphocytes (**C**) were measured in BALF. n=6-8; Significantly different from saline control: $^{+}p<0.05$; $^{++}$ $p<0.01$. Significantly different from OVA control: $^{*}p<0.05$; $^{**}p<0.01$; $^{***}p<0.001$.

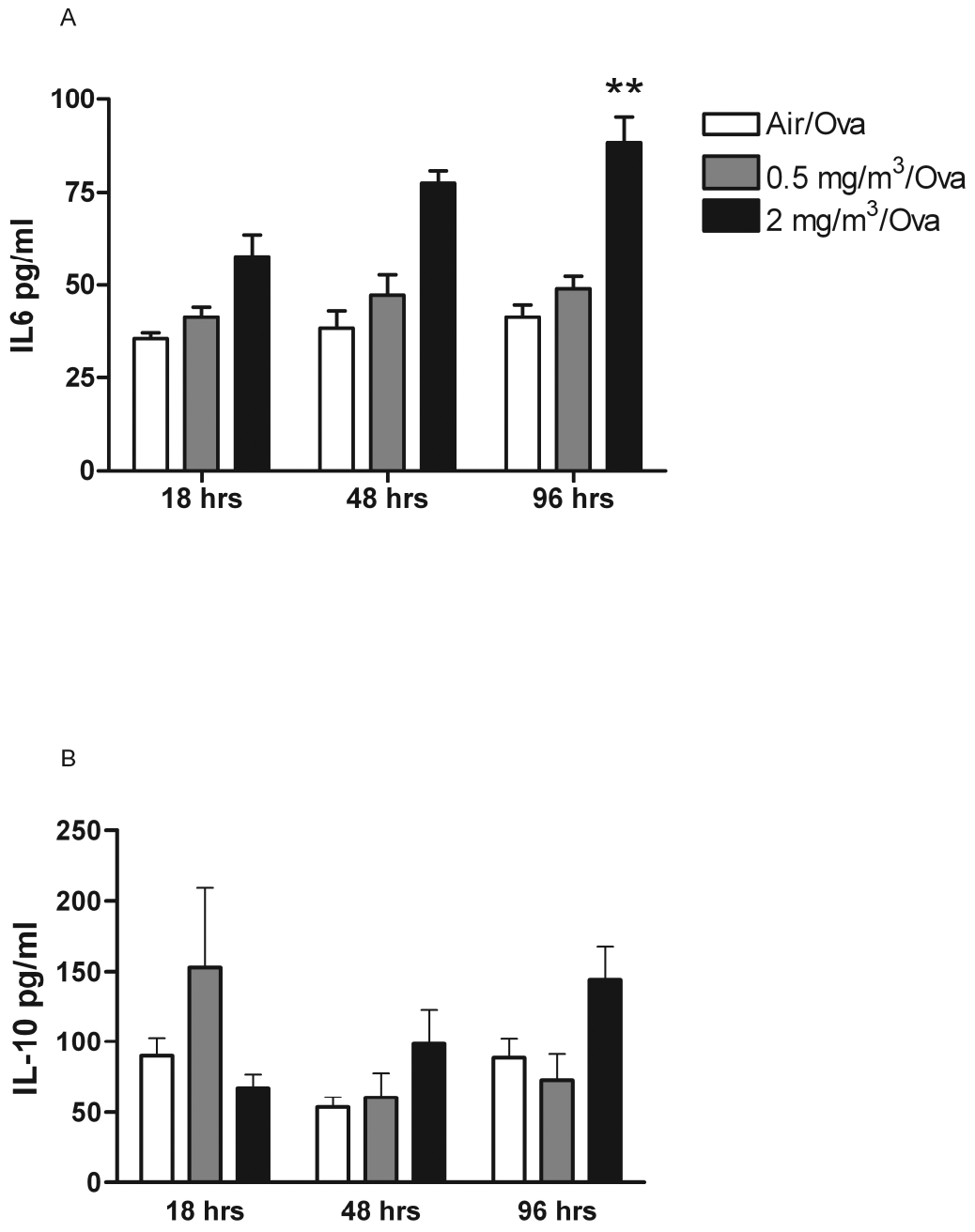

Figure 4.4 Quantification of IL-6 and IL-10 protein levels. Mice were exposed to filtered air or DE at a particle concentration of 500 or 2000 µg/m^{3}on days 0-4 for 4 hr/day, intranasally instilled with OVA or saline on days 0, 1, 2, 18, challenged with OVA on day 28, and necropsied 18, 48, and 96 hrs later. IL-6 (**A**) and IL-10 (**B**) protein levels were measured by ELISA in the BALF of the same mice as described in Figure 1. n= 6-8; Significantly different from OVA control: $^{**}p<0.01$.

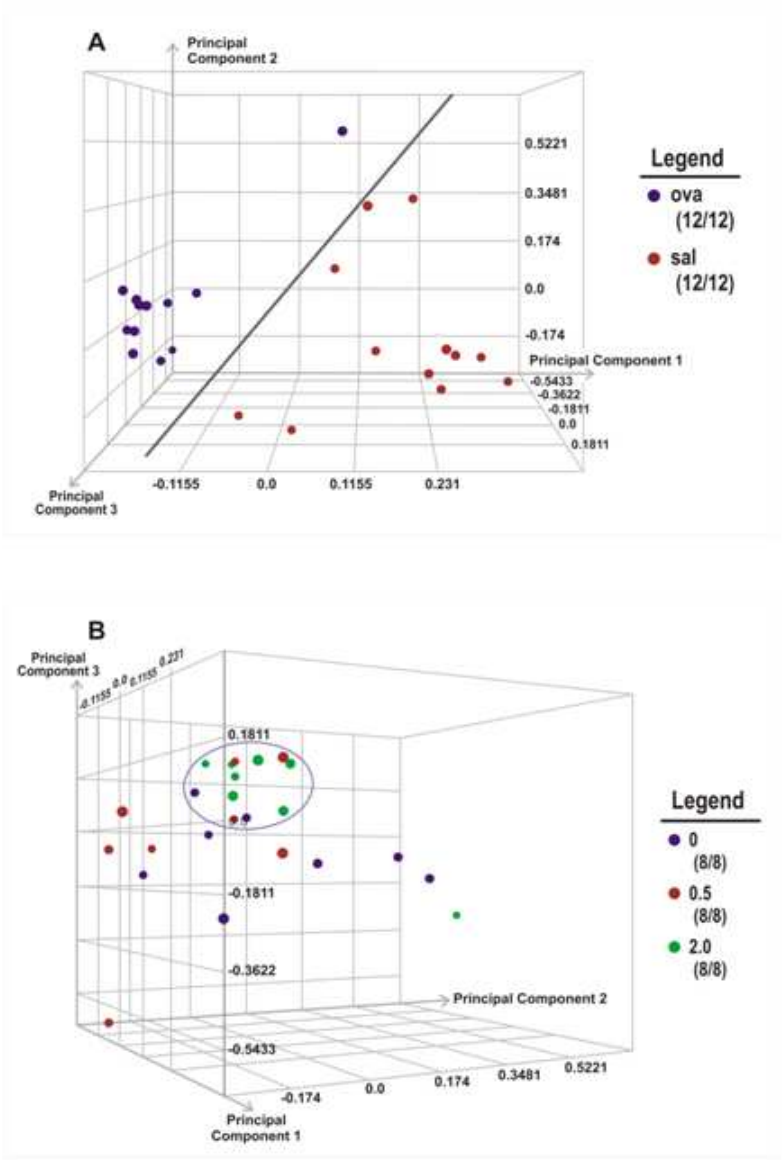

Figure 4.5 Principle component analysis plot from microarray data. Mice were necropsied 4 hours after the last diesel exposure on Day 4. RNA was isolated from the lungs and hybridized to Affymetrix Mouse 430A gene chips (n=4). PCA plots were created in Rosetta Resolver. Each plot contains gene chips from all mice and each dot represents a gene chip. Gene chips were highlighted according to the immunization protocol (blue-OVA treatment or red-saline treatment) (**A**) or the diesel concentration (blue- air/saline and air/OVA, red-500 µg DE/m^3/saline and 500 µg DE/m^3/OVA, green-2000 µg DE/m^3/saline and 2000 µg DE/m^3/OVA) (**B**).

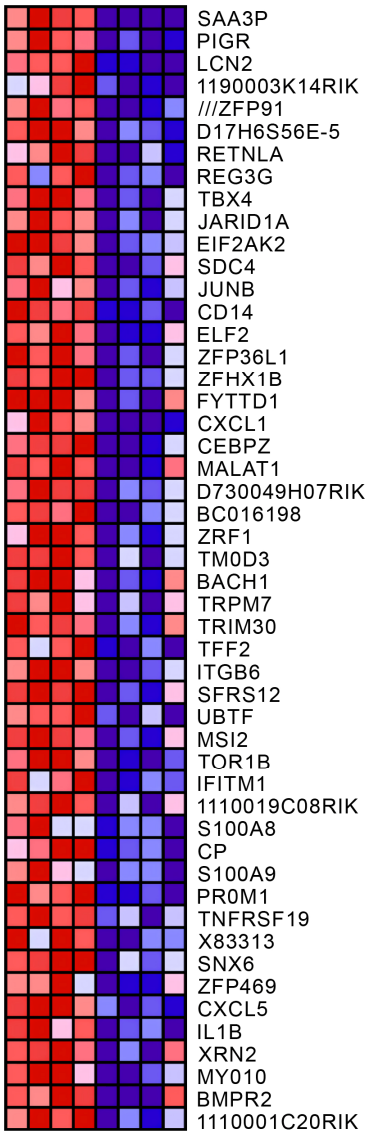

Figure 4.6 Heat map of top 50 genes associated with high DE in non-allergic mice. In the heat map, expression values for the top 50 genes in each chip is represented as a color, where the range of colors (red, pink, light blue, dark blue) shows the range of expression values (high, moderate, low, lowest). Lanes 1-4 are high DE/saline and 5-8 are air/saline.

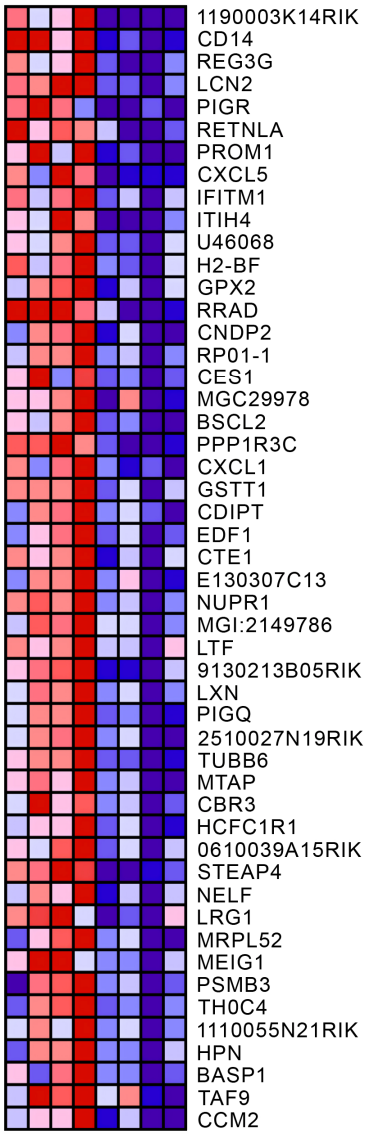

Figure 4.7 Heat map of top 50 genes associated with high DE in OVA-allergic mice. In the heat map, expression values for the top 50 genes in each chip is represented as a color, where the range of colors (red, pink, light blue, dark blue) shows the range of expression values (high, moderate, low, lowest). Lanes 1-4 are high DE/OVA and 5-8 are air/OVA.

Chapter 5

Discussion

Over the past several decades the prevalence, morbidity, and mortality of asthma has been increasing at an alarming rate, making it a major public health concern. Increases in ambient particulate matter (PM) have been correlated with a rise in hospitalization associated with respiratory illnesses such as asthma [118, 183]. Diesel exhaust particles (DEP) are a major constituent of ambient particulate matter in urban environments and occupational settings. Several studies in humans and animals have shown that diesel exhaust (DE) as well as DEP can act as an immunological adjuvant to increase the severity of allergen induced asthma [114, 115, 123, 128, 134, 184-186]. However, there is still a fundamental lack of understanding as to what component or components are responsible for these effects and the underlying mechanisms through which they act. The purpose of this research was to investigate the relative adjuvant potency of 3 chemically distinct DEP given with an allergen, and to identify the cellular mechanisms responsible for this effect.

The heterogeneous nature of DEP samples adds to the difficulty in determining what effects are common among all DEP exposures versus specific characteristics of a particular sample. Several studies investigating the adjuvant potential of the particle itself have demonstrated its ability to induce antigen-specific IgE antibodies when given with antigen [194, 195, 262]. Nygaard et al. [262] studied the adjuvant effect of polystyrene particles (PSP) of various sizes (0.0588 to 11.14 μm), carbon black (CB; 0.035 μm), and DEP (0.030 μm) in mice. The results demonstrated the smaller PSP (0.0588 and 0.202 μm), CB, and DEP increased allergen-specific IgE serum levels. Furthermore linear regression analysis indicated particle diameter and surface area were predictive of IgE response [262]. Another body of evidence supports the notion that adsorbed chemical

substances found on the particles such as polycyclic aromatic hydrocarbons (PAHs) can induce allergic adjuvancy [191-195]. Most of the mechanistic studies have focused on the role of oxidative stress and the generation of reactive oxygen species (ROS) from organic rich DEP or DEP extracts. The present work investigated the relative adjuvant potency of three different DEP samples, N-DEP, A-DEP, and C-DEP which differed in the percentage of dichloromethane (DCM) extractable organic material (EOM) (1.5%, 68.6%, and 18.9%, respectively) in a mucosal sensitization model adopted from Steerenberg *et al.* [199].

Results of this research show that DEP induces asthma-like parameters of antigen-specific IgG1, airway hyperresponsiveness (AHR) and inflammation, as well as alterations in local lung cytokine levels and increases in lung permeability. In addition, on a comparative mass basis, the three samples induced a gradation of post-challenge adjuvancy and this was not solely dependent on the organic content. Immune and inflammatory endpoints demonstrate C-DEP/OVA ≈ A-DEP/OVA >> N-DEP/OVA with respect to post-challenge adjuvancy as measured by eosinophilic inflammation and T_H2 cytokines in the BALF, serum OVA-specific IgG1 antibodies, and airway hyperresponsiveness.

Human and rodent studies have shown DEP induced allergic asthma is characterized by recruitment of T helper 2 (T_H2) lymphocytes and subsequent production of T_H2 cytokines like IL-4, IL-5, IL-10, and IL-13, which perpetuate the inflammatory response. The importance of T_H2 cells in allergic asthma is underlined by a study in which adoptive transfer of these cells into naïve mice led to an allergic asthma phenotype [205]. Conversely, removal of these cells prevented induction of asthma in sensitized

mice. Thymus activation regulated chemokine (TARC), mainly produced by dendritic cells, selectively induces the migration of CCR4-expressing T_H2 cells [206, 207] and is thought to play a crucial role in allergic asthma. In the present study, TARC levels post-challenge in the BALF were significantly increased in C-DEP + OVA exposed mice compared to all groups and this was accompanied by a significant increase in lymphocytes.

While most reports on PM-induced adjuvancy have focused on immune effects post-challenge, we were also interested in assessing early signaling events caused by DEP in the context of antigen sensitization. C-DEP/OVA, consistent with the strong degree of adjuvancy post-challenge, increased the influx of eosinophils, neutrophils, and lymphocytes, increased the production of T_H2 cytokines, and decreased the production of the T_H1 cytokine IL-12 in the BALF, 18 hrs after sensitization. On the other hand, post-sensitization differential cell counts and production of T_H1 and T_H2 cytokines were not significantly different for the organic rich A-DEP/OVA compared to OVA control although this group induced a strong adjuvant effect post-challenge suggesting the kinetics of the response may be different. The elemental carbon rich N-DEP/OVA exposures induced a mild T_H2 phenotype post-sensitization followed by a mild adjuvant effect post-challenge.

There is much evidence that the organic chemical compounds, such as PAHs, quinones, and nitro-PAHs, absorbed on the surface of DEP play a role in ROS production which in turn causes oxidative stress. If the level of oxidative stress exceeds the cells natural antioxidant defense mechanisms then inflammatory cytokines and chemokines,

which may contribute to the adjuvant effect of DEP, are produced. The amount of DCM extractable organic material present in the A-DEP sample was about 3.5 times greater than C-DEP; however, both samples when given with allergen induced similar degrees of adjuvancy post challenge. One possible explanation is the adjuvant response was saturated. In other words the A-DEP sample may produce the same degree of adjuvancy at a lower dose than the C-DEP. An alternate explanation for these effects induced by exposure to the different DEP samples is the presence of particular species of compounds in the organic fraction, rather than the overall amount, could be responsible for the toxic effects. Xia et al [165] demonstrated the quinone-enriched polar fraction of DEP was more potent than the PAH-enriched aromatic fraction in ROS production suggesting a greater ability to cause oxidative stress. Therefore, it is possible that C-DEP contains a more potent compound. Complete chemical analysis of the compounds present in the fractionated DCM EOM of the DEP samples may be informative in further examination of this hypothesis.

To elucidate possible mechanisms and biomarkers for these effects, early signaling events and global gene expression changes in the lung were assessed. Certain exposures to DEP induce lung inflammation. DE and DEP have been shown to induce pulmonary inflammation manifested by neutrophil infiltration and elevated levels of total protein, albumin, LDH, and ROS in the lung as well as up-regulation of inflammatory pathways [201, 217, 219, 223, 224]. Based on these observations, it was no surprise that the cytokine-cytokine receptor pathway was a significantly altered pathway common to all DEP/saline exposures. The genes in this pathway included inflammatory, T_H1, and T_H2 cytokines and chemokines, but the majority of them were associated with neutrophil

signaling in the DEP/saline exposures. In agreement with these findings, all three DEP/saline samples induced an increase in neutrophils in the BALF at this time point, although the increase was not significant [219].

Toll-like receptor signaling was also altered in all DEP/saline exposures. Toll-like receptors (TLRs) play important roles in the initiation of both innate and adaptive immune responses [225, 226]. Their activation is usually associated with viral or bacterial exposure; however, TLRs can also signal in response to endogenous molecules and environmental pollutants. NO_2 adjuvant effects are dependent on TLR2 [227] and airway hyperresponsiveness, induced by chronic ozone exposure, is dependent on TLR4 [228]. In addition, Zhou *et al.* [229] reported heat shock induced increases in TLR2 and TLR4 mRNA and protein expression in monocytes. Furthermore, DEP has been shown to induce TLR4 expression in the lung [230] and TLR4 deficient mice develop airway inflammation to a lesser degree in response to DEP compared to control [231]. Our results demonstrated that the toll-like receptor interaction pathway was altered by all three DEP/saline exposures, providing further evidence that the TLR pathway is involved in DEP induced inflammatory responses.

The cytokine-cytokine receptor interaction and toll-like receptor signal pathways were also common pathways associated with all three DEP/OVA exposures but with a greater enrichment of genes in both pathways. In addition, GeneGo pathway analysis revealed significantly altered immune response, inflammatory, and apoptosis pathways. We have previously shown all three DEP/OVA exposures induced allergic adjuvancy after antigen challenge suggesting the pathways presented here may be important early signaling pathways in DEP induced allergic disease.

Li *et al.* [174] proposed a hierarchical oxidative stress model to explain DEP induced effects whereby low levels of oxidative stress induce antioxidant defense mechanisms to restore redox balance in the cell (tier 1). Intermediate levels of oxidative stress (tier 2) activate MAPK and NF-κB cascades, which induce inflammation, while high levels of oxidative stress (tier 3) activate apoptosis and apoptosis/necrosis pathways[174].

The study presented in chapter 3 demonstrated altered transcription of genes in all three tiers simultaneously with DEP/OVA exposure *in vivo.* Antioxidant transcription factor and enzymes such as Nrf2, heme oxygenase 1 (HO-1), and superoxide dismutase 2 (SOD2) were up-regulated in response to all three DEP/OVA exposures indicative of low oxidative stress levels according to the tiered model. The tier 2 responses were also up-regulated in the lungs of mice exposed to all three DEP samples when given with OVA (i.e. MAPKs, NF-κB, as well as inflammatory, T_H1, and T_H2 cytokines and chemokines). In addition, A- and C-DEP/OVA exposures altered apoptosis (tier 3) pathways; however, C-DEP/OVA significantly altered the greatest number of these pathways. Furthermore, the apoptosis pathway representation appears to coincide with the combined phenotypic allergic responses of the three DEP/OVA. Although ROS production was not measured, the results suggest that C-DEP/OVA, according to the hierarchical stress model, induced high levels of oxidative stress.

While the hierarchical oxidative stress model suggests a dose-dependent response, because we were examining whole lungs rather than individual cell lines it is possible the discrepancy seen in this study was due to cell turnover rates, varying concentration of DEP throughout the lung, as well as differences in the response of different cell types to

DEP.

It has been established that DEP organic compounds can generate reactive oxygen species (ROS) [232] and excessive ROS production can lead to a variety of cellular responses including DNA damage [233]. In fact, oxidative DNA damage has been detected in mouse lung DNA after DEP exposure [234]. Although the A-DEP sample contained the greatest amount of DCM EOM, in the present study, C-DEP/OVA exposure was unique in significantly altering cell cycle and DNA damage pathways. Global transcriptional analysis of lung tissue revealed up-regulation of cell cycle control genes including 6 cyclin genes, 7 cell division cycle genes, 7 members of the family of MAP kinases, 2 cyclin-dependent kinases, RAS p21 protein activator 3 (Rasa3), and 5 other RAS related proteins. This suggests the amount of DCM EOM does not directly relate to the ability of the sample to generate ROS.

In addition to the role of oxidative stress, the cytotoxicity and immune-modulating effects of DEP have been examined in a number of studies. DEP has been shown to induce the degranulation of eosinophils and enhance their adhesiveness to epithelial cells [263]. Also, DEP exposure may disrupt the epithelial barrier, which would further increase the cell's response to increased levels of proinflammatory cytokines [264] and allow antigens like OVA to become more easily available to antigen-presenting dendritic cells thus increasing adjuvancy [265]. The pathology results presented in chapter 2 demonstrate C-DEP/OVA exposure to induce the greatest amount peribronchial and perivascular inflammation.

All DEP samples with or without OVA had altered cytokine and toll-like receptor pathways suggesting these responses are a DEP chemical class signature rather than an

effect of a particular component of DEP (i.e. the percentage of DCM EOM). All DEP/OVA exposures increased transcription of genes involved in each tier of the hierarchical stress response model described by Li *et al*. [166, 174, 175]. CDEP/OVA exposure significantly altered the most number of apoptosis pathways as well as cell cycle and DNA damage pathways suggesting the C-DEP is the most bioactive sample. This comprehensive approach using gene expression analysis to examine pathway changes at a transcriptional level provides a clearer picture of the events occurring in the lung after DEP exposure in the presence or absence of antigen. Genomic analysis revealed a wide range of altered pathways suggesting this method may be more sensitive and can be used for identifying mechanisms involved in adverse effects of inhaled pollutants.

In conclusion the data suggest that three DEP samples appear to have signature responses. For example the C-DEP/OVA treatment increased eosinophil and lymphocyte lung infiltration, TARC, MCP-1, IL-4, and IL-5 production in the BALF, and altered transcription of immune, inflammation, protein degradation, cell adhesion, DNA damage, and cell cycle networks. These post-sensitization responses were associated with a strong adjuvant response after antigen challenge. A-DEP/OVA exposure induced transcriptional changes in networks associated with immune responses, inflammation, and cell adhesion but to a less extent than C-DEP/OVA. This exposure also resulted in a strong degree of adjuvancy post-challenge. The N-DEP/OVA exposure increased TARC and IL-5 production in the BALF and altered transcription of immune, inflammation, and cell adhesion networks post-sensitization. This response was associated with mild adjuvancy post-challenge. An in-depth analysis of the particle chemistry for each sample would

provide a means to relate chemical compounds with allergic potential.

In addition, this work also explored immune responses in mice acutely exposed to moderate doses of DE in an OVA mucosal sensitization model and identified possible mechanisms using genomics. Many studies have used instillation boluses of DEP or DEP extracts to explore the mechanisms of diesel enhanced allergic immune responses. While these methods are simpler and cheaper than inhalation, and can be used for hazard identification, they are less representative of real world exposures than inhalation exposures. Previous inhalation studies have used chronic exposures, between 5-34 weeks, and antigen administration has often been systemic or in combination with adjuvants such as alum. These studies have shown increases in neutrophils and eosinophils in the BALF [14, 252] but it is not clear if short term, moderate dose exposures would have the same effect on mucosal immunization. Moreover, these inhalation studies have not investigated the signaling mechanisms responsible for increased immunity and clinical disease.

The study described in chapter 4, exposed mice to DE generated from an engine used to power an air compressor. This is the same engine and operation procedures used to generate the C-DEP sample. The two goals of this study were: 1) to investigate the adjuvant effects, post antigen challenge, of a short term inhalation exposure to moderate doses (500 and 2000 $\mu g/m^3$) of DE; and 2) to identify global gene changes associated with altered immune function. Our data demonstrate for the first time that even short term inhalation exposure to moderate concentrations of DE, when given with an antigen, can induce allergic lung disease after antigen challenge. Furthermore, these adjuvant effects were associated with changes in gene expression 4 hrs after DE exposure in mice

given antigen that were distinct from changes in animals exposed to DE alone.

The post-challenge results demonstrate DE exposure with antigen resulted in mild adjuvancy as evidenced by significant increases in eosinophils, neutrophils, lymphocytes, and IL-6 in the BALF. Saline and OVA control mice did not induce an asthma phenotype after the 2° OVA challenge and DE alone only increased neutrophils, indicating the combination exposure of DE and antigen was essential to promote the development of allergic lung disease.

For the second goal, transcriptional analysis of RNA isolated from whole lung tissue of mice 4 hrs after the last DE exposure was assessed. GSEA was applied to identify pathway level changes associated with DE and DE + OVA exposures. DE inhalation has been shown to induce lung inflammation in humans [253] and in mice [14, 254]. In agreement with these studies, the DE exposures caused an up-regulation of neutrophil homing chemokines genes (CCL4, CXCL1, -5, and -6) and inflammatory cytokines (IL-1β, CXCL2 [mouse equivalent to IL-8], and GMCSF) as well as 32 other signaling molecules including numerous interleukins and TNF subtypes, and an array of CC and CXC chemokines. Similar pathways were altered with the C-DEP instillation exposures.

Cell cycle control genes such as cyclin E2, cell division cycle associated 7, cyclin-dependent kinase 8, E2F transcription factor 5, mitogen-activated protein kinase kinase kinase 5 (MAP3K5), and mitogen-activated protein kinase 6 (MAPK6), retinoblastoma 1 (Rb1) were increased with DE inhalation and also in the C-DEP/OVA exposure. In addition, we observed in both exposure systems, an up-regulation of several genes up-stream of this pathway such as Jun-B oncogene (JunB), trans-acting

transcription factor 1 (Sp1), and early growth response 1 (Egr1) that could be driving this proliferative response.

Global transcriptional analysis of lung tissue from mice in the high DE/OVA treatment group expressed increased transcription of 45 genes involved in the NADH and $FADH_2$ respiratory chain located in the inner membrane of the mitochondria. These include 6 ATP synthases, 6 ATPases, 8 cytochrome c oxidases, 20 NADH dehydrogenases, and 2 ubiquinol-cytochrome c reductases, the majority of which were up-regulated. The genomic profile for the DEP/OVA group also altered a significant number of genes reflecting phase I metabolism, including cytochrome P450s, dehydrogenases, carboxylesterases, and reductases, and a consistent induction of phase II transferases. This was very similar to the pathways up-regulated in the C-DEP/OVA exposures. These data confirm *in vitro* findings that have shown polycyclic aromatic hydrocarbons (PAH) induce oxidative stress indirectly, through biotransformation by cytochrome P450, expoxide hydrolase, and dihydrodiol dehydrogenase to generate redox active quinones [261].

In conclusion, mice exposed to high DE and C-DEP altered inflammatory and cell cycle control pathways post-sensitization. Consistent with the Li *et al* premise, DE and C-DEP exposure in the context of antigen immunization induced oxidative stress pathways, possibly through disruption of the inner mitochondrial membrane. These effects were associated with adjuvancy post-challenge. Genomic alterations in lung tissues after both high DE/saline and high DE/OVA exposures are more likely to reflect molecular changes within the resident lung cell population rather than the infiltration of new cells because the cell differential counts were unchanged compared to saline and

OVA controls at that time point; however a significant influx of eosinophils, neutrophils and lymphocytes were present in the lung post-sensitization for the C-DEP/OVA exposure.

This comprehensive approach using gene expression analysis to examine changes at a cellular and molecular level combined with more traditional immunotoxicity endpoints provide a clearer picture of the events occurring in the lung after DE and DEP exposure in the presence or absence of antigen. Genomic analysis revealed a wide range of altered pathways suggesting this method may be more sensitive and can be used for identifying mechanisms involved in adverse effects of inhaled pollutants.

T_H2 cells play a crucial role in the initiation, progression, and persistence of allergic asthma. While previous studies have suggested that a disturbance in balance between T_H1 and T_H2 cells underlies the allergic response to otherwise harmless antigen, the data presented here indicates other immuno-modulating mechanisms may be responsible for the adjuvant effect of DE and DEP + OVA exposure in mice. Regulatory T (Treg) cells are capable of preventing allergic sensitization and progression of allergic responses. Down-regulation or apoptosis of these cells is a possible mechanism by which DEP may induce adjuvany. A- and C-DEP/OVA exposures led to a strong allergic response after antigen challenge. The genomic data presented in chapter 3 indicated altered expression of apoptosis pathways after sensitization was unique to these exposures. Cell death of Treg cells may provide an explanation for the DEP induced adjuvant effect. Investigation of Treg cell numbers in the lung after DEP/OVA exposures as well as the relative susceptibility of this cell population to the cytotoxic effects of DEP *ex vivo*, may be informative in further examination of this hypothesis.

Appendix 1

Significantly altered gene sets by N-DEP/saline compared to saline

NAME	SIZE	ES	NES	FDR q-val
CARIES_PULP_HIGH_UP	68	0.81	2.85	< 1.00E-06
LAL_KO_3MO_UP	46	0.84	2.80	< 1.00E-06
FLECHNER_KIDNEY_TRANSPLANT_ REJECTION_UP	72	0.78	2.79	< 1.00E-06
LINDSTEDT_DEND_8H_VS_48H_UP	58	0.81	2.78	< 1.00E-06
LAL_KO_6MO_UP	58	0.80	2.75	< 1.00E-06
WIELAND_HEPATITIS_B_INDUCED	71	0.77	2.71	< 1.00E-06
GALINDO_ACT_UP	75	0.74	2.66	< 1.00E-06
YANG_OSTECLASTS_SIG	39	0.84	2.61	< 1.00E-06
NAKAJIMA_MCS_UP	85	0.70	2.55	< 1.00E-06
BLEO_HUMAN_LYMPH_HIGH_24HRS_UP	86	0.69	2.54	< 1.00E-06
BASSO_GERMINAL_CENTER_CD40_UP	82	0.69	2.54	< 1.00E-06
HINATA_NFKB_UP	89	0.69	2.52	< 1.00E-06
NADLER_OBESITY_UP	57	0.73	2.51	< 1.00E-06
SANA_TNFA_ENDOTHELIAL_UP	61	0.72	2.50	< 1.00E-06
NEMETH_TNF_UP	82	0.69	2.49	< 1.00E-06
MUNSHI_MM_VS_PCS_UP	64	0.67	2.34	< 1.00E-06
MUNSHI_MM_UP	57	0.69	2.34	7.18E-05
NI2_MOUSE_UP	40	0.74	2.33	6.78E-05
TNFA_NFKB_DEP_UP	17	0.86	2.33	6.43E-05
SHIPP_FL_VS_DLBCL_DN	30	0.74	2.24	6.11E-05
LINDSTEDT_DEND_UP	44	0.69	2.23	5.81E-05
TAVOR_CEBP_UP	42	0.69	2.22	5.55E-05
HOUSTIS_ROS	32	0.73	2.21	5.31E-05
MARTINELLI_IFNS_DIFF	16	0.83	2.19	5.09E-05
ZUCCHI_EPITHELIAL_DN	36	0.68	2.19	4.88E-05
TPA_SENS_MIDDLE_UP	55	0.64	2.17	1.39E-04
ROSS_CBF_MYH	38	0.70	2.17	2.21E-04
CROONQUIST_IL6_RAS_UP	18	0.81	2.15	2.99E-04
ZHAN_MULTIPLE_MYELOMA_VS_ NORMAL_DN	33	0.71	2.15	2.89E-04
NAKAJIMA_MCSMBP_MAST	37	0.69	2.14	3.19E-04
ABBUD_LIF_UP	45	0.66	2.14	3.09E-04
KNUDSEN_PMNS_UP	65	0.62	2.14	2.99E-04
JECHLINGER_EMT_UP	56	0.63	2.12	4.73E-04
DAC_BLADDER_UP	23	0.76	2.12	4.59E-04
DAC_IFN_BLADDER_UP	16	0.82	2.12	4.46E-04
PEART_HISTONE_DN	63	0.61	2.11	4.34E-04
RADAEVA_IFNA_UP	38	0.67	2.10	4.22E-04
ZELLER_MYC_UP	23	0.73	2.10	4.11E-04
CANCER_UNDIFFERENTIATED_META_ UP	62	0.61	2.10	4.62E-04
MARSHALL_SPLEEN_BAL	25	0.74	2.09	4.50E-04
PROTEASOMEPATHWAY	21	0.73	2.09	4.69E-04
TNFALPHA_ALL_UP	66	0.59	2.08	5.41E-04

EMT_UP	55	0.60	2.08	5.29E-04
SCHUMACHER_MYC_UP	47	0.63	2.07	5.17E-04
PASSERINI_INFLAMMATION	23	0.73	2.07	5.05E-04
APPEL_IMATINIB_UP	29	0.70	2.07	4.94E-04
MYC_TARGETS	39	0.65	2.07	4.84E-04
ADIP_DIFF_CLUSTER4	31	0.68	2.07	4.99E-04
CMV_24HRS_UP	61	0.61	2.06	4.89E-04
OXIDATIVE_PHOSPHORYLATION	55	0.61	2.06	5.28E-04
CMV_ALL_UP	81	0.57	2.05	6.36E-04
HOFMANN_MDS_CD34_LOW_AND_ HIGH_RISK	31	0.68	2.05	7.14E-04
FERRANDO_MLL_T_ALL_DN	71	0.57	2.03	9.73E-04
IFNALPHA_NL_UP	19	0.74	2.01	1.16E-03
ERM_KO_SERTOLI_DN	17	0.77	2.01	1.18E-03
AGED_MOUSE_NEOCORTEX_UP	60	0.59	2.01	1.16E-03
INOS_ALL_UP	47	0.61	2.01	1.16E-03
CANTHARIDIN_DN	45	0.61	2.00	1.22E-03
COLLER_MYC_UP	17	0.77	2.00	1.43E-03
ROS_MOUSE_AORTA_DN	68	0.57	2.00	1.40E-03
PROTEASOME	17	0.75	2.00	1.38E-03
NKTPATHWAY	28	0.67	1.99	1.53E-03
HADDAD_CD45CD7_PLUS_VS_MINUS_ UP	52	0.58	1.99	1.51E-03
IL6_FIBRO_UP	35	0.63	1.99	1.48E-03
HEARTFAILURE_VENTRICLE_DN	56	0.59	1.99	1.55E-03
APOPTOSIS	64	0.56	1.98	1.84E-03
TAKEDA_NUP8_HOXA9_3D_DN	20	0.71	1.97	1.85E-03
LIAN_MYELOID_DIFF_GRANULE	28	0.67	1.96	2.33E-03
HADDAD_HSC_CD7_UP	52	0.58	1.96	2.39E-03
ST_TUMOR_NECROSIS_FACTOR_ PATHWAY	28	0.67	1.96	2.56E-03
MOOTHA_VOXPHOS	73	0.55	1.95	2.71E-03
CHAUHAN_2ME2	42	0.60	1.95	2.76E-03
RIBOSOMAL_PROTEINS	78	0.54	1.95	2.77E-03
TNFALPHA_4HRS_UP	34	0.63	1.94	2.91E-03
LEE_MYC_TGFA_UP	54	0.57	1.94	2.89E-03
MOREAUX_TACI_HI_IN_PPC_UP	43	0.59	1.94	2.97E-03
BHATTACHARYA_ESC_UP	57	0.57	1.94	3.07E-03
BRCA_BRCA1_POS	68	0.56	1.94	3.09E-03
IFNALPHA_HCC_UP	23	0.70	1.94	3.13E-03
DSRNA_UP	32	0.64	1.94	3.09E-03
PROTEASOME_DEGRADATION	32	0.64	1.93	3.26E-03
BENNETT_SLE_UP	19	0.70	1.93	3.39E-03
TARTE_PC	65	0.55	1.93	3.58E-03
CMV_HCMV_TIMECOURSE_12HRS_ UP	21	0.69	1.93	3.58E-03
TNFALPHA_30MIN_UP	37	0.61	1.92	3.71E-03
UVB_NHEK3_C0	73	0.54	1.92	3.89E-03
GOLDRATH_CYTOLYTIC	24	0.67	1.92	3.84E-03
LIAN_MYELOID_DIFF_RECEPTORS	33	0.61	1.92	3.84E-03
PARK_RARALPHA_UP	34	0.61	1.91	4.34E-03

IL2PATHWAY	21	0.68	1.90	4.71E-03
STEMCELL_COMMON_DN	54	0.56	1.90	4.66E-03
AGED_MOUSE_CEREBELLUM_UP	58	0.55	1.89	5.69E-03
DER_IFNG_UP	54	0.56	1.88	6.10E-03
CCR5PATHWAY	18	0.70	1.87	7.21E-03
HALMOS_CEBP_UP	41	0.57	1.86	8.29E-03
ZHAN_MM_CD138_MF_VS_REST	30	0.62	1.85	8.56E-03
HOHENKIRK_MONOCYTE_DEND_ UP	85	0.51	1.85	8.52E-03
ST_GAQ_PATHWAY	24	0.65	1.85	8.95E-03
PHOTOSYNTHESIS	21	0.67	1.85	9.02E-03
IFN_GAMMA_UP	35	0.59	1.84	9.97E-03
IFNA_UV-CMV_COMMON_HCMV_6HRS_ UP	20	0.67	1.84	9.88E-03

ES = enrichment score; NES = normalized enrichment score; FDR = false discovery rate

Appendix 2

Significantly altered gene sets by A-DEP/saline compared to saline

NAME	SIZE	ES	NES	FDR q-val
CARIES_PULP_HIGH_UP	68	0.77	2.89	< 1.00E-06
LAL_KO_3MO_UP	46	0.78	2.73	< 1.00E-06
LAL_KO_6MO_UP	58	0.73	2.65	< 1.00E-06
DNA_REPLICATION_REACTOME	41	0.75	2.55	< 1.00E-06
ELECTRON_TRANSPORT_CHAIN	86	0.65	2.55	< 1.00E-06
CANCER_UNDIFFERENTIATED_META_UP	62	0.69	2.51	< 1.00E-06
MOOTHA_VOXPHOS	73	0.67	2.48	< 1.00E-06
YANG_OSTECLASTS_SIG	39	0.74	2.45	< 1.00E-06
MANALO_HYPOXIA_DN	73	0.65	2.44	< 1.00E-06
CANCER_NEOPLASTIC_META_UP	59	0.68	2.44	< 1.00E-06
YU_CMYC_UP	37	0.72	2.38	< 1.00E-06
GALINDO_ACT_UP	75	0.62	2.37	< 1.00E-06
OXIDATIVE_PHOSPHORYLATION	55	0.66	2.36	< 1.00E-06
FLECHNER_KIDNEY_TRANSPLANT_ REJECTION_UP	72	0.62	2.34	< 1.00E-06
LINDSTEDT_DEND_8H_VS_48H_UP	58	0.65	2.32	< 1.00E-06
CANTHARIDIN_DN	45	0.66	2.31	< 1.00E-06
SERUM_FIBROBLAST_CELLCYCLE	88	0.58	2.30	< 1.00E-06
FERRANDO_MLL_T_ALL_DN	71	0.61	2.30	< 1.00E-06
SCHUMACHER_MYC_UP	47	0.66	2.29	< 1.00E-06
WIELAND_HEPATITIS_B_INDUCED	71	0.62	2.29	< 1.00E-06
ADIP_DIFF_CLUSTER4	31	0.72	2.28	< 1.00E-06
P21_ANY_DN	27	0.74	2.28	< 1.00E-06
HOUSTIS_ROS	32	0.71	2.27	< 1.00E-06
PEART_HISTONE_DN	63	0.62	2.27	< 1.00E-06
IDX_TSA_UP_CLUSTER3	81	0.60	2.26	4.59E-05
NEMETH_TNF_UP	82	0.59	2.25	4.42E-05
CMV_IE86_UP	42	0.67	2.24	4.25E-05
BLEO_HUMAN_LYMPH_HIGH_24HRS_UP	86	0.57	2.21	4.10E-05
INOS_ALL_UP	47	0.64	2.21	3.96E-05
MENSSEN_MYC_UP	30	0.70	2.21	3.83E-05
UVB_NHEK2_UP	55	0.61	2.17	2.29E-04
NI2_MOUSE_UP	40	0.64	2.16	2.97E-04
PROTEASOME_DEGRADATION	32	0.67	2.15	4.35E-04
RIBOSOMAL_PROTEINS	78	0.56	2.15	4.57E-04
BHATTACHARYA_ESC_UP	57	0.59	2.12	5.44E-04
HG_PROGERIA_DN	24	0.71	2.12	5.29E-04
NAKAJIMA_MCS_UP	85	0.55	2.12	5.47E-04
COLLER_MYC_UP	17	0.76	2.10	6.62E-04
HEARTFAILURE_VENTRICLE_DN	56	0.58	2.09	6.74E-04
OLDAGE_DN	45	0.61	2.09	6.58E-04
BASSO_GERMINAL_CENTER_CD40_UP	82	0.54	2.07	9.37E-04
DOX_RESIST_GASTRIC_UP	30	0.65	2.06	1.26E-03
ZELLER_MYC_UP	23	0.69	2.04	1.70E-03
UVB_NHEK1_C1	41	0.60	2.03	1.69E-03

MOREAUX_TACI_HI_IN_PPC_UP	43	0.60	2.03	1.70E-03
RIBAVIRIN_RSV_UP	18	0.72	2.01	2.22E-03
P21_P53_ANY_DN	35	0.62	2.01	2.17E-03
BREAST_DUCTAL_CARCINOMA_GENES	19	0.71	2.01	2.30E-03
CMV_24HRS_UP	61	0.55	2.00	2.42E-03
REN_E2F1_TARGETS	37	0.60	2.00	2.52E-03
IDX_TSA_UP_CLUSTER5	82	0.52	2.00	2.49E-03
CROONQUIST_IL6_STARVE_UP	32	0.62	1.99	2.51E-03
TNFALPHA_ALL_UP	66	0.53	1.99	2.60E-03
TSA_CD4_UP	24	0.65	1.99	2.55E-03
PYRIMIDINE_METABOLISM	55	0.55	1.98	2.90E-03
HINATA_NFKB_UP	89	0.51	1.97	3.15E-03
MYC_TARGETS	39	0.59	1.96	3.66E-03
ADIP_DIFF_CLUSTER5	34	0.59	1.95	4.09E-03
SHIPP_FL_VS_DLBCL_DN	30	0.61	1.95	4.06E-03
TNFA_NFKB_DEP_UP	17	0.71	1.95	4.23E-03
ATP_SYNTHESIS	20	0.67	1.95	4.18E-03
TNFALPHA_30MIN_UP	37	0.58	1.95	4.12E-03
HPV31_DN	37	0.58	1.94	4.28E-03
P21_P53_MIDDLE_DN	17	0.71	1.94	4.23E-03
TAVOR_CEBP_UP	42	0.57	1.93	4.64E-03
PHOTOSYNTHESIS	21	0.67	1.93	4.74E-03
PROTEASOMEPATHWAY	21	0.65	1.92	5.43E-03
TARTE_PC	65	0.52	1.91	5.70E-03
TYPE_III_SECRETION_SYSTEM	20	0.67	1.91	5.66E-03
CMV_ALL_UP	81	0.50	1.91	5.88E-03
UEDA_MOUSE_SCN	86	0.49	1.91	5.82E-03
G1_TO_S_CELL_CYCLE_REACTOME	65	0.51	1.90	6.40E-03
STRESS_TPA_SPECIFIC_UP	34	0.59	1.90	6.36E-03
CELL_CYCLE	71	0.50	1.90	6.42E-03
FLAGELLAR_ASSEMBLY	20	0.67	1.89	6.60E-03
ABBUD_LIF_UP	45	0.54	1.89	7.01E-03
KNUDSEN_PMNS_UP	65	0.51	1.88	7.46E-03
TPA_SENS_MIDDLE_UP	55	0.53	1.88	7.62E-03
CARBON_FIXATION	18	0.66	1.88	7.67E-03
MMS_HUMAN_LYMPH_HIGH_24HRS_UP	18	0.69	1.88	7.58E-03
ZHAN_MM_CD138_PR_VS_REST	28	0.62	1.87	7.97E-03
ZUCCHI_EPITHELIAL_DN	36	0.58	1.87	8.21E-03
TIS7_OVEREXP_DN	17	0.67	1.87	8.23E-03
ZHAN_MULTIPLE_MYELOMA_VS_ NORMAL_DN	33	0.58	1.87	8.23E-03
ROS_MOUSE_AORTA_DN	68	0.50	1.87	8.17E-03
BRENTANI_DNA_METHYLATION_AND_ MODIFICATION	23	0.63	1.86	8.83E-03
NADLER_OBESITY_UP	57	0.52	1.86	8.73E-03
BLEO_MOUSE_LYMPH_LOW_24HRS_DN	24	0.63	1.86	8.70E-03
ET743_SARCOMA_UP	56	0.51	1.86	8.63E-03
UVB_NHEK3_C6	25	0.61	1.85	9.32E-03

ES = enrichment score; NES = normalized enrichment score; FDR = false discovery rate

Appendix 3

Significantly altered gene sets by C-DEP/saline compared to saline

NAME	SIZE	ES	NES	FDR q-val
CARIES_PULP_HIGH_UP	68	0.77	2.90	< 1.00E-06
GALINDO_ACT_UP	75	0.72	2.79	< 1.00E-06
YANG_OSTECLASTS_SIG	39	0.79	2.74	< 1.00E-06
LINDSTEDT_DEND_8H_VS_48H_UP	58	0.70	2.69	< 1.00E-06
HINATA_NFKB_UP	89	0.65	2.64	< 1.00E-06
NAKAJIMA_MCS_UP	85	0.65	2.58	< 1.00E-06
NEMETH_TNF_UP	82	0.64	2.57	< 1.00E-06
LAL_KO_6MO_UP	58	0.68	2.57	< 1.00E-06
WIELAND_HEPATITIS_B_INDUCED	71	0.66	2.53	< 1.00E-06
LAL_KO_3MO_UP	46	0.73	2.52	< 1.00E-06
HOUSTIS_ROS	32	0.75	2.49	< 1.00E-06
SANA_TNFA_ENDOTHELIAL_UP	61	0.66	2.48	< 1.00E-06
FLECHNER_KIDNEY_TRANSPLANT_ REJECTION_UP	72	0.64	2.47	< 1.00E-06
BLEO_HUMAN_LYMPH_HIGH_24HRS_UP	86	0.61	2.45	< 1.00E-06
NADLER_OBESITY_UP	57	0.66	2.45	< 1.00E-06
ADIP_DIFF_CLUSTER4	31	0.74	2.44	< 1.00E-06
MYC_TARGETS	39	0.71	2.44	< 1.00E-06
TNFA_NFKB_DEP_UP	17	0.86	2.42	< 1.00E-06
NI2_MOUSE_UP	40	0.71	2.41	< 1.00E-06
INOS_ALL_UP	47	0.68	2.39	< 1.00E-06
TPA_SENS_MIDDLE_UP	55	0.66	2.38	< 1.00E-06
TSA_CD4_UP	24	0.76	2.35	< 1.00E-06
CANCER_UNDIFFERENTIATED_META_UP	62	0.62	2.35	< 1.00E-06
ZELLER_MYC_UP	23	0.76	2.33	< 1.00E-06
ZUCCHI_EPITHELIAL_DN	36	0.70	2.33	< 1.00E-06
CMV_IE86_UP	42	0.66	2.26	5.58E-05
CMV_24HRS_UP	61	0.59	2.26	5.37E-05
MUNSHI_MM_UP	57	0.59	2.24	1.03E-04
DAC_BLADDER_UP	23	0.74	2.23	1.47E-04
PASSERINI_INFLAMMATION	23	0.71	2.19	3.21E-04
BASSO_GERMINAL_CENTER_CD40_UP	82	0.56	2.19	3.11E-04
IDX_TSA_UP_CLUSTER3	81	0.56	2.18	4.32E-04
MARTINELLI_IFNS_DIFF	16	0.79	2.18	4.19E-04
CMV_ALL_UP	81	0.54	2.17	4.47E-04
P21_ANY_DN	27	0.69	2.16	4.73E-04
MANALO_HYPOXIA_DN	73	0.55	2.16	4.97E-04
MUNSHI_MM_VS_PCS_UP	64	0.58	2.15	5.20E-04
FERRANDO_MLL_T_ALL_DN	71	0.56	2.15	5.06E-04
SHIPP_FL_VS_DLBCL_DN	30	0.66	2.14	5.30E-04
MMS_HUMAN_LYMPH_HIGH_24HRS_UP	18	0.76	2.14	5.16E-04
DAC_IFN_BLADDER_UP	16	0.78	2.14	5.37E-04
DNA_REPLICATION_REACTOME	41	0.62	2.13	5.24E-04
PROTEASOME_DEGRADATION	32	0.66	2.13	5.43E-04
ROSS_CBF_MYH	38	0.61	2.12	7.18E-04

HG_PROGERIA_DN	24	0.70	2.11	7.33E-04
ROS_MOUSE_AORTA_DN	68	0.55	2.10	8.96E-04
OLDAGE_DN	45	0.60	2.09	1.05E-03
COLLER_MYC_UP	17	0.76	2.09	1.14E-03
KNUDSEN_PMNS_UP	65	0.55	2.08	1.29E-03
TARTE_PC	65	0.54	2.07	1.37E-03
PROTEASOME	17	0.75	2.07	1.37E-03
DER_IFNG_UP	54	0.56	2.06	1.37E-03
CANCER_NEOPLASTIC_META_UP	59	0.55	2.06	1.40E-03
CHAUHAN_2ME2	42	0.60	2.06	1.48E-03
SCHUMACHER_MYC_UP	47	0.60	2.06	1.45E-03
UVB_NHEK2_UP	55	0.57	2.06	1.50E-03
NKTPATHWAY	28	0.65	2.06	1.50E-03
MENSSEN_MYC_UP	30	0.64	2.06	1.52E-03
SERUM_FIBROBLAST_CELLCYCLE	88	0.52	2.05	1.54E-03
TAVOR_CEBP_UP	42	0.59	2.05	1.58E-03
PROTEASOMEPATHWAY	21	0.69	2.04	1.71E-03
IFNALPHA_NL_UP	19	0.71	2.04	1.68E-03
JECHLINGER_EMT_UP	56	0.55	2.04	1.70E-03
ABBUD_LIF_UP	45	0.59	2.04	1.76E-03
IL6_FIBRO_UP	35	0.60	2.03	1.79E-03
PEART_HISTONE_DN	63	0.53	2.02	2.33E-03
AS3_FIBRO_DN	26	0.65	2.01	2.34E-03
YU_CMYC_UP	37	0.59	2.01	2.34E-03
P21_P53_MIDDLE_DN	17	0.71	2.01	2.31E-03
STRESS_TPA_SPECIFIC_UP	34	0.61	2.01	2.40E-03
DSRNA_UP	32	0.60	2.00	2.60E-03
ERM_KO_SERTOLI_DN	17	0.71	1.99	2.64E-03
RADAEVA_IFNA_UP	38	0.59	1.99	2.73E-03
TNFALPHA_4HRS_UP	34	0.60	1.99	2.90E-03
CANTHARIDIN_DN	45	0.55	1.98	2.97E-03
IFN_GAMMA_UP	35	0.59	1.98	3.04E-03
HOFMANN_MDS_CD34_LOW_AND_ HIGH_RISK	31	0.61	1.97	3.31E-03
ADIP_DIFF_CLUSTER5	34	0.59	1.97	3.27E-03
TIS7_OVEREXP_DN	17	0.69	1.97	3.22E-03
LIAN_MYELOID_DIFF_RECEPTORS	33	0.59	1.97	3.36E-03
MARSHALL_SPLEEN_BAL	25	0.63	1.95	4.34E-03
NAKAJIMA_MCSMBP_MAST	37	0.58	1.94	4.80E-03
TAKEDA_NUP8_HOXA9_3D_DN	20	0.67	1.93	5.19E-03
PYRIMIDINE_METABOLISM	55	0.52	1.93	5.34E-03
TNFALPHA_ALL_UP	66	0.51	1.92	6.17E-03
CMV_HCMV_TIMECOURSE_12HRS_UP	21	0.65	1.92	6.12E-03
HEARTFAILURE_VENTRICLE_DN	56	0.52	1.92	6.14E-03
IFNALPHA_HCC_UP	23	0.64	1.91	6.44E-03
HYPOXIA_REVIEW	68	0.50	1.91	6.64E-03
LINDSTEDT_DEND_UP	44	0.54	1.91	6.87E-03
CROONQUIST_IL6_RAS_UP	18	0.67	1.90	7.79E-03
LEE_MYC_TGFA_UP	54	0.51	1.89	7.81E-03
EMT_UP	55	0.51	1.89	8.20E-03
LEE_ACOX1_UP	58	0.51	1.89	8.21E-03

BENNETT_SLE_UP	19	0.65	1.88	8.45E-03
ZHAN_MMPC_SIMAL	41	0.55	1.88	8.40E-03
P21_P53_ANY_DN	35	0.57	1.88	8.63E-03
BREAST_DUCTAL_CARCINOMA_ GENES	19	0.65	1.88	8.74E-03

ES = enrichment score; NES = normalized enrichment score; FDR = false discovery rate

Appendix 4

Significantly altered gene sets by N-DEP/OVA compared to OVA

NAME	SIZE	ES	NES	FDR q-val
CARIES_PULP_HIGH_UP	68	0.81	2.76	< 1.00E-06
LAL_KO_3MO_UP	46	0.83	2.61	< 1.00E-06
LAL_KO_6MO_UP	58	0.79	2.60	< 1.00E-06
NEMETH_TNF_UP	82	0.74	2.59	< 1.00E-06
WIELAND_HEPATITIS_B_INDUCED	71	0.74	2.54	< 1.00E-06
NADLER_OBESITY_UP	57	0.76	2.51	< 1.00E-06
YANG_OSTECLASTS_SIG	39	0.82	2.50	< 1.00E-06
LINDSTEDT_DEND_8H_VS_48H_UP	58	0.73	2.45	< 1.00E-06
NAKAJIMA_MCS_UP	85	0.69	2.44	< 1.00E-06
SANA_TNFA_ENDOTHELIAL_UP	61	0.71	2.41	< 1.00E-06
BASSO_GERMINAL_CENTER_CD40_UP	82	0.69	2.40	< 1.00E-06
GALINDO_ACT_UP	75	0.69	2.40	< 1.00E-06
FLECHNER_KIDNEY_TRANSPLANT_ REJECTION_UP	72	0.69	2.39	< 1.00E-06
HINATA_NFKB_UP	89	0.64	2.26	< 1.00E-06
NI2_MOUSE_UP	40	0.70	2.16	3.02E-04
BLEO_HUMAN_LYMPH_HIGH_24HRS_UP	86	0.60	2.14	2.83E-04
GOLDRATH_CYTOLYTIC	24	0.77	2.14	3.32E-04
BRENTANI_IMMUNE_FUNCTION	42	0.68	2.13	3.75E-04
JECHLINGER_EMT_UP	56	0.64	2.11	5.30E-04
ADIP_DIFF_CLUSTER3	28	0.73	2.10	5.03E-04
TNFA_NFKB_DEP_UP	17	0.80	2.09	5.83E-04
YU_CMYC_DN	53	0.65	2.09	5.57E-04
YAGI_AML_PROGNOSIS	31	0.70	2.07	7.26E-04
ROSS_MLL_FUSION	60	0.62	2.05	1.12E-03
LIAN_MYELOID_DIFF_RECEPTORS	33	0.69	2.03	1.47E-03
EMT_UP	55	0.61	2.02	1.50E-03
PASSERINI_INFLAMMATION	23	0.74	2.01	1.69E-03
APPEL_IMATINIB_UP	29	0.70	2.01	1.96E-03
ABBUD_LIF_UP	45	0.64	2.01	1.89E-03
TAKEDA_NUP8_HOXA9_3D_DN	20	0.74	2.01	1.86E-03
LINDSTEDT_DEND_DN	53	0.61	2.01	1.87E-03
CMV_ALL_UP	81	0.56	2.01	1.81E-03
TAVOR_CEBP_UP	42	0.63	1.99	2.34E-03
STEMCELL_COMMON_DN	54	0.60	1.98	2.89E-03
SCHUMACHER_MYC_UP	47	0.61	1.97	3.54E-03
ERM_KO_SERTOLI_DN	17	0.75	1.96	3.66E-03
DAC_IFN_BLADDER_UP	16	0.77	1.95	4.26E-03
SANA_IFNG_ENDOTHELIAL_UP	45	0.62	1.95	4.26E-03
WANG_HOXA9_VS_MEIS1_UP	25	0.68	1.94	4.75E-03
LIAN_MYELOID_DIFF_GRANULE	28	0.68	1.93	5.19E-03
CMV_24HRS_UP	61	0.58	1.93	5.58E-03
MARTINELLI_IFNS_DIFF	16	0.75	1.93	5.45E-03
TARTE_PC	65	0.56	1.92	5.48E-03
MYC_TARGETS	39	0.63	1.92	5.46E-03

WANG_MLL_CBP_VS_GMP_UP	42	0.61	1.91	6.10E-03
XU_CBP_UP	25	0.68	1.91	6.53E-03
LOTEM_LEUKEMIA_UP	22	0.69	1.91	6.39E-03
LINDSTEDT_DEND_UP	44	0.61	1.90	6.60E-03
LU_IL4BCELL	62	0.56	1.90	6.79E-03
ZELLER_MYC_UP	23	0.69	1.90	6.99E-03
CASPASEPATHWAY	20	0.69	1.90	6.89E-03
ROSS_CBF_MYH	38	0.62	1.90	6.76E-03
CMV_8HRS_UP	27	0.66	1.88	8.38E-03
TPA_SENS_MIDDLE_UP	55	0.57	1.88	8.27E-03
DSRNA_UP	32	0.63	1.87	8.52E-03
NAKAJIMA_MCSMBP_MAST	37	0.61	1.87	8.37E-03
CROONQUIST_IL6_RAS_UP	18	0.72	1.87	8.38E-03
GENOTOXINS_ALL_24HRS_REG	22	0.68	1.87	8.26E-03
HOHENKIRK_MONOCYTE_DEND_UP	85	0.53	1.87	8.40E-03
SHIPP_FL_VS_DLBCL_DN	30	0.63	1.87	8.34E-03

ES = enrichment score; NES = normalized enrichment score; FDR = false discovery rate

Appendix 5

Significantly altered gene sets by A-DEP/OVA compared to OVA

NAME	SIZE	ES	NES	FDR q-val
YANG_OSTECLASTS_SIG	39	0.86	2.84	< 1.00E-06
LAL_KO_6MO_UP	58	0.74	2.59	< 1.00E-06
NAKAJIMA_MCS_UP	85	0.68	2.58	< 1.00E-06
LINDSTEDT_DEND_8H_VS_48H_UP	58	0.73	2.58	< 1.00E-06
LAL_KO_3MO_UP	46	0.76	2.56	< 1.00E-06
NADLER_OBESITY_UP	57	0.72	2.56	< 1.00E-06
GALINDO_ACT_UP	75	0.70	2.54	< 1.00E-06
SANA_TNFA_ENDOTHELIAL_UP	61	0.71	2.52	< 1.00E-06
CARIES_PULP_HIGH_UP	68	0.70	2.50	< 1.00E-06
NEMETH_TNF_UP	82	0.66	2.43	< 1.00E-06
JECHLINGER_EMT_UP	56	0.67	2.32	< 1.00E-06
HINATA_NFKB_UP	89	0.60	2.29	< 1.00E-06
TNFA_NFKB_DEP_UP	17	0.85	2.29	< 1.00E-06
NI2_MOUSE_UP	40	0.70	2.26	7.14E-05
ERM_KO_SERTOLI_DN	17	0.83	2.25	6.67E-05
BASSO_GERMINAL_CENTER_CD40_UP	82	0.61	2.24	6.25E-05
WIELAND_HEPATITIS_B_INDUCED	71	0.62	2.22	5.88E-05
EMT_UP	55	0.63	2.21	5.56E-05
PASSERINI_INFLAMMATION	23	0.75	2.19	5.26E-05
NAKAJIMA_MCSMBP_MAST	37	0.68	2.17	5.00E-05
TPA_SENS_MIDDLE_UP	55	0.62	2.16	4.76E-05
LIAN_MYELOID_DIFF_RECEPTORS	33	0.69	2.14	1.40E-04
BENNETT_SLE_UP	19	0.77	2.13	2.24E-04
TGFBETA_C2_UP	17	0.79	2.12	2.14E-04
TAKEDA_NUP8_HOXA9_3D_DN	20	0.76	2.12	2.48E-04
RADAEVA_IFNA_UP	38	0.65	2.10	3.19E-04
IL1_CORNEA_UP	53	0.60	2.08	5.72E-04
DAC_BLADDER_UP	23	0.72	2.08	5.89E-04
DAC_IFN_BLADDER_UP	16	0.79	2.08	6.03E-04
MARTINELLI_IFNS_DIFF	16	0.77	2.07	6.89E-04
TAVOR_CEBP_UP	42	0.62	2.06	7.32E-04
AS3_FIBRO_DN	26	0.70	2.05	7.74E-04
HEARTFAILURE_VENTRICLE_DN	56	0.59	2.03	1.03E-03
CANCER_UNDIFFERENTIATED_META_UP	62	0.56	2.01	1.43E-03
FLECHNER_KIDNEY_TRANSPLANT_ REJECTION_UP	72	0.55	2.01	1.39E-03
ADIP_DIFF_CLUSTER4	31	0.64	2.01	1.38E-03
KNUDSEN_PMNS_UP	65	0.56	2.00	1.39E-03
AGED_MOUSE_CEREBELLUM_UP	58	0.58	1.99	1.66E-03
CMV_ALL_UP	81	0.54	1.98	1.90E-03
BLEO_HUMAN_LYMPH_HIGH_24HRS_UP	86	0.52	1.98	2.06E-03
MATRIX_METALLOPROTEINASES	24	0.69	1.98	2.04E-03
DORSEY_DOXYCYCLINE_UP	23	0.68	1.96	2.53E-03
PASSERINI_EM	34	0.62	1.96	2.56E-03
TSA_CD4_UP	24	0.66	1.95	2.62E-03

CROONQUIST_IL6_RAS_UP	18	0.70	1.95	2.70E-03
ZUCCHI_EPITHELIAL_DN	36	0.60	1.94	3.52E-03
CMV_8HRS_UP	27	0.64	1.93	4.18E-03
IFNALPHA_HCC_UP	23	0.66	1.92	4.21E-03
SANA_IFNG_ENDOTHELIAL_UP	45	0.58	1.92	4.35E-03
APPEL_IMATINIB_UP	29	0.63	1.92	4.30E-03
SHEPARD_POS_REG_OF_CELL_ PROLIFERATION	85	0.52	1.92	4.22E-03
CROONQUIST_IL6_STROMA_UP	34	0.60	1.92	4.34E-03
SERUM_FIBROBLAST_CELLCYCLE	88	0.50	1.91	4.61E-03
DSRNA_UP	32	0.61	1.91	4.91E-03
MYC_TARGETS	39	0.58	1.90	5.89E-03
INSULIN_NIH3T3_UP	15	0.72	1.89	6.12E-03
CHAUHAN_2ME2	42	0.56	1.89	6.17E-03
CAMPTOTHECIN_PROBCELL_DN	21	0.66	1.89	6.08E-03
LINDSTEDT_DEND_DN	53	0.55	1.89	6.21E-03
LEE_DENA_UP	55	0.54	1.88	6.31E-03
ROSS_MLL_FUSION	60	0.53	1.88	6.51E-03
CCR5PATHWAY	18	0.68	1.88	6.64E-03
PEART_HISTONE_DN	63	0.52	1.88	6.61E-03
IRITANI_ADPROX_DN	45	0.55	1.87	7.03E-03
ABBUD_LIF_UP	45	0.56	1.87	7.16E-03
MUNSHI_MM_UP	57	0.53	1.87	7.10E-03
ZHAN_MULTIPLE_MYELOMA_VS_ NORMAL_DN	33	0.61	1.87	7.10E-03
NKTPATHWAY	28	0.62	1.85	9.28E-03

ES = enrichment score; NES = normalized enrichment score; FDR = false discovery rate

Appendix 6

Significantly altered gene sets by C-DEP/OVA compared to OVA

NAME	SIZE	ES	NES	FDR q-val
CARIES_PULP_HIGH_UP	68	0.80	2.94	< 1.00E-06
WIELAND_HEPATITIS_B_INDUCED	71	0.76	2.83	< 1.00E-06
NEMETH_TNF_UP	82	0.73	2.77	< 1.00E-06
YANG_OSTECLASTS_SIG	39	0.82	2.73	< 1.00E-06
LINDSTEDT_DEND_8H_VS_48H_UP	58	0.76	2.73	< 1.00E-06
FLECHNER_KIDNEY_TRANSPLANT_ REJECTION_UP	72	0.73	2.71	< 1.00E-06
IFNA_HCMV_6HRS_UP	38	0.80	2.64	< 1.00E-06
LAL_KO_6MO_UP	58	0.76	2.64	< 1.00E-06
GALINDO_ACT_UP	75	0.71	2.62	< 1.00E-06
LAL_KO_3MO_UP	46	0.77	2.60	< 1.00E-06
SANA_TNFA_ENDOTHELIAL_UP	61	0.73	2.59	< 1.00E-06
CMV_ALL_UP	81	0.67	2.50	< 1.00E-06
SANA_IFNG_ENDOTHELIAL_UP	45	0.74	2.50	< 1.00E-06
RADAEVA_IFNA_UP	38	0.76	2.49	< 1.00E-06
CMV_8HRS_UP	27	0.81	2.48	< 1.00E-06
BASSO_GERMINAL_CENTER_CD40_UP	82	0.66	2.48	< 1.00E-06
NAKAJIMA_MCS_UP	85	0.65	2.46	< 1.00E-06
DER_IFNA_UP	53	0.69	2.45	< 1.00E-06
CANCER_NEOPLASTIC_META_UP	59	0.69	2.45	< 1.00E-06
DER_IFNB_UP	76	0.65	2.41	< 1.00E-06
HINATA_NFKB_UP	89	0.63	2.41	< 1.00E-06
CMV_HCMV_TIMECOURSE_12HRS_UP	21	0.82	2.39	< 1.00E-06
CANCER_UNDIFFERENTIATED_META_UP	62	0.66	2.34	< 1.00E-06
CMV_24HRS_UP	61	0.66	2.34	< 1.00E-06
MANALO_HYPOXIA_DN	73	0.62	2.33	< 1.00E-06
NADLER_OBESITY_UP	57	0.66	2.32	< 1.00E-06
IFNA_UV-CMV_COMMON_HCMV_6HRS_UP	20	0.81	2.32	< 1.00E-06
SCHUMACHER_MYC_UP	47	0.68	2.32	< 1.00E-06
DER_IFNG_UP	54	0.66	2.28	< 1.00E-06
IFN_ANY_UP	71	0.61	2.27	< 1.00E-06
PEART_HISTONE_DN	63	0.63	2.26	< 1.00E-06
IFN_BETA_UP	55	0.64	2.26	< 1.00E-06
ADIP_DIFF_CLUSTER4	31	0.72	2.25	< 1.00E-06
IFNALPHA_NL_UP	19	0.80	2.25	< 1.00E-06
IFN_GAMMA_UP	35	0.69	2.23	< 1.00E-06
GOLDRATH_CYTOLYTIC	24	0.75	2.21	< 1.00E-06
IFNALPHA_HCC_UP	23	0.74	2.20	< 1.00E-06
CANTHARIDIN_DN	45	0.65	2.20	< 1.00E-06
MOREAUX_TACI_HI_IN_PPC_UP	43	0.66	2.19	< 1.00E-06
DAC_IFN_BLADDER_UP	16	0.82	2.19	< 1.00E-06
BENNETT_SLE_UP	19	0.79	2.18	< 1.00E-06
STRESS_TPA_SPECIFIC_UP	34	0.69	2.17	2.91E-05
TNFA_NFKB_DEP_UP	17	0.81	2.17	2.84E-05
TARTE_PC	65	0.60	2.17	2.77E-05

BLEO_HUMAN_LYMPH_HIGH_24HRS_UP	86	0.57	2.17	2.71E-05
DSRNA_UP	32	0.69	2.16	2.65E-05
TSA_CD4_UP	24	0.73	2.15	5.32E-05
JECHLINGER_EMT_UP	56	0.61	2.14	1.30E-04
INOS_ALL_UP	47	0.62	2.14	1.27E-04
IFN_ALL_UP	16	0.79	2.14	1.25E-04
IFN_ALPHA_UP	34	0.67	2.13	1.95E-04
LIAN_MYELOID_DIFF_RECEPTORS	33	0.67	2.13	1.91E-04
BRCA_BRCA1_POS	68	0.58	2.13	2.11E-04
ERM_KO_SERTOLI_DN	17	0.78	2.12	2.07E-04
COLLER_MYC_UP	17	0.78	2.12	2.03E-04
AMINOACYL_TRNA_BIOSYNTHESIS	18	0.75	2.10	4.86E-04
PROTEASOMEPATHWAY	21	0.73	2.09	5.20E-04
HSC_INTERMEDIATEPROGENITORS_ADULT	88	0.54	2.09	5.11E-04
PASSERINI_INFLAMMATION	23	0.70	2.08	6.52E-04
LINDSTEDT_DEND_DN	53	0.59	2.07	6.83E-04
ROSS_CBF_MYH	38	0.63	2.07	7.52E-04
LU_IL4BCELL	62	0.57	2.06	7.81E-04
DNA_REPLICATION_REACTOME	41	0.64	2.06	7.68E-04
STRESS_GENOTOXIC_SPECIFIC_DN	36	0.63	2.06	9.11E-04
SERUM_FIBROBLAST_CELLCYCLE	88	0.54	2.05	9.35E-04
YAGI_AML_PROGNOSIS	31	0.65	2.05	9.21E-04
EMT_UP	55	0.58	2.05	9.07E-04
PROTEASOME_DEGRADATION	32	0.65	2.05	9.12E-04
NI2_MOUSE_UP	40	0.62	2.05	9.88E-04
HSC_INTERMEDIATEPROGENITORS_SHARED	80	0.54	2.05	9.74E-04
LINDSTEDT_DEND_UP	44	0.61	2.04	1.05E-03
TRNA_SYNTHETASES	17	0.75	2.03	1.19E-03
SHIPP_FL_VS_DLBCL_DN	30	0.66	2.02	1.29E-03
INSULIN_ADIP_INSENS_UP	17	0.73	2.02	1.36E-03
PROTEASOME	17	0.74	2.01	1.46E-03
GOLDRATH_CELLCYCLE	28	0.65	2.01	1.52E-03
ZHAN_MULTIPLE_MYELOMA_SUBCLASSES_ DIFF	26	0.67	2.01	1.68E-03
YU_CMYC_DN	53	0.58	2.00	1.72E-03
UV-CMV_UNIQUE_HCMV_6HRS_UP	83	0.53	2.00	1.72E-03
CHOLESTEROL_BIOSYNTHESIS	15	0.76	2.00	1.69E-03
TAKEDA_NUP8_HOXA9_3D_DN	20	0.70	2.00	1.69E-03
YU_CMYC_UP	37	0.61	1.99	1.77E-03
UEDA_MOUSE_SCN	86	0.53	1.98	2.20E-03
APOPTOSIS	64	0.55	1.98	2.34E-03
ZELLER_MYC_UP	23	0.68	1.96	3.06E-03
DAC_BLADDER_UP	23	0.67	1.96	3.11E-03
MYC_TARGETS	39	0.58	1.94	3.99E-03
BLEO_MOUSE_LYMPH_HIGH_24HRS_DN	32	0.62	1.94	3.97E-03
CMV_HCMV_6HRS_UP	19	0.70	1.94	3.99E-03
HDACI_COLON_CUR24HRS_UP	28	0.63	1.94	3.96E-03
UNDERHILL_PROLIFERATION	18	0.69	1.93	4.03E-03
MENSSEN_MYC_UP	30	0.63	1.93	4.16E-03
IL1_CORNEA_UP	53	0.55	1.93	4.15E-03
FASPATHWAY	25	0.65	1.93	4.18E-03

MUNSHI_MM_UP	57	0.54	1.92	5.04E-03
IDX_TSA_UP_CLUSTER3	81	0.51	1.92	5.09E-03
ST_TUMOR_NECROSIS_FACTOR_PATHWAY	28	0.64	1.91	5.10E-03
PYRIMIDINE_METABOLISM	55	0.54	1.91	5.39E-03
KNUDSEN_PMNS_UP	65	0.53	1.91	5.40E-03
NFKBPATHWAY	23	0.65	1.90	5.53E-03
HEARTFAILURE_VENTRICLE_DN	56	0.53	1.90	5.62E-03
CMV_UV-CMV_COMMON_HCMV_6HRS_UP	17	0.70	1.90	6.00E-03
ABBUD_LIF_UP	45	0.56	1.88	7.06E-03
HPV31_DN	37	0.57	1.88	7.03E-03
LOTEM_LEUKEMIA_UP	22	0.65	1.88	7.17E-03
TPA_SENS_MIDDLE_UP	55	0.54	1.88	7.59E-03
CASPASEPATHWAY	20	0.67	1.88	7.62E-03
UVC_HIGH_D3_DN	35	0.59	1.87	7.75E-03
WANG_MLL_CBP_VS_GMP_UP	42	0.56	1.87	8.33E-03
MARSHALL_SPLEEN_BAL	25	0.62	1.86	9.11E-03
XU_CBP_UP	25	0.61	1.86	9.64E-03
MUNSHI_MM_VS_PCS_UP	64	0.51	1.86	9.70E-03
GENOTOXINS_ALL_24HRS_REG	22	0.64	1.86	9.65E-03

ES = enrichment score; NES = normalized enrichment score; FDR = false discovery rate

Appendix 7

Significantly altered gene sets by high DE/saline compared to air/saline

NAME	SIZE	ES	NES	NOM p-val
WANG_MLL_CBP_VS_GMP_UP	42	0.5829	1.8836	< 1.00E-06
HSC_MATURE_SHARED	169	0.4647	1.8517	< 1.00E-06
CARIES_PULP_HIGH_UP	68	0.5137	1.8385	< 1.00E-06
HSC_MATURE_ADULT	232	0.4448	1.8207	< 1.00E-06
NEMETH_TNF_DN	26	0.5976	1.7882	0.00430
SA_MMP_CYTOKINE_CONNECTION	15	0.6905	1.7827	0.00938
UVB_NHEK3_C2	35	0.5643	1.7761	0.00546
GSK3PATHWAY	26	0.5953	1.7462	0.00147
ZHAN_PCS_MULTIPLE_MYELOMA_SPKD	20	0.6155	1.7248	0.00436
TAKEDA_NUP8_HOXA9_16D_DN	126	0.4403	1.7221	< 1.00E-06
CORDERO_KRAS_KD_VS_CONTROL_DN	48	0.5109	1.7068	< 1.00E-06
LE_MYELIN_UP	91	0.4602	1.6978	0.00122
NI2_MOUSE_UP	40	0.5196	1.6940	0.00409
YANG_OSTECLASTS_SIG	39	0.5290	1.6935	0.00955
IGF1MTORPATHWAY	19	0.6039	1.6913	0.01351
CHEN_HOXA5_TARGETS_UP	135	0.4345	1.6912	< 1.00E-06
UVB_NHEK3_C5	30	0.5573	1.6886	0.00980
HOHENKIRK_MONOCYTE_DEND_DN	100	0.4442	1.6822	0.00122
TENEDINI_MEGAKARYOCYTIC_GENES	47	0.5038	1.6754	0.00530
HCC_SURVIVAL_GOOD_VS_POOR_DN	118	0.4318	1.6661	0.00118

ES = enrichment score; NES = normalized enrichment score; NOM p-val = nominal p-value

Appendix 8

Significantly altered gene sets by high DE/OVA compared to air/OVA

NAME	SIZE	ES	NES	NOM p-val
ELECTRON_TRANSPORT_CHAIN	86	0.5388	1.8950	< 1.00E-06
MOOTHA_VOXPHOS	73	0.5432	1.8901	< 1.00E-06
CANTHARIDIN_DN	45	0.5841	1.8698	< 1.00E-06
WANG_MLL_CBP_VS_GMP_UP	42	0.5782	1.8590	< 1.00E-06
FETAL_LIVER_VS_ADULT_LIVER_GNF2	53	0.5481	1.8214	< 1.00E-06
LVAD_HEARTFAILURE_DN	33	0.5996	1.8206	< 1.00E-06
MITOCHONDRIA	355	0.4661	1.7823	< 1.00E-06
GLUTATHIONE_METABOLISM	28	0.5990	1.7704	0.0012
FLECHNER_KIDNEY_TRANSPLANT_ REJECTION_UP	72	0.5018	1.7340	< 1.00E-06
CMV_HCMV_TIMECOURSE_14HRS_UP	33	0.5748	1.7278	0.0012
WIELAND_HEPATITIS_B_INDUCED	71	0.4953	1.7061	< 1.00E-06
INNEREAR_UP	34	0.5598	1.7037	0.0012
HUMAN_MITODB_6_2002	352	0.4416	1.7015	< 1.00E-06
ROSS_MLL_FUSION	60	0.5003	1.6858	0.0022
AMINOACYL_TRNA_BIOSYNTHESIS	18	0.6183	1.6649	0.0076
PYRIMIDINE_METABOLISM	55	0.5008	1.6546	0.0011
FATTY_ACID_DEGRADATION	23	0.5875	1.6440	0.0036
OXIDATIVE_PHOSPHORYLATION	55	0.4895	1.6302	0.0011
ABBUD_LIF_UP	45	0.5048	1.6222	0.0045
ROS_MOUSE_AORTA_UP	23	0.5807	1.6160	0.0086

ES = enrichment score; NES = normalized enrichment score; NOM p-val = nominal p-value

References

1. Abbey, D.E., et al., *Estimated long-term ambient concentrations of PM10 and development of respiratory symptoms in a nonsmoking population.* Arch Environ Health, 1995. **50**(2): p. 139-52.

2. Abbey, D.E., et al., *Chronic respiratory symptoms associated with estimated long-term ambient concentrations of fine particulates less than 2.5 microns in aerodynamic diameter (PM2.5) and other air pollutants.* J Expo Anal Environ Epidemiol, 1995. **5**(2): p. 137-59.

3. Dockery, D.W. and C.A. Pope, 3rd, *Acute respiratory effects of particulate air pollution.* Annu Rev Public Health, 1994. **15**: p. 107-32.

4. Pope, C.A., 3rd, et al., *Particulate air pollution as a predictor of mortality in a prospective study of U.S. adults.* Am J Respir Crit Care Med, 1995. **151**(3 Pt 1): p. 669-74.

5. Oberdorster, G. and M.J. Utell, *Ultrafine particles in the urban air: to the respiratory tract--and beyond?* Environ Health Perspect, 2002. **110**(8): p. A440-1.

6. Wilson, W.E., et al., *Monitoring of particulate matter outdoors.* Chemosphere, 2002. **49**(9): p. 1009-43.

7. Gilmour, M.I., et al., *Comparative toxicity of size-fractionated airborne particulate matter obtained from different cities in the United States.* Inhal Toxicol, 2007. **19 Suppl 1**: p. 7-16.

8. Schins, R.P., et al., *Inflammatory effects of coarse and fine particulate matter in relation to chemical and biological constituents.* Toxicol Appl Pharmacol, 2004. **195**(1): p. 1-11.

9. Oberdorster, G., J. Ferin, and B.E. Lehnert, *Correlation between particle size, in vivo particle persistence, and lung injury.* Environ Health Perspect, 1994. **102 Suppl 5**: p. 173-9.

10. Lippmann, M. and R.B. Schlesinger, *Toxicological bases for the setting of health-related air pollution standards.* Annu Rev Public Health, 2000. **21**: p. 309-33.

11. Monteiller, C., et al., *The pro-inflammatory effects of low-toxicity low-solubility particles, nanoparticles and fine particles, on epithelial cells in vitro: the role of surface area.* Occup Environ Med, 2007. **64**(9): p. 609-15.

12. Dick, C.A., et al., *The role of free radicals in the toxic and inflammatory effects of four different ultrafine particle types.* Inhal Toxicol, 2003. **15**(1): p. 39-52.

13. Aust, A.E., et al., *Particle characteristics responsible for effects on human lung epithelial cells.* Res Rep Health Eff Inst, 2002(110): p. 1-65; discussion 67-76.

14. Miyabara, Y., et al., *Diesel exhaust enhances allergic airway inflammation and hyperresponsiveness in mice.* Am J Respir Crit Care Med, 1998. **157**(4 Pt 1): p. 1138-44.

15. Steerenberg, P.A., et al., *Adjuvant activity of various diesel exhaust and ambient particle in two allergic models.* J Toxicol Environ Health A, 2003. **66**(15): p. 1421-1439.

16. Whitekus, M.J., et al., *Thiol antioxidants inhibit the adjuvant effects of aerosolized diesel exhaust particles in a murine model for ovalabumin sensitization.* J Immun, 2002. **168**: p. 2560-2567.

17. de Raat, W.K. and F.A. de Meijere, *Polycyclic aromatic hydrocarbon (PAH) concentrations in ambient airborne particles from local traffic and distant sources; variation of the PAH profile.* Sci Total Environ, 1991. **103**(1): p. 1-17.

18. Kinney, P.L., et al., *Airborne concentrations of PM(2.5) and diesel exhaust particles on Harlem sidewalks: a community-based pilot study.* Environ Health Perspect, 2000. **108**(3): p. 213-8.

19. Fruin, A., *Fine particle and black carbon concentrations inside vehicles*. in *10th annual conferance of the international society of exposure analysis*. 2000.

20. HEI, *Health effects of diesel exhaust: epidemiology. In: Diesel Exhaust: A critical analysis of emissions, exposure and health effects*. 1995, Health Effects Institute: Cambridge. p. 251-292.

21. Singh, P., et al., *Sample characterization of automobile and forklift diesel exhaust particles and comparative pulmonary toxicity in mice.* Environ Health Perspect, 2004. **112**(8): p. 820-5.

22. Schafer, T. and J. Ring, *Epidemiology of allergic diseases.* Allergy, 1997. **52**(38 Suppl): p. 14-22; discussion 35-6.

23. von Mutius, E., et al., *International patterns of tuberculosis and the prevalence of symptoms of asthma, rhinitis, and eczema.* Thorax, 2000. **55**(6): p. 449-53.

24. *American Academy of Allergy, Asthma, and Immunology 56th annual meeting. San Diego, California, USA. March 3-8, 2000. Abstracts.* J Allergy Clin Immunol, 2000. **105**(1 Pt 2): p. S1-462.

25. Gold, D.R. and D. Acevedo-Garcia, *Immigration to the United States and acculturation as risk factors for asthma and allergy.* J Allergy Clin Immunol, 2005. **116**(1): p. 38-41.

26. Ober, C. and S. Hoffjan, *Asthma genetics 2006: the long and winding road to gene discovery.* Genes Immun, 2006. **7**(2): p. 95-100.

27. Black, P.N. and S. Sharpe, *Dietary fat and asthma: is there a connection?* Eur Respir J, 1997. **10**(1): p. 6-12.

28. Rumold, R., M. Jyrala, and D. Diaz-Sanchez, *Secondhand smoke induces allergic sensitization in mice.* J Immunol, 2001. **167**(8): p. 4765-70.

29. Bornehag, C.G., et al., *Association between ventilation rates in 390 Swedish homes and allergic symptoms in children.* Indoor Air, 2005. **15**(4): p. 275-80.

30. Etzel, R.A., *How environmental exposures influence the development and exacerbation of asthma.* Pediatrics, 2003. **112**(1 Pt 2): p. 233-9.

31. Pierson, W.E. and J.Q. Koenig, *Respiratory effects of air pollution on allergic disease.* J Allergy Clin Immunol, 1992. **90**(4 Pt 1): p. 557-66.

32. Gilmour, M.I., et al., *How exposure to environmental tobacco smoke, outdoor air pollutants, and increased pollen burdens influences the incidence of asthma.* Environ Health Perspect, 2006. **114**(4): p. 627-33.

33. Peden, D.B., *Air pollutants, exercise, and risk of developing asthma in children.* Clin J Sport Med, 2003. **13**(1): p. 62-3.

34. CDC, *Asthma at a Glance*, N.C.f.E.H. (NCEH), Editor. 1999, CDC.

35. Holt, P.G. and W.R. Thomas, *Sensitization to airborne environmental allergens: unresolved issues.* Nat Immunol, 2005. **6**(10): p. 957-60.

36. Ostro, B., *The association of air pollution and mortality: examining the case for inference.* Arch Environ Health, 1993. **48**(5): p. 336-42.

37. Atkinson, R.W., et al., *Acute effects of particulate air pollution on respiratory admissions: results from APHEA 2 project. Air Pollution and Health: a European Approach.* Am J Respir Crit Care Med, 2001. **164**(10 Pt 1): p. 1860-6.

38. Abbey, D.E., et al., *Long-term ambient concentrations of total suspended particulates and oxidants as related to incidence of chronic disease in California Seventh-Day Adventists.* Environ Health Perspect, 1991. **94**: p. 43-50.

39. Gordian, M.E., et al., *Particulate air pollution and respiratory disease in Anchorage, Alaska.* Environ Health Perspect, 1996. **104**(3): p. 290-7.

40. van Vliet, P., et al., *Motor vehicle exhaust and chronic respiratory symptoms in children living near freeways.* Environ Res, 1997. **74**(2): p. 122-32.

41. Mosmann, T.R., et al., *Two types of murine helper T cell clone. I. Definition according to profiles of lymphokine activities and secreted proteins.* J Immunol, 1986. **136**(7): p. 2348-57.

42. Peden, D.B., *Development of atopy and asthma: candidate environmental influences and important periods of exposure.* Environ Health Perspect, 2000. **108 Suppl 3**: p. 475-82.

43. Kay, A.B., et al., *Eosinophils and eosinophil-associated cytokines in allergic inflammation.* Int Arch Allergy Immunol, 1997. **113**(1-3): p. 196-9.

44. Kay, A.B. and C.J. Corrigan, *Asthma. Eosinophils and neutrophils.* Br Med Bull, 1992. **48**(1): p. 51-64.

45. Kitayama, J., et al., *The C-C chemokine receptor CCR3 participates in stimulation of eosinophil arrest on inflammatory endothelium in shear flow.* J Clin Invest, 1998. **101**(9): p. 2017-24.

46. Sanderson, C.J., *Interleukin-5, eosinophils, and disease.* Blood, 1992. **79**(12): p. 3101-9.

47. Denburg, J.A., *The origins of basophils and eosinophils in allergic inflammation.* J Allergy Clin Immunol, 1998. **102**(5): p. S74-6.

48. O'Byrne P, M. and D.S. Postma, *The many faces of airway inflammation. Asthma and chronic obstructive pulmonary disease. Asthma Research Group.* Am J Respir Crit Care Med, 1999. **159**(5 Pt 2): p. S41-63.

49. Mautino, G., et al., *Balance in asthma between matrix metalloproteinases and their inhibitors.* J Allergy Clin Immunol, 1999. **104**(3 Pt 1): p. 530-3.

50. Bruijnzeel, P.L., *Contribution of eosinophil-derived mediators in asthma.* Int Arch Allergy Appl Immunol, 1989. **90 Suppl 1**: p. 57-63.

51. Onadeko, B.O., et al., *Serum eosinophil cationic protein as a predictor of disease activity in acute and chronic asthma.* East Afr Med J, 1999. **76**(9): p. 524-9.

52. Coffman, R.L., et al., *B cell stimulatory factor-1 enhances the IgE response of lipopolysaccharide-activated B cells.* J Immunol, 1986. **136**(12): p. 4538-41.

53. Pawankar, R., et al., *Nasal mast cells in perennial allergic rhinitics exhibit increased expression of the Fc epsilonRI, CD40L, IL-4, and IL-13, and can induce IgE synthesis in B cells.* J Clin Invest, 1997. **99**(7): p. 1492-9.

54. Goust, J.M., *Immediate hypersensitivity.* Immunol Ser, 1993. **58**: p. 343-59.

55. Dabbagh, K., et al., *IL-4 induces mucin gene expression and goblet cell metaplasia in vitro and in vivo.* J Immunol, 1999. **162**(10): p. 6233-7.

56. Doucet, C., et al., *IL-4 and IL-13 specifically increase adhesion molecule and inflammatory cytokine expression in human lung fibroblasts.* Int Immunol, 1998. **10**(10): p. 1421-33.

57. Hsieh, C.S., et al., *Differential regulation of T helper phenotype development by interleukins 4 and 10 in an alpha beta T-cell-receptor transgenic system.* Proc Natl Acad Sci U S A, 1992. **89**(13): p. 6065-9.

58. Seder, R.A., et al., *The presence of interleukin 4 during in vitro priming determines the lymphokine-producing potential of CD4+ T cells from T cell receptor transgenic mice.* J Exp Med, 1992. **176**(4): p. 1091-8.

59. Kopf, M., et al., *Disruption of the murine IL-4 gene blocks Th2 cytokine responses.* Nature, 1993. **362**(6417): p. 245-8.

60. Moser, R., J. Fehr, and P.L. Bruijnzeel, *IL-4 controls the selective endothelium-driven transmigration of eosinophils from allergic individuals.* J Immunol, 1992. **149**(4): p. 1432-8.

61. Kips, J.C., *Cytokines in asthma.* Eur Respir J Suppl, 2001. **34**: p. 24s-33s.

62. Mahanty, S. and T.B. Nutman, *The biology of interleukin-5 and its receptor.* Cancer Invest, 1993. **11**(5): p. 624-34.

63. Foster, P.S., et al., *Interleukin 5 deficiency abolishes eosinophilia, airways hyperreactivity, and lung damage in a mouse asthma model.* J Exp Med, 1996. **183**(1): p. 195-201.

64. Minty, A., et al., *Interleukin-13 is a new human lymphokine regulating inflammatory and immune responses.* Nature, 1993. **362**(6417): p. 248-50.

65. Zurawski, G. and J.E. de Vries, *Interleukin 13 elicits a subset of the activities of its close relative interleukin 4.* Stem Cells, 1994. **12**(2): p. 169-74.

66. Humbert, M., et al., *Elevated expression of messenger ribonucleic acid encoding IL-13 in the bronchial mucosa of atopic and nonatopic subjects with asthma.* J Allergy Clin Immunol, 1997. **99**(5): p. 657-65.

67. Naseer, T., et al., *Expression of IL-12 and IL-13 mRNA in asthma and their modulation in response to steroid therapy.* Am J Respir Crit Care Med, 1997. **155**(3): p. 845-51.

68. Grunig, G., et al., *Requirement for IL-13 independently of IL-4 in experimental asthma.* Science, 1998. **282**(5397): p. 2261-3.

69. Wills-Karp, M., et al., *Interleukin-13: central mediator of allergic asthma.* Science, 1998. **282**(5397): p. 2258-61.

70. de Vries, J.E., *The role of IL-13 and its receptor in allergy and inflammatory responses.* J Allergy Clin Immunol, 1998. **102**(2): p. 165-9.

71. Borish, L., et al., *Interleukin-10 regulation in normal subjects and patients with asthma.* J Allergy Clin Immunol, 1996. **97**(6): p. 1288-96.

72. Robinson, D.S., et al., *Increased interleukin-10 messenger RNA expression in atopic allergy and asthma.* Am J Respir Cell Mol Biol, 1996. **14**(2): p. 113-7.

73. van Scott, M.R., et al., *IL-10 reduces Th2 cytokine production and eosinophilia but augments airway reactivity in allergic mice.* Am J Physiol Lung Cell Mol Physiol, 2000. **278**(4): p. L667-74.

74. Moore, K.W., et al., *Interleukin-10.* Annu Rev Immunol, 1993. **11**: p. 165-90.

75. Seitz, M., et al., *Interleukin-10 differentially regulates cytokine inhibitor and chemokine release from blood mononuclear cells and fibroblasts.* Eur J Immunol, 1995. **25**(4): p. 1129-32.

76. Sironi, M., et al., *Divergent effects of interleukin-10 on cytokine production by mononuclear phagocytes and endothelial cells.* Eur J Immunol, 1993. **23**(10): p. 2692-5.

77. Lukacs, N.W., et al., *Differential recruitment of leukocyte populations and alteration of airway hyperreactivity by C-C family chemokines in allergic airway inflammation.* J Immunol, 1997. **158**(9): p. 4398-404.

78. Nakae, S., et al., *IL-1 is required for allergen-specific Th2 cell activation and the development of airway hypersensitivity response.* Int Immunol, 2003. **15**(4): p. 483-90.

79. Broide, D.H. and G.S. Firestein, *Endobronchial allergen challenge in asthma. Demonstration of cellular source of granulocyte macrophage colony-stimulating factor by in situ hybridization.* J Clin Invest, 1991. **88**(3): p. 1048-53.

80. Hirata, N., et al., *Allergen exposure induces the expression of endothelial adhesion molecules in passively sensitized human bronchus: time course and the role of cytokines.* Am J Respir Cell Mol Biol, 1998. **18**(1): p. 12-20.

81. Ohkawara, Y., et al., *Human lung mast cells and pulmonary macrophages produce tumor necrosis factor-alpha in sensitized lung tissue after IgE receptor triggering.* Am J Respir Cell Mol Biol, 1992. **7**(4): p. 385-92.

82. Albuquerque, R.V., et al., *Association of polymorphisms within the tumour necrosis factor (TNF) genes and childhood asthma.* Clin Exp Allergy, 1998. **28**(5): p. 578-84.

83. Gosset, P., et al., *Tumor necrosis factor alpha and interleukin-6 production by human mononuclear phagocytes from allergic asthmatics after IgE-dependent stimulation.* Am Rev Respir Dis, 1992. **146**(3): p. 768-74.

84. Bhandari, V., *Developmental differences in the role of interleukins in hyperoxic lung injury in animal models.* Front Biosci, 2002. **7**: p. d1624-33.

85. Mattoli, S., et al., *Levels of endothelin in the bronchoalveolar lavage fluid of patients with symptomatic asthma and reversible airflow obstruction.* J Allergy Clin Immunol, 1991. **88**(3 Pt 1): p. 376-84.

86. Elias, J.A., et al., *Cytokine- and virus-stimulated airway smooth muscle cells produce IL-11 and other IL-6-type cytokines.* Am J Physiol, 1997. **273**(3 Pt 1): p. L648-55.

87. Rochester, C.L., et al., *Eosinophil-fibroblast interactions. Granule major basic protein interacts with IL-1 and transforming growth factor-beta in the stimulation of lung fibroblast IL-6-type cytokine production.* J Immunol, 1996. **156**(11): p. 4449-56.

88. Akira, S., T. Taga, and T. Kishimoto, *Interleukin-6 in biology and medicine.* Adv Immunol, 1993. **54**: p. 1-78.

89. Broide, D.H., et al., *Cytokines in symptomatic asthma airways.* J Allergy Clin Immunol, 1992. **89**(5): p. 958-67.

90. Vercelli, D., et al., *Endogenous interleukin 6 plays an obligatory role in interleukin 4-dependent human IgE synthesis.* Eur J Immunol, 1989. **19**(8): p. 1419-24.

91. Silberstein, D.S., et al., *Enhancement of human eosinophil cytotoxicity and leukotriene synthesis by biosynthetic (recombinant) granulocyte-macrophage colony-stimulating factor.* J Immunol, 1986. **137**(10): p. 3290-4.

92. Marini, M., et al., *Expression of the potent inflammatory cytokines, granulocyte-macrophage-colony-stimulating factor and interleukin-6 and interleukin-8, in bronchial epithelial cells of patients with asthma.* J Allergy Clin Immunol, 1992. **89**(5): p. 1001-9.

93. Virchow, J.C., Jr., et al., *Inflammatory determinants of asthma severity: mediator and cellular changes in bronchoalveolar lavage fluid of patients with severe asthma.* J Allergy Clin Immunol, 1996. **98**(5 Pt 2): p. S27-33; discussion S33-40.

94. Virchow, J.C., Jr., et al., *T cells and cytokines in bronchoalveolar lavage fluid after segmental allergen provocation in atopic asthma.* Am J Respir Crit Care Med, 1995. **151**(4): p. 960-8.

95. Cox, G., et al., *Promotion of eosinophil survival by human bronchial epithelial cells and its modulation by steroids.* Am J Respir Cell Mol Biol, 1991. **4**(6): p. 525-31.

96. Masuda, T., et al., *Airway epithelial cells enhance eosinophil survival.* Respiration, 1992. **59**(4): p. 238-42.

97. Vignola, A.M., et al., *Evaluation of apoptosis of eosinophils, macrophages, and T lymphocytes in mucosal biopsy specimens of patients with asthma and chronic bronchitis.* J Allergy Clin Immunol, 1999. **103**(4): p. 563-73.

98. Lambrecht, B.N., et al., *Dendritic cells are required for the development of chronic eosinophilic airway inflammation in response to inhaled antigen in sensitized mice.* J Immunol, 1998. **160**(8): p. 4090-7.

99. Stampfli, M.R., et al., *GM-CSF transgene expression in the airway allows aerosolized ovalbumin to induce allergic sensitization in mice.* J Clin Invest, 1998. **102**(9): p. 1704-14.

100. Banchereau, J. and R.M. Steinman, *Dendritic cells and the control of immunity.* Nature, 1998. **392**(6673): p. 245-52.

101. Lei, X.F., et al., *Compartmentalized transgene expression of granulocyte-macrophage colony-stimulating factor (GM-CSF) in mouse lung enhances allergic airways inflammation.* Clin Exp Immunol, 1998. **113**(2): p. 157-65.

102. Omata, N., et al., *Monocyte chemoattractant protein-1 selectively inhibits the acquisition of CD40 ligand-dependent IL-12-producing capacity of monocyte-derived dendritic cells and modulates Th1 immune response.* J Immunol, 2002. **169**(9): p. 4861-6.

103. Roggen, E.L., et al., *Interactions between dendritic cells and epithelial cells in allergic disease.* Toxicol Lett, 2006. **162**(1): p. 71-82.

104. Zhou, B., et al., *Thymic stromal lymphopoietin as a key initiator of allergic airway inflammation in mice.* Nat Immunol, 2005. **6**(10): p. 1047-53.

105. Hirata, H., et al., *Production of TARC and MDC by naive T cells in asthmatic patients.* J Clin Immunol, 2003. **23**(1): p. 34-45.

106. Raghow, R., *Role of transforming growth factor-beta in repair and fibrosis.* Chest, 1991. **99**(3 Suppl): p. 61S-65S.

107. Raghu, G., et al., *Collagen synthesis by normal and fibrotic human lung fibroblasts and the effect of transforming growth factor-beta.* Am Rev Respir Dis, 1989. **140**(1): p. 95-100.

108. Minshall, E.M., et al., *Eosinophil-associated TGF-beta1 mRNA expression and airways fibrosis in bronchial asthma.* Am J Respir Cell Mol Biol, 1997. **17**(3): p. 326-33.

109. Gruber, B.L., M.J. Marchese, and R.R. Kew, *Transforming growth factor-beta 1 mediates mast cell chemotaxis.* J Immunol, 1994. **152**(12): p. 5860-7.

110. Postlethwaite, A.E., et al., *Stimulation of the chemotactic migration of human fibroblasts by transforming growth factor beta.* J Exp Med, 1987. **165**(1): p. 251-6.

111. Wahl, S.M., et al., *Transforming growth factor type beta induces monocyte chemotaxis and growth factor production.* Proc Natl Acad Sci U S A, 1987. **84**(16): p. 5788-92.

112. Kelley, J., et al., *Cytokine signaling in lung: transforming growth factor-beta secretion by lung fibroblasts.* Am J Physiol, 1991. **260**(2 Pt 1): p. L123-8.

113. Wade, J.F., 3rd and L.S. Newman, *Diesel asthma. Reactive airways disease following overexposure to locomotive exhaust.* J Occup Med, 1993. **35**(2): p. 149-54.

114. Rusznak, C., J.L. Devalia, and R.J. Davies, *The impact of pollution on allergic disease.* Allergy, 1994. **49**(18 Suppl): p. 21-7.

115. D'Amato, G., *Outdoor air pollution in urban areas and allergic respiratory diseases.* Monaldi Arch Chest Dis, 1999. **54**(6): p. 470-4.

116. Hajat, S., et al., *Association of air pollution with daily GP consultations for asthma and other lower respiratory conditions in London.* Thorax, 1999. **54**(7): p. 597-605.

117. Nicolai, T., *Environmental air pollution and lung disease in children.* Monaldi Arch Chest Dis, 1999. **54**(6): p. 475-8.

118. Brunekreef, B., et al., *Air pollution from truck traffic and lung function in children living near motorways.* Epidemiology, 1997. **8**(3): p. 298-303.

119. Delfino, R.J., et al., *Asthma symptoms in Hispanic children and daily ambient exposures to toxic and criteria air pollutants.* Environ Health Perspect, 2003. **111**(4): p. 647-56.

120. Gauderman, W.J., et al., *Childhood asthma and exposure to traffic and nitrogen dioxide.* Epidemiology, 2005. **16**(6): p. 737-43.

121. Diaz-Sanchez, D., et al., *Enhanced nasal cytokine production in human beings after in vivo challenge with diesel exhaust particles.* J Allergy Clin Immunol, 1996. **98**(1): p. 114-23.

122. Diaz-Sanchez, D., et al., *Combined diesel exhaust particulate and ragweed allergen challenge markedly enhances human in vivo nasal ragweed-specific IgE and skews cytokine production to a T helper cell 2-type pattern.* J Immunol, 1997. **158**(5): p. 2406-13.

123. Lovik, M., et al., *Diesel exhaust particles and carbon black have adjuvant activity on the local lymph node response and systemic IgE production to ovalbumin.* Toxicology, 1997. **121**(2): p. 165-78.

124. Miyabara, Y., et al., *Effects of diesel exhaust on allergic airway inflammation in mice.* J Allergy Clin Immunol, 1998. **102**(5): p. 805-12.

125. Nel, A.E., et al., *Enhancement of allergic inflammation by the interaction between diesel exhaust particles and the immune system.* J Allergy Clin Immunol, 1998. **102**(4 Pt 1): p. 539-54.

126. Takano, H., et al., *Diesel exhaust particles enhance antigen-induced airway inflammation and local cytokine expression in mice.* Am J Respir Crit Care Med, 1997. **156**(1): p. 36-42.

127. Takafuji, S., et al., *Enhancing effect of suspended particulate matter on the IgE antibody production in mice.* Int Arch Allergy Appl Immunol, 1989. **90**(1): p. 1-7.

128. Fujimaki, H., et al., *Inhalation of diesel exhaust enhances antigen-specific IgE antibody production in mice.* Toxicology, 1997. **116**(1-3): p. 227-33.

129. Lambert, A.L., et al., *Enhanced allergic sensitization by residual oil fly ash particles is mediated by soluble metal constituents.* Toxicol Appl Pharmacol, 2000. **165**(1): p. 84-93.

130. Maejima, K., et al., *Comparison of the effects of various fine particles on IgE antibody production in mice inhaling Japanese cedar pollen allergens.* J Toxicol Environ Health, 1997. **52**(3): p. 231-48.

131. de Haar, C., et al., *Ultrafine carbon black particles cause early airway inflammation and have adjuvant activity in a mouse allergic airway disease model.* Toxicol Sci, 2005. **87**(2): p. 409-18.

132. Nygaard, U.C., et al., *Ambient air particles from four European cities increase the primary cellular response to allergen in the draining lymph node.* Toxicology, 2005. **207**(2): p. 241-54.

133. van Zijverden, M., et al., *Diesel exhaust, carbon black, and silica particles display distinct Th1/Th2 modulating activity.* Toxicol Appl Pharmacol, 2000. **168**(2): p. 131-9.

134. Diaz-Sanchez, D., et al., *Diesel exhaust particles induce local IgE production in vivo and alter the pattern of messenger RNA isoforms.* J Clin Invest, 1994. **94**: p. 1417-1425.

135. Diaz-Sanchez, D., et al., *Nasal challenge with diesel exhaust particles can induce sensitization to a neoallergen in the human mucosa.* J Allergy Clin Immunol, 1999. **104**(6): p. 1183-8.

136. Granum, B. and M. Lovik, *The effect of particles on allergic immune responses.* Toxicol Sci, 2002. **65**(1): p. 7-17.

137. Singh, P., M. Madden, and M.I. Gilmour, *Effects of Diesel Exhaust Particles and Carbon Black on Induction of Dust Mite Allergy in Brown Norway Rats.* J Immunotoxicology, 2005. **2**: p. 41-49.

138. Kongerud, J., et al., *Nasal responses in asthmatic and nonasthmatic subjects following exposure to diesel exhaust particles.* Inhal Toxicol, 2006. **18**(9): p. 589-94.

139. Lambrecht, B.N., et al., *Myeloid dendritic cells induce Th2 responses to inhaled antigen, leading to eosinophilic airway inflammation.* J Clin Invest, 2000. **106**(4): p. 551-9.

140. Lambrecht, B.N. and H. Hammad, *Taking our breath away: dendritic cells in the pathogenesis of asthma.* Nat Rev Immunol, 2003. **3**(12): p. 994-1003.

141. de Heer, H.J., et al., *Essential role of lung plasmacytoid dendritic cells in preventing asthmatic reactions to harmless inhaled antigen.* J Exp Med, 2004. **200**(1): p. 89-98.

142. van Rijt, L.S. and B.N. Lambrecht, *Dendritic cells in asthma: a function beyond sensitization.* Clin Exp Allergy, 2005. **35**(9): p. 1125-34.

143. Rengasamy, A., et al., *Diesel exhaust particle-induced alterations of pulmonary phase I and phase II enzymes of rats.* J Toxicol Environ Health A, 2003. **66**(2): p. 153-67.

144. Schuetzle, D., *Sampling of vehicle emissions for chemical analysis and biological testing.* Environ Health Perspect, 1983. **47**: p. 65-80.

145. Bunger, J., et al., *Mutagenicity of diesel exhaust particles from two fossil and two plant oil fuels.* Mutagenesis, 2000. **15**(5): p. 391-7.

146. Conney, A.H., *Induction of microsomal enzymes by foreign chemicals and carcinogenesis by polycyclic aromatic hydrocarbons: G. H. A. Clowes Memorial Lecture.* Cancer Res, 1982. **42**(12): p. 4875-917.

147. Thakker, D.R., et al., *Metabolism of benzo[a]pyrene: conversion of (+/-)-trans-7,8-dihydroxy-7,8-dihydrobenzo[a]pyrene to highly mutagenic 7,8-diol-9,10-epoxides.* Proc Natl Acad Sci U S A, 1976. **73**(10): p. 3381-5.

148. Yang, S.K., et al., *Enzymatic conversion of benzo(a)pyrene leading predominantly to the diol-epoxide r-7,t-8-dihydroxy-t-9,10-oxy-7,8,9,10-tetrahydrobenzo(a)pyrene through a single enantiomer of r-7, t-8-dihydroxy-7,8-dihydrobenzo(a)pyrene.* Proc Natl Acad Sci U S A, 1976. **73**(8): p. 2594-8.

149. Cavalieri, E.L. and E.G. Rogan, *Central role of radical cations in metabolic activation of polycyclic aromatic hydrocarbons.* Xenobiotica, 1995. **25**(7): p. 677-88.

150. Chen, L., et al., *Expanded analysis of benzo[a]pyrene-DNA adducts formed in vitro and in mouse skin: their significance in tumor initiation.* Chem Res Toxicol, 1996. **9**(5): p. 897-903.

151. Penning, T.M., et al., *Generation of reactive oxygen species during the enzymatic oxidation of polycyclic aromatic hydrocarbon trans-dihydrodiols catalyzed by dihydrodiol dehydrogenase.* Chem Res Toxicol, 1996. **9**(1): p. 84-92.

152. Smithgall, T.E., R.G. Harvey, and T.M. Penning, *Spectroscopic identification of ortho-quinones as the products of polycyclic aromatic trans-dihydrodiol oxidation catalyzed by dihydrodiol dehydrogenase. A potential route of proximate carcinogen metabolism.* J Biol Chem, 1988. **263**(4): p. 1814-20.

153. Takano, H., et al., *Lung expression of cytochrome P450 1A1 as a possible biomarker of exposure to diesel exhaust particles.* Arch Toxicol, 2002. **76**(3): p. 146-51.

154. Devanesan, P.D., et al., *Identification and quantitation of benzo[a]pyrene-DNA adducts formed by rat liver microsomes in vitro.* Chem Res Toxicol, 1992. **5**(2): p. 302-9.

155. Bond, J.A., J.L. Mauderly, and R.K. Wolff, *Concentration- and time-dependent formation of DNA adducts in lungs of rats exposed to diesel exhaust.* Toxicology, 1990. **60**(1-2): p. 127-35.

156. Hemminki, K., et al., *DNA adducts among personnel servicing and loading diesel vehicles.* Carcinogenesis, 1994. **15**(4): p. 767-9.

157. Cho, H.Y., et al., *Role of NRF2 in protection against hyperoxic lung injury in mice.* Am J Respir Cell Mol Biol, 2002. **26**(2): p. 175-82.

158. Li, N., et al., *Comparison of the pro-oxidative and proinflammatory effects of organic diesel exhaust particle chemicals in bronchial epithelial cells and macrophages.* J Immunol, 2002. **169**(8): p. 4531-41.

159. Xiao, G.G., et al., *Use of proteomics to demonstrate a hierarchical oxidative stress response to diesel exhaust particle chemicals in a macrophage cell line.* J Biol Chem, 2003. **278**(50): p. 50781-50790.

160. Li, N., et al., *Nrf2 is a key transcription factor that regulates antioxidant defense in macrophages and epithelial cells: protecting against the proinflammatory and oxidizing effects of diesel exhaust chemicals.* J Immunol, 2004. **173**(5): p. 3467-81.

161. Wang, M., et al., *Use of a fluorescent phosphoprotein dye to characterize oxidative stress-induced signaling pathway components in macrophage and epithelial cultures exposed to diesel exhaust particle chemicals.* Electrophoresis, 2005. **26**(11): p. 2092-108.

162. Xiao, G.G., et al., *Use of proteomics to demonstrate a hierarchical oxidative stress response to diesel exhaust particle chemicals in a macrophage cell line.* J Biol Chem, 2003. **278**(50): p. 50781-90.

163. Pandya, R.J., et al., *Diesel exhaust and asthma: hypotheses and molecular mechanisms of action.* Environ Health Perspect, 2002. **110 Suppl 1**: p. 103-12.

164. Hiura, T.S., et al., *Chemicals in diesel exhaust particles generate reactive oxygen radicals and induce apoptosis in macrophages.* J Immunol, 1999. **163**(10): p. 5582-91.

165. Xia, T., et al., *Quinones and aromatic chemical compounds in particulate matter induce mitochondrial dysfunction: implications for ultrafine particle toxicity.* Environ Health Perspect, 2004. **112**(14): p. 1347-58.

166. Li, N., et al., *Ultrafine particulate pollutants induce oxidative stress and mitochondrial damage.* Environ Health Perspect, 2003. **111**(4): p. 455-60.

167. Pennie, W.D., et al., *Application of genomics to the definition of the molecular basis for toxicity.* Toxicol Lett, 2001. **120**(1-3): p. 353-8.

168. Thomas, R.S., et al., *Application of genomics to toxicology research.* Environ Health Perspect, 2002. **110 Suppl 6**: p. 919-23.

169. Reynolds, L.J. and R.J. Richards, *Can toxicogenomics provide information on the bioreactivity of diesel exhaust particles?* Toxicology, 2001. **165**(2-3): p. 145-52.

170. Sato, H., et al., *Identification, by cDNA microarray, of A-raf and proliferating cell nuclear antigen as genes induced in rat lung by exposure to diesel exhaust.* Res Commun Mol Pathol Pharmacol, 1999. **105**(1-2): p. 77-86.

171. Koike, E., et al., *cDNA microarray analysis of gene expression in rat alveolar macrophages in response to organic extract of diesel exhaust particles.* Toxicol Sci, 2002. **67**(2): p. 241-6.

172. Koike, E., et al., *cDNA microarray analysis of rat alveolar epithelial cells following exposure to organic extract of diesel exhaust particles.* Toxicol Appl Pharmacol, 2004. **201**(2): p. 178-85.

173. Verheyen, G.R., et al., *Microarray analysis of the effect of diesel exhaust particles on in vitro cultured macrophages.* Toxicol In Vitro, 2004. **18**(3): p. 377-91.

174. Li, N., et al., *Particulate air pollutants and asthma. A paradigm for the role of oxidative stress in PM-induced adverse health effects.* Clin Immunol, 2003. **109**(3): p. 250-65.

175. Li, N., et al., *Use of a stratiefied oxidative stress model to study the biological effects of ambient concentrated and diesel exhaust particulate matter.* Inhalation Toxicology, 2002. **14**: p. 459-486.

176. D'Amato, G., G. Liccardi, and M. D'Amato, *Environmental risk factors (outdoor air pollution and climatic changes) and increased trend of respiratory allergy.* J Investig Allergol Clin Immunol, 2000. **10**(3): p. 123-8.

177. Maziak, W., et al., *Are asthma and allergies in children and adolescents increasing? Results from ISAAC phase I and phase III surveys in Munster, Germany.* Allergy, 2003. **58**(7): p. 572-9.

178. Galassi, C., et al., *Changes in prevalence of asthma and allergies among children and adolescents in Italy: 1994-2002.* Pediatrics, 2006. **117**(1): p. 34-42.

179. Carvajal-Uruena, I., et al., *[Geographic variation in the prevalence of asthma symptoms in Spanish children and adolescents. International Study of Asthma and Allergies in Childhood (ISAAC) Phase 3, Spain]*. Arch Bronconeumol, 2005. **41**(12): p. 659-66.

180. Chellini, E., et al., *[Changes in social characteristics and risk factors for asthma and allergies among children and adolescents in Italy]*. Epidemiol Prev, 2005. **29**(2 Suppl): p. 80-5.

181. Migliore, E., et al., *[Prevalence of asthma and allergies among migrant children and adolescents in Italy]*. Epidemiol Prev, 2005. **29**(2 Suppl): p. 36-41.

182. Sestini, P., et al., *[Frequency of asthma and allergies in Italian children and adolescents: results from SIDRIA-2]*. Epidemiol Prev, 2005. **29**(2 Suppl): p. 24-31.

183. Pope, C.A., 3rd, *Epidemiology of fine particulate air pollution and human health: biologic mechanisms and who's at risk?* Environ Health Perspect, 2000. **108 Suppl 4**: p. 713-23.

184. D'Amato, G., et al., *Outdoor air pollution, climatic changes and allergic bronchial asthma.* Eur Respir J, 2002. **20**(3): p. 763-76.

185. Dong, C.C., et al., *Effect of diesel exhaust particles on allergic reactions and airway responsiveness in ovalbumin-sensitized brown Norway rats.* Toxicol Sci, 2005. **88**(1): p. 202-12.

186. Steerenberg, P.A., et al., *Adjuvant activity of various diesel exhaust and ambient particles in two allergic models.* J Toxicol Environ Health A, 2003. **66**(15): p. 1421-39.

187. Kobayashi, T. and T. Ito, *Diesel exhaust particulates induce nasal mucosal hyperresponsiveness to inhaled histamine aerosol.* Fundam Appl Toxicol, 1995. **27**(2): p. 195-202.

188. Hughes, T.J., J. Lewtas, and L.D. Claxton, *Development of a standard reference material for diesel mutagenicity in the Salmonella plate incorporation assay.* Mutat Res, 1997. **391**(3): p. 243-58.

189. Nilsen, A., R. Hagemann, and I. Eide, *The adjuvant activity of diesel exhaust particles and carbon black on systemic IgE production to ovalbumin in mice after intranasal instillation.* Toxicology, 1997. **124**(3): p. 225-32.

190. Suzuki, T., et al., *Adjuvant activity of diesel exhaust particulates (DEP) in production of anti-IgE and anti-IgG1 antibodies to mite allergen in mice.* J Clin Lab Immunol, 1996. **48**(5): p. 187-99.

191. Diaz-Sanchez, D., *The role of diesel exhaust particles and their associated polyaromatic hydrocarbons in the induction of allergic airway disease.* Allergy, 1997. **52**(38 Suppl): p. 52-6; discussion 57-8.

192. Hao, M., et al., *Diesel exhaust particles exert acute effects on airway inflammation and function in murine allergen provocation models.* J Allergy Clin Immunol, 2003. **112**(5): p. 905-14.

193. Al-Humadi, N.H., et al., *The effect of diesel exhaust particles (DEP) and carbon black (CB) on thiol changes in pulmonary ovalbumin allergic sensitized Brown Norway rats.* Exp Lung Res, 2002. **28**(5): p. 333-49.

194. Granum, B., et al., *Fine particles of widely different composition have an adjuvant effect on the production of allergen-specific antibodies.* Toxicol Lett, 2001. **118**(3): p. 171-81.

195. Granum, B., P.I. Gaarder, and M. Lovik, *IgE adjuvant effect caused by particles - immediate and delayed effects.* Toxicology, 2001. **156**(2-3): p. 149-59.

196. Yanagisawa, R., et al., *Components of diesel exhaust particles differentially affect Th1/Th2 response in a murine model of allergic airway inflammation.* Clin Exp Allergy, 2006. **36**(3): p. 386-95.

197. Sagai, M., et al., *Biological effects of diesel exhaust particles. I. In vitro production of superoxide and in vivo toxicity in mouse.* Free Radic Biol Med, 1993. **14**(1): p. 37-47.

198. Cao, D., et al., *Diesel exhaust particulate-induced activation of Stat3 requires activities of EGFR and Src in airway epithelial cells.* Am J Physiol Lung Cell Mol Physiol, 2007. **292**(2): p. L422-9.

199. Steerenberg, P.A., et al., *Optimization of route of administration for coexposure to ovalbumin and particle matter to induce adjuvant activity in respiratory allergy in the mouse.* Inhal Toxicol, 2003. **15**(13): p. 1309-25.

200. Hamelmann, E., et al., *Noninvasive measurement of airway responsiveness in allergic mice using barometric plethysmography.* Am J Respir Crit Care Med, 1997. **156**(3 Pt 1): p. 766-75.

201. Singh, P., et al., *Sample Characterization of Automobile and Forklift Diesel Exhaust Particles and Comparative Pulmonary Toxicity in Mice* Environ Health Perspect, 2004. **112**(8): p. 820-825.

202. Metzger, J.M. and L.B. Peterson, *Cyclosporin A enhances the pulmonary granuloma response induced by Schistosoma mansoni eggs.* Immunopharmacology, 1988. **15**(2): p. 103-15.

203. Kaneko, M., et al., *Allergen-specific IgG1 and IgG3 through Fc gamma RII induce eosinophil degranulation.* J Clin Invest, 1995. **95**(6): p. 2813-21.

204. Ito, K., et al., *IgG1 antibodies to house dust mite (Dermatophagoides farinae) and late asthmatic response.* Int Arch Allergy Appl Immunol, 1986. **81**(1): p. 69-74.

205. Huang, T.J., et al., *Allergen-specific Th1 cells counteract efferent Th2 cell-dependent bronchial hyperresponsiveness and eosinophilic inflammation partly via IFN-gamma.* J Immunol, 2001. **166**(1): p. 207-17.

206. Imai, T., et al., *Molecular cloning of a novel T cell-directed CC chemokine expressed in thymus by signal sequence trap using Epstein-Barr virus vector.* J Biol Chem, 1996. **271**(35): p. 21514-21.

207. Peh, S.C., L.H. Kim, and S. Poppema, *TARC, a CC chemokine, is frequently expressed in classic Hodgkin's lymphoma but not in NLP Hodgkin's lymphoma, T-cell-rich B-cell lymphoma, and most cases of anaplastic large cell lymphoma.* Am J Surg Pathol, 2001. **25**(7): p. 925-9.

208. Berin, M.C., et al., *Regulated production of the T helper 2-type T-cell chemoattractant TARC by human bronchial epithelial cells in vitro and in human lung xenografts.* Am J Respir Cell Mol Biol, 2001. **24**(4): p. 382-9.

209. Kawasaki, S., et al., *Intervention of thymus and activation-regulated chemokine attenuates the development of allergic airway inflammation and hyperresponsiveness in mice.* J Immunol, 2001. **166**(3): p. 2055-62.

210. Takano, H., et al., *Inhalation of diesel exhaust enhances allergen-related eosinophil recruitment and airway hyperresponsiveness in mice.* Toxicol Appl Pharmacol, 1998. **150**(2): p. 328-37.

211. Fiorentino, D.F., M.W. Bond, and T.R. Mosmann, *Two types of mouse T helper cell. IV. Th2 clones secrete a factor that inhibits cytokine production by Th1 clones.* J Exp Med, 1989. **170**(6): p. 2081-95.

212. Fiorentino, D.F., et al., *IL-10 acts on the antigen-presenting cell to inhibit cytokine production by Th1 cells.* J Immunol, 1991. **146**(10): p. 3444-51.

213. Schandene, L., et al., *B7/CD28-dependent IL-5 production by human resting T cells is inhibited by IL-10.* J Immunol, 1994. **152**(9): p. 4368-74.

214. Zuany-Amorim, C., et al., *Modulation by IL-10 of antigen-induced IL-5 generation, and CD4+ T lymphocyte and eosinophil infiltration into the mouse peritoneal cavity.* J Immunol, 1996. **157**(1): p. 377-84.

215. Zuany-Amorim, C., et al., *Interleukin-10 inhibits antigen-induced cellular recruitment into the airways of sensitized mice.* J Clin Invest, 1995. **95**(6): p. 2644-51.

216. Sydbom, A., et al., *Health effects of diesel exhaust emissions.* Eur Respir J, 2001. **17**(4): p. 733-746.

217. Bayram, H., et al., *The effect of diesel exhaust particles on cell function and release of inflammatory mediators from human bronchial epithelial cells in vitro.* Am J Respir Cell Mol Biol, 1998. **18**(3): p. 441-8.

218. Takafuji, S., et al., *Diesel-exhaust particulates inoculated by the intranasal route have an adjuvant activity for IgE production in mice.* J Allergy Clin Immunol, 1987. **79**(4): p. 639-45.

219. Stevens, T., W. Linak, and M.I. Gilmour, *Differential Potentiation of Allergic Lung Disease in Mice Exposed to Chemically Distinct Diesel Samples.* Toxicol Sci. **submitted**.

220. Subramanian, A., et al., *Gene set enrichment analysis: a knowledge-based approach for interpreting genome-wide expression profiles.* Proc Natl Acad Sci U S A, 2005. **102**(43): p. 15545-50.

221. Bild, A. and P.G. Febbo, *Application of a priori established gene sets to discover biologically important differential expression in microarray data.* Proc Natl Acad Sci U S A, 2005. **102**(43): p. 15278-9.

222. Heo, Y., A. Saxon, and O. Hankinson, *Effect of diesel exhaust particles and their components on the allergen-specific IgE and IgG1 response in mice.* Toxicology, 2001. **159**(3): p. 143-58.

223. Ito, T., et al., *Peroxynitrite formation by diesel exhaust particles in alveolar cells: Links to pulmonary inflammation.* Environ Toxicol Pharmacol, 2000. **9**(1-2): p. 1-8.

224. Stevens, T., et al., *Increased transcription of immune and metabolic pathways in naive and allergic mice exposed to diesel exhaust.* Toxicol Sci, 2008. **102**(2): p. 359-70.

225. Medzhitov, R., P. Preston-Hurlburt, and C.A. Janeway, Jr., *A human homologue of the Drosophila Toll protein signals activation of adaptive immunity.* Nature, 1997. **388**(6640): p. 394-7.

226. Visintin, A., et al., *Regulation of Toll-like receptors in human monocytes and dendritic cells.* J Immunol, 2001. **166**(1): p. 249-55.

227. Bevelander, M., et al., *Nitrogen dioxide promotes allergic sensitization to inhaled antigen.* J Immunol, 2007. **179**(6): p. 3680-8.

228. Hollingsworth, J.W., 2nd, et al., *The role of Toll-like receptor 4 in environmental airway injury in mice.* Am J Respir Crit Care Med, 2004. **170**(2): p. 126-32.

229. Zhou, J., et al., *Heat shock up-regulates expression of Toll-like receptor-2 and Toll-like receptor-4 in human monocytes via p38 kinase signal pathway.* Immunology, 2005. **114**(4): p. 522-30.

230. Takano, H., et al., *Diesel exhaust particles enhance lung injury related to bacterial endotoxin through expression of proinflammatory cytokines, chemokines, and intercellular adhesion molecule-1.* Am J Respir Crit Care Med, 2002. **165**(9): p. 1329-35.

231. Inoue, K., et al., *The role of toll-like receptor 4 in airway inflammation induced by diesel exhaust particles.* Arch Toxicol, 2006. **80**(5): p. 275-9.

232. Casillas, A.M., et al., *Enhancement of allergic inflammation by diesel exhaust particles: permissive role of reactive oxygen species.* Ann Allergy Asthma Immunol, 1999. **83**(6 Pt 2): p. 624-9.

233. Risom, L., P. Moller, and S. Loft, *Oxidative stress-induced DNA damage by particulate air pollution.* Mutat Res, 2005. **592**(1-2): p. 119-37.

234. Nagashima, M., et al., *Formation of an oxidative DNA damage, 8-hydroxydeoxyguanosine, in mouse lung DNA after intratracheal instillation of diesel exhaust particles and effects of high dietary fat and beta-carotene on this process.* Carcinogenesis, 1995. **16**(6): p. 1441-5.

235. Brauer, M., et al., *Estimating long-term average particulate air pollution concentrations: application of traffic indicators and geographic information systems.* Epidemiology, 2003. **14**(2): p. 228-39.

236. Delfino, R.J., et al., *Respiratory symptoms and peak expiratory flow in children with asthma in relation to volatile organic compounds in exhaled breath and ambient air.* J Expo Anal Environ Epidemiol, 2003. **13**(5): p. 348-63.

237. Hwang, B.F., et al., *Traffic related air pollution as a determinant of asthma among Taiwanese school children.* Thorax, 2005. **60**(6): p. 467-73.

238. Heinrich, J. and H.E. Wichmann, *Traffic related pollutants in Europe and their effect on allergic disease.* Curr Opin Allergy Clin Immunol, 2004. **4**(5): p. 341-8.

239. Lwebuga-Mukasa, J.S., et al., *Association between traffic volume and health care use for asthma among residents at a U.S.-Canadian border crossing point.* J Asthma, 2004. **41**(3): p. 289-304.

240. McConnell, R., et al., *Asthma in exercising children exposed to ozone: a cohort study.* Lancet, 2002. **359**(9304): p. 386-91.

241. McDonnell, W.F., et al., *Long-term ambient ozone concentration and the incidence of asthma in nonsmoking adults: the AHSMOG Study.* Environ Res, 1999. **80**(2 Pt 1): p. 110-21.

242. Froines, J.R., et al., *Exposure of firefighters to diesel emissions in fire stations.* Am Ind Hyg Assoc J, 1987. **48**(3): p. 202-7.

243. Nauss, K. *Diesel Exhaust: A Critical Analysis of Emissions, Exposure, and Health Effects*. Cambridge, MA., Health Effects Institute, 1995; pp. 13–18.

244. Matsumoto, A., et al., *Repeated exposure to low-dose diesel exhaust after allergen challenge exaggerates asthmatic responses in mice.* Clin Immunol, 2006. **121**(2): p. 227-35.

245. Li, N., et al., *Induction of heme oxygenase-1 expression in macrophages by diesel exhaust particle chemicals and quinones via the antioxidant-responsive element.* J Immunol, 2000. **165**(6): p. 3393-401.

246. Maejima, K., et al., *Effects of the inhalation of diesel exhaust, Kanto loam dust, or diesel exhaust without particles on immune responses in mice exposed to Japanese cedar (Cryptomeria japonica) pollen.* Inhal Toxicol, 2001. **13**(11): p. 1047-63.

247. Fujimaki, H. and Y. Kurokawa, *Diesel exhaust-associated gas components enhance chemokine production by cervical lymph-node cells from mice immunized with sugi basic proteins.* Inhal Toxicol, 2004. **16**(1): p. 61-5.

248. Gilmour, M.I. and M.J. Selgrade, *A model of immune-mediated lung disease in rats sensitized to house dust mite and upregulation of immunity following exposure to nitrogen dioxide.* Chest, 1996. **109**(3 Suppl): p. 69S.

249. Whitekus, M.J., et al., *Thiol antioxidants inhibit the adjuvant effects of aerosolized diesel exhaust particles in a murine model for ovalbumin sensitization.* J Immunol, 2002. **168**(5): p. 2560-7.

250. Blalock, E.M., et al., *Harnessing the power of gene microarrays for the study of brain aging and Alzheimer's disease: statistical reliability and functional correlation.* Ageing Res Rev, 2005. **4**(4): p. 481-512.

251. Farraj, A.K., J.R. Harkema, and N.E. Kaminski, *Allergic rhinitis induced by intranasal sensitization and challenge with trimellitic anhydride but not with dinitrochlorobenzene or oxazolone in A/J mice.* Toxicol Sci, 2004. **79**(2): p. 315-25.

252. Ichinose, T., et al., *Long-term exposure to diesel exhaust enhances antigen-induced eosinophilic inflammation and epithelial damage in the murine airway.* Toxicol Sci, 1998. **44**(1): p. 70-9.

253. Salvi, S., et al., *Acute inflammatory responses in the airways and peripheral blood after short-term exposure to diesel exhaust in healthy human volunteers.* Am J Respir Crit Care Med, 1999. **159**(3): p. 702-9.

254. Saito, Y., et al., *Long-term inhalation of diesel exhaust affects cytokine expression in murine lung tissues: comparison between low- and high-dose diesel exhaust exposure.* Exp Lung Res, 2002. **28**: p. 493-506.

255. Boland, S., et al., *Diesel exhaust particles are taken up by human airway epithelial cells in vitro and alter cytokine production.* Am J Physiol, 1999. **276**(4 Pt 1): p. L604-13.

256. Boland, S., et al., *Mechanisms of GM-CSF increase by diesel exhaust particles in human airway epithelial cells.* Am J Physiol Lung Cell Mol Physiol, 2000. **278**(1): p. L25-32.

257. Barnhart, M.I., et al., *Ultrastructure and morphometry of the alveolar lung of guinea pigs chronically exposed to diesel engine exhaust: six month's experience.* J Appl Toxicol, 1981. **1**(2): p. 88-103.

258. Wright, E.S., *Effects of short-term exposure to diesel exhaust on lung cell proliferation and phospholipid metabolism.* Exp Lung Res, 1986. **10**(1): p. 39-55.

259. Kato, A., H. Kyono, and N. Kuwabara, *[Electron-microscopic observations on rat lungs after long term inhalation of diesel emissions--non-neoplastic lesions]*. Nihon Kyobu Shikkan Gakkai Zasshi, 1992. **30**(2): p. 238-47.

260. Bayram, H., et al., *Regulation of human lung epithelial cell numbers by diesel exhaust particles.* Eur Respir J, 2006. **27**(4): p. 705-13.

261. Penning, T.M., et al., *Dihydrodiol dehydrogenases and polycyclic aromatic hydrocarbon activation: generation of reactive and redox active o-quinones.* Chem Res Toxicol, 1999. **12**(1): p. 1-18.

262. Nygaard, U.C., et al., *The capacity of particles to increase allergic sensitization is predicted by particle number and surface area, not by particle mass.* Toxicol Sci, 2004. **82**(2): p. 515-24.

263. Terada, N., et al., *Diesel exhaust particulates enhance eosinophil adhesion to nasal epithelial cells and cause degranulation.* Int Arch Allergy Immunol, 1997. **114**(2): p. 167-74.

264. Coyne, C.B., et al., *Regulation of airway tight junctions by proinflammatory cytokines.* Mol Biol Cell, 2002. **13**(9): p. 3218-34.

265. Lambert, A.L., et al., *Residual oil fly ash exposure enhances allergic sensitization to house dust mite.* Toxicol Appl Pharmacol, 1999. **158**(3): p. 269-77.